THE FLOCCULATION DYNAMICS OF COHESIVE SEDIMENTS IN THE ST LUCIA AND MFOLOZI ESTUARIES, SOUTH AFRICA

Christopher Mark Maine

Submitted in fulfilment of the requirements for the degree of
Master of Science in Engineering
In the
Civil Engineering Programme
University of KwaZulu-Natal
Durban
2011

Supervisor: Professor DD Stretch

ABSTRACT

Increasing turbidities due to land use changes and poor catchment management can cause negative impacts on estuaries worldwide. High turbidity has an impact on the biological functioning of estuaries which are amongst our most productive ecosystems. This study focuses on the St Lucia estuary on the east coast of South Africa, a UNESCO World Heritage Site and Ramsar wetland of international importance. Increased turbidity due to suspended inorganic sediments has been identified as an important threat to the sustainability of biodiversity in the St Lucia system. In order to determine the influence of increased cohesive sediment loads on the estuarine system it is necessary to understand how flocculation affects the fate and transport of cohesive sediment. Flocculation describes the processes of aggregate formation and breakup. Suspended sediment concentration, salinity and turbulent shear rates have been identified as key drivers of estuarine flocculation. This study investigates flocculation by measuring how the floc size distribution and settling velocities of flocs vary with the key drivers. A laboratory technique was developed where flocculation was simulated in an agitated beaker. Digital imaging techniques were used to measure changes in the size of flocs within the beaker and floc settling velocities in a still settling column. Results show reduced aggregation and floc size with increases in turbulent shear. Floc settling velocities were observed to increase with floc size while the effective density was observed to decrease. The study is concluded by investigating potential applications for the results obtained.

PREFACE

I, Christopher Mark Maine, hereby declare that the whole of this dissertation is my own work and has not been submitted in part, or in whole to any other University. Where use has been made of the work of others, it has been duly acknowledged in the text. This research work has been carried out in the Centre for Research in Environmental, Coastal and Hydraulic Engineering, School of Civil Engineering, Surveying and Construction, University of Kwa-Zulu Natal, Durban, under the supervision of Professor D.D. Stretch.

....

C.M. Maine Date

As the candidate's supervisor, I have approved this dissertation for submission.

....

Professor D.D. Stretch Date

ACKNOWLEDGEMENTS

I would like to express my gratitude to the following:

- Professor Derek Stretch, for his support, motivation and guidance
- The technical support staff at the School of Civil Engineering workshop and environmental laboratory, particularly Logan Govender, Fathima Ali, Mogadesen Moodley, Peter Naidoo and Sydney
- The School of Biological Sciences, particularly Professor R Perisinotto and Dr K Tirok for assistance with equipment
- Colleagues Justin Pringle and Andrew Maro, for assistance on field trips, support and motivation
- Ezemvelo KZN Wildlife, particularly Dr Ricky Taylor, Caroline Fox and S'bu for assistance with field trips
- iSimangaliso Wetland Park Authority, particularly Nerosha Govender, for assistance with access to the park.

Research was made possible by funding from the following sources:

- SANPAD Education & Research Trust, Project number 10/90
- NRF SEACHANGE Programme, Grant number 71051 (Society, Ecosystems & Change).
- External subsistence funding through the NRF Scarce Skills Scholarship

TABLE OF CONTENTS

LIST OF FIGURES

LIST OF PLATES

Schematic diagrams, photographs and maps are referred to as plates.

LIST OF TABLES

CHAPTER 1

INTRODUCTION

Chapter 1 introduces the research undertaken in this investigation. It outlines the key objectives of the investigation. The motivation for the research is then discussed. The chapter is concluded by a brief outline of the dissertation.

1.1. Introduction

The focus of the investigation is to understand the behaviour of cohesive sediments in the St Lucia-Mfolozi estuaries. The research has been undertaken to answer a key question to understanding sediment transport: “How does flocculation influence the fate and transport of fine suspended sediments in the Mfolozi/St Lucia estuarine complex?” Flocculation is a property of cohesive sediments characterized by the tendency of fine sediments to combine and form aggregates (Van Leussen, 1994; Maggi, 2007). Flocculation is the dynamic combination of aggregation and floc breakup processes (Maggi, 2007). It is a physico-chemical process controlled by a set of driving parameters. Collisions between particles are required for aggregates to form. The collision frequency is driven by turbulence and the number of particles present (suspended sediment concentration). Colliding particles have a potential to stick together and form aggregates. The flocculation potential is controlled by two chemical drivers: ionic strength salinity and organic matter content (Van Leussen, 1994; Maggi, 2006). These drivers control the strength of the flocs which form. Floc breakup is driven by turbulent shear.

Flocculation has been observed to occur in estuaries where saline water stimulates the aggregation of suspended particular matter. It is also influenced by other estuarine processes. The aggregates which form are sensitive to the strengths of the flocculation drivers (Mikes & Manning, 2010).When flocs form, their settling velocities increase. Large flocs have been observed to dominate the vertical settling flux of suspended sediment in the water column (Dyer &Manning, 1999). Flocculation therefore enhances the settling rate of cohesive sediment.

Sediments from the area of interest are known to contain cohesive properties (Linsay et al., 1996). It is anticipated that their behaviour is influenced by the drivers mentioned above. It is therefore reasonable to understand sediment transport characteristics by first investigating flocculation.

1.2. Objectives

The aim of this research is to determine the sediment transport characteristics of sediment from the Mfolozi and St Lucia estuaries. A quantitative estimate of the settling rate of Mfolozi sediment is required and is intended for use in future sediment transport modelling. This will provide a means for determining the influence of Mfolozi sediment on a combined Mfolozi-St Lucia estuarine mouth. Given the cohesive nature of Mfolozi and St Lucia sediments, the investigation focuses on flocculation. The study aims to obtain a comprehensive understanding of flocculation and its effect on sediment settling characteristics. The results of the study are also intended to aid in understanding the influence of flocculation on re-suspension and deposition processes caused by high energy events in Lake St Lucia. The aim may be elaborated by the following objectives:

- To investigate the influence of the flocculation drivers (suspended sediment concentration, turbulence and salinity) on the development and destruction of aggregates
- To investigate the settling velocities of aggregates and their sensitivity to the drivers of flocculation.
- To integrate observed flocculation behaviour with settling velocities to understand the settling characteristics of Mfolozi and St Lucia sediments.
- To obtain accurate estimates of the settling velocity of Mfolozi and St Lucia sediments for use in future sediment transport studies.

1.3. Motivation

The research focuses on the Mfolozi and St Lucia estuarine systems. It seeks to investigate the probable influence of the Mfolozi river sediment on siltation in the St Lucia estuarine system. The Mfolozi River previously entered the St Lucia estuary. It was however separated in 1952 from the St Lucia estuary. Fears of siltation in the St Lucia system have long influenced the management policy to maintain separate Mfolozi and St Lucia systems. Since 1952 the St Lucia system has suffered from a deficiency in its freshwater supply. This lead to Lake St Lucia drying significantly during droughts. These problems are exacerbated by the prevailing hypersaline conditions occurring in the lake. Recent publications have highlighted the importance of the Mfolozi River as a supply of freshwater to the St Lucia system. There is thus a need to investigate the feasibility of restoring (or partially restoring) the historical combined St Lucia-Mfolozi estuarine system.

This requires an investigation into the influence of Mfolozi sediments on siltation in the St Lucia system. Sediments from the Mfolozi River are predominantly fine cohesive sediment. The settling and transport characteristics of cohesive sediment are influenced by the process of flocculation. This study seeks to understand the process of flocculation in order to provide a basis for modelling cohesive sediment transport in a combined St Lucia-Mfolozi estuary. This will ultimately provide a detailed understanding of the sedimentation characteristics of the historically combined system.

1.4. Outline of Dissertation

Chapter 2 contains a literature review where a theoretical background of the field of study is presented. It covers the physical and chemical aspects of cohesive sediment flocculation. The study area is described at the end of the chapter.

Chapter 3 contains the methodology of the investigation. A short review of the available laboratory techniques is presented. The laboratory procedure employed is described in detail. This is followed by a description of the how the data and images obtained from laboratory tests were processed.

Chapter 4 contains the results of the investigation. It presents and discusses the results of material composition tests, aggregation and deflocculating experiments, and settling velocity measurements. Problems encountered during the investigation are discussed. Possible applications for results are suggested.

Chapter 5 presents conclusions to the investigation and recommendations for further research.

CHAPTER 2

LITERATURE REVIEW

The literature review begins by defining cohesive sediment and describing various classes of aggregates which form when cohesive sediment flocculates. The chemical aspects of flocculation are discussed. The kinetics of flocculation are discussed, paying particular attention to turbulence and its role in floc formation and breakup. This is followed by a section on the settling characteristics of cohesive sediment. The chapter ends with a description of the Mfolozi and St Lucia estuaries, the problems they are faced with, and the relevance of this investigation to solving those problems.

2.1. Introduction to cohesive sediment

Cohesive sediments are found in most river systems around the world. It is these sediments that give rivers and estuaries a turbid or 'muddy' appearance. Cohesive sediments remain in suspension for longer periods of time than non-cohesive sediments. The transport properties of cohesive sediments are controlled by the process of flocculation (Mikes & Manning, 2010). Cohesive sediment is composed of fine grained clay and silt particles (Milligan & Hill, 1998) as opposed to non-cohesive sediment, which primarily consists of sand and other large grained particles. Cohesive sediment is characterized by its tendency to aggregate into larger particles known as flocs. The behaviour of flocs is fundamentally different to that of sand. The behaviour is a complex response to the strength of various ambient conditions and driving factors within an estuarine system (Mikes & Manning, 2010; Maggi, 2006). It is influenced by both physical and chemical factors.

Flocculation has an influence on water quality and siltation in river and estuarine systems (Maggi, 2006; Van Leussen, 1994). Flocculation has been linked to the transport of contaminants and pollutants in river systems (Maggi, 2006). Flocculation has been linked to sedimentation processes in harbours, lakes, rivers and estuaries (Maggi, 2006; Van Leussen, 1994). Its effect on the turbidity of water columns influences the biological productivity of aquatic systems by influencing light penetration.

In order to understand the influence of cohesive sediment loads on estuarine systems it is necessary to understand the process of flocculation. This enables the prediction of sediment behaviour under various conditions.

The estuarine environment is characterized by a complex hydrodynamic system. Estuaries contain a variation of physical, chemical and biological parameters influencing the interaction between suspended sediment particles (Maggi, 2006). Interactions between particles may be constructive or destructive interactions. These are termed aggregation and fragmentation. These antagonistic processes are collectively defined by the term flocculation. The balance between aggregation and fragmentation is dependent on the relative strengths of each of the ambient driving parameters. The primary driving factors in the estuarine flocculation process are salinity, turbulence, suspended particulate matter concentration, the material composition of suspended sediment (including biological compounds and micro-organisms) and the time duration for which the conditions remain (Mikes et al., 2002; Mikes & Manning, 2010; Verney et al, 2009, Van Leussen, 1994; Kumar et al., 2010).

2.2. Classification of cohesive sediment

Soil is typically classified as clay, silt, sand or gravel. Soil classification is size-based. The particle-size classification developed by the Massachusetts Institute of technology is shown below in table 2-1 (Das, 2006). The MIT classification is generally used to distinguish clay, silt, and sand particles.

Table 2-1: MIT particle size classification

Clay	Silt	Sand	Gravel
<2μm	2 - 60μm	60 - 2000μm	>2000μm

The definition of cohesive sediment is not as clear as the particle size classification above. Clay is considered cohesive sediment. It is clay minerals that give sediments cohesive properties (Bureau of Reclamation, 2006). Clays are flake-shaped particles composed of clay minerals and mica. Examples of clay minerals are: Kaolinite, Illite, Montmorrilonite, Bentonite, Smectite, and Chlorite (Das, 2006). Silt contains both cohesive and non-cohesive particles. Silt typically contains fine grains of quartz and large clay-type particles containing clay minerals (Das, 2006). Silt is generally considered as a cohesive sediment because has cohesive properties. For the purpose of this dissertation silt is considered cohesive sediment. Sands are considered non-cohesive. Cohesive sediment also contains and is influenced by organic materials Bureau of Reclamation 2006).

The definition of clay and cohesive sediment should not be restricted to particle size but rather mineral composition. It is the mineral composition rather than the particle size which influences sediment behaviour. Size classification does however provide a good estimation of the clay and silt content of a soil and hence its cohesive properties. Soils dominated by silt and clay-sized particles are considered cohesive.

2.3. Aggregates

The term floc describes a sediment structure consisting of a combination of smaller particles. Aggregates occur naturally as sediment flocs, biological flocs (e.g.: fecal pellets, marine snow) and combinations thereof (Van Leussen, 1994). Sediment flocs are important as their size and settling velocities influence cohesive sediment transport in rivers and estuaries. Thus sediment flocs are the main focus of this study. The tendency of a suspension of particles to coagulate to form flocs is referred to as the *stability* of a solution (van Leussen, 1994; Maggi, 2006, Mietta et al., 2009a, Mietta et al., 2009b). A stable solution is one that contains a suspension of particles where there is no potential for coagulation to occur. Conversely an unstable solution is one where suspended particles have some potential to coagulate. Estuarine and river flocs seldom occur as a suspension of primary particles in a stable form (Eisma et al., 1996). Due to the cohesive nature of clay minerals, particles interact and flocculate upon suspension into rivers and estuaries (Mikes & Manning, 2010). Suspended particles will coagulate until a quasi-steady equilibrium is reached where the floc size distribution remains relatively constant and the rate of floc formation and floc break-up are equal. The resultant floc size distribution is dependent on the strengths of the drivers of the flocculation process.

Sediment flocs have been classified by their size. A range of floc sizes may be observed under different conditions as a response to the relative strengths of the drivers of flocculation. Sediment flocs are commonly classified as microflocs and macroflocs (Mikes & Manning, 2010; Maggi, 2006; Verney, 2006). A broader classification is proposed by van Leussen (1994), where suspended particulate matter may be classified as primary particles, flocculus, flocs and aggregates. The size of suspended particulate matter may also be classified by an order. Primary particles may be classified as zero-order aggregates while microflocs and the larger macroflocs are classified as first and second order aggregates respectively (Mikes, 2010; Maggi, 2006; Van Leussen, 1994). Higher order aggregates are formed from combinations of lower order aggregates. Aggregates of different orders each have characteristic size ranges, settling velocities, densities and strength properties. An understanding of the floc size distribution and settling characteristics will aid in indicating the typical behaviour of a suspension.

2.3.1. Zero order aggregates -Clay mineral aggregates:

The primary particles that form the basis of estuarine flocs are clay and silt particles. Clay particles are typically classified by a size range less than 2μm (Das, 2007). The particles are flat, plate-like in structure, and exhibit a large surface to volume ratio. The particles are clay minerals such as Kaolinite, Montmorillonite and Illite (Van Leussen, 1994; Das, 2007). These particles contain a negative surface charge. This is responsible for their cohesive properties.

Dissolved ions form a layer around suspended clay particles known as the Stern layer (Van Leussen, 1994; Maggi, 2006). A further layer of ions may develop depending on the surface charge. The ion layers form energy barriers to particle collisions. A large layer of ions surrounding a particle will serve as a significant barrier to particle contact and prevent aggregation (Maggi, 2006; Mietta et al, 2009a; Mietta et al., 2009b; Van Leussen, 1994). The strength of the ionic layers is dependent on the clay minerals present, the pH and the salinity of the ambient fluid (Mietta et al, 2009a; Mietta et al., 2009b; Maggi, 2006; Van Leussen, 1994; Mikes & Manning, 2010; Verney, 2006). This will be discussed further under the chemical process of coagulation.

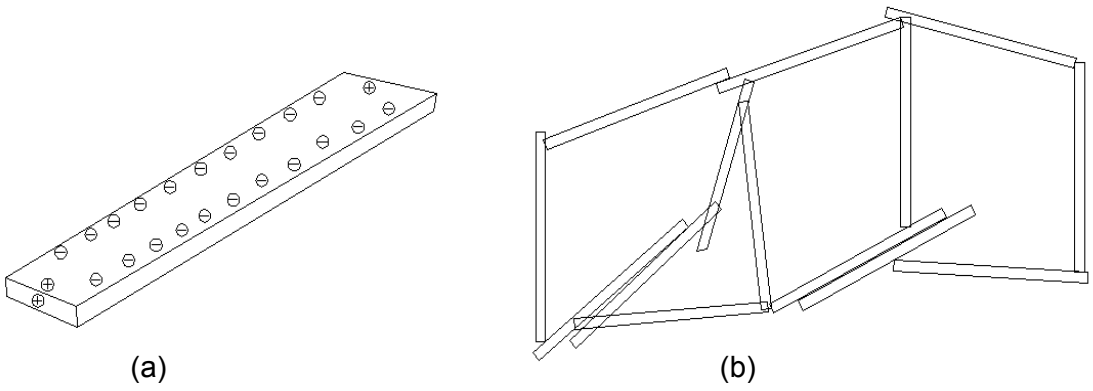

Plate 2-1: (a) Typical clay mineral structure (size: 1-2μm), (b) Typical structure (10-20μm) of a fine microfloc, (adapted from Van Leussen, 1994 and Das, 2007)

Silt particles are typically larger than clay particles and do not contain a negative surface charge. Silt particles do participate in the flocculation process. The proportion of silt and clay particles in suspension influences the size, density and strength of the flocs that form (Wolanski & Gibbs, 1995; Wolanski et al., 1993, Wolanski et al., 1998). Silt particles have weak cohesive properties in comparison to clay particles. Silt dominant conditions produce flocs which are typically larger and weaker than clay dominated flocs (Wolanski & Gibbs, 1995).

2.3.2. First order aggregates – Microflocs

Microflocs are small aggregates typically less than 150μm in size (Dyer &Manning, 1999). Microflocs are formed from a combination of zero order aggregates. They are robust, spherical

in nature and highly resistant to disruption by turbulence (Mikes et al., 2002; Mikes & Manning, 2010; Verney et al, 2009; Maggi, 2006). Microflocs are held together by electrochemical forces and biochemical forces (Mikes, 2010). These flocs are typically dense in comparison to larger aggregate structures. The dense, resilient nature of the flocs is attributed to the nature of particle connections and number of contacts between particles (Manning & Dyer, 1999; Maggi, 2006). The particles are formed by the physico-chemical process of coagulation and are typically stable in suspension in rivers (Mikes & Manning, 2010). Microflocs become unstable where changes in salinity or ph occur, resulting in further aggregation and the formation of second order aggregates. There are several size classifications of microflocs observed in literature: 10-20 µm (Mikes and Manning 2010), 100 µm (Mikes et al., 2002), 125 µm (Eisma, 1993); 5-20 µm (Maggi, 2006) and 150 µm (Dyer & Manning, 1999). It is generally agreed upon that microflocs are smaller than 150µm in diameter. The settling velocity of microflocs is typically of the order 0.001mm/s (Manning & Dyer, 1999). The settling velocity is low in comparison to larger aggregates.

2.3.3. Second order aggregates – Macroflocs

Macroflocs are large aggregations of microflocs which form under favourable hydrodynamic conditions in estuaries. The formation is sensitive to turbulence, salinity and biological and organic compounds in suspension (Mikes & Manning, 2010; Van Leussen, 1994).Low turbulence and salinity are typically necessary for the formation of macroflocs to occur (Mikes & Manning, 2010). Macroflocs range in size from 160µm to a few mm (Eisma et al., 1996; Mikes & Manning, 2010; Verney et al, 2009; Dyer & Manning, 1999, Van Leussen, 1994). Macroflocs are porous in nature and are characterized by a low density in comparison to microflocs (Mikes & Manning, 2010; Dyer & Manning, 1999; Kranenburg, 1999). Large aggregates, particularly macroflocs, dominate the vertical settling flux of suspended sediment in the water column (Dyer& Manning, 1999). The settling velocity of macroflocs ranges from 1-15mm/s (Mikes & Manning, 2010).

Second order aggregates are fragile due to their loosely bonded porous structure (Mikes & Manning, 2010, Verney et al., 2009, Van Leussen, 1994). They are vulnerable to changes in ambient turbulent conditions (Maggi, 2006; Eisma et al., 1996). Turbulent shear is a primary cause of floc breakage. The fragility of macroflocs limits the techniques available for floc observation and sampling, to the extent that flocs may only be observed by camera and image analysis or by special sampling techniques (Eisma et al., 1996; Milligan & Hill, 1998; Dyer & Manning, 1999; Mikes & Manning, 2010, Gibbs & Konwar, 1982). Upon disruption macroflocs break up into the range of microflocs of which they are composed (Dyer & Manning, 1999). It is thus necessary to investigate macroflocs by the least invasive method possible. Conversely microflocs are resistant to breakup during sampling and are suitable for optical and electron

microscope analysis (Mikes & Manning, 2010). Macroflocs are depicted in figure 2-2 below. They are distinctly larger than the surrounding microflocs.

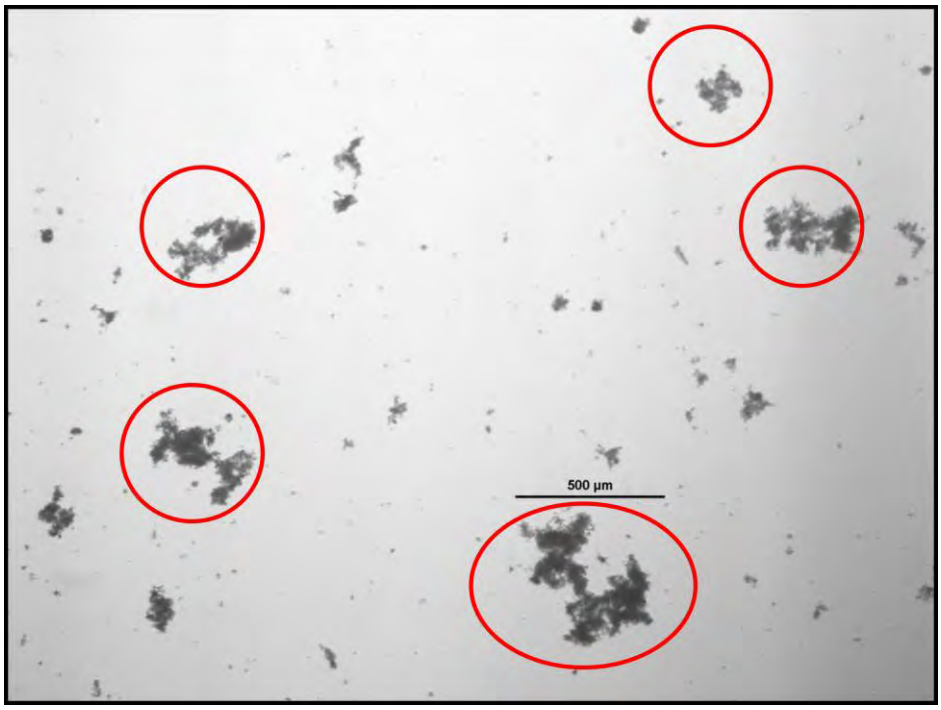

Plate 2-2: Microscope image depicting macroflocs and microflocs. Macroflocs are distinguished by red ellipses. The solid black bar represents 500µm

2.3.4. Biological aggregates

Biological aggregates occur naturally and in engineered systems. Biological aggregates are composed of biological microorganisms, suspended nutrients and fecal pellets (Van Leussen, 1994). Sediment flocs also contain organic material including microorganisms (Verney et al., 2009). A common biological aggregate is marine snow, which describes large aggregates of phytoplankton which form in marine environments (Van Leussen, 1994). Phytoplankton, particularly diatoms, have been found to increase the flocculation potential of suspended matter in estuaries (Verney et al., 2009). Estuarine flocs generally contain organic elements such as microorganisms, fecal pellets, and nutrients (Mikes & Manning, 2010). Organic matter reduces the density and settling velocity of estuarine flocs. Fecal pellets are aggregations formed as a result of the digestive processes of aquatic organisms (Van Leussen, 1994). Excretions such as polysaccharide chains play an important role in the flocculation process by forming bridges between particles and aggregates, effectively holding the floc together (Van Leussen, 1994). This will be discussed in detail in the following section.

2.4. The influence of chemical and biological parameters on the flocculation potential of sediment

2.4.1. Chemical properties of aggregates

Primary particles contain a negative surface charge which results in the development of layers of dissolved ions around the surface of the particle. This is commonly referred to as the double layer (Van Leussen, 1994; Maggi, 2006; Mietta et al., 2009a; Mietta et al., 2009b; Das, 2007). The strength of the surface charge influences the size of the double layer that forms. The strength of the electric charge is commonly expressed by a parameter known as Zeta potential (ξ-potential) (Mietta et al., 2009b, Van Leussen, 1994). The double layer forms an energy barrier which hinders contact between particles. The repulsive forces between particles are proportional to the ξ-potential. Figure 2-1 illustrates the ξ-potential of the double layer as a function of the distance to the surface of the particle. Repulsive forces increase with decreasing distance to the surface of the particle. Once the energy barrier is overcome, attractive forces exist on the surface of clay particles. The energy barrier needs to be overcome in order for a collision between two particles to become effective and coagulation to occur. Coagulated particles are held together by Van Der Waal's intermolecular forces (Van Leussen, 1994).

The size of the double layer is sensitive to the ionic strength (salinity) and pH of the ambient fluid (Mikes & Manning, 2010; Mietta et al., 2009a, b; Van Leussen, 1994; Larson, 2002). The influence of salinity on the flocculation of cohesive sediment has been widely investigated in literature (Van Leussen, 1994; Kumar et al, 2010; Larsen & Johansen, 1998; Mietta et al, 2009a, b; Mikes et al., 2002; Verney, 2006; Mikes & Manning, 2010; Verney et al., 2009; Milligan & hill, 1998). The process is known as *salt flocculation*.

2.4.2. Salt Flocculation

The size of the double layer reduces with increasing ionic strength (Mietta et al., 2008a, b; Van Leussen, 1994; Maggi, 2006). The energy barrier to flocculation decreases with increased salinity. This allows particles to move closer together. It increases the probability of effective collisions between flocs. Salinity therefore increases the potential for coagulation to occur. The reduction in the size of the double layer with increased salinity is depicted in plate2-3.

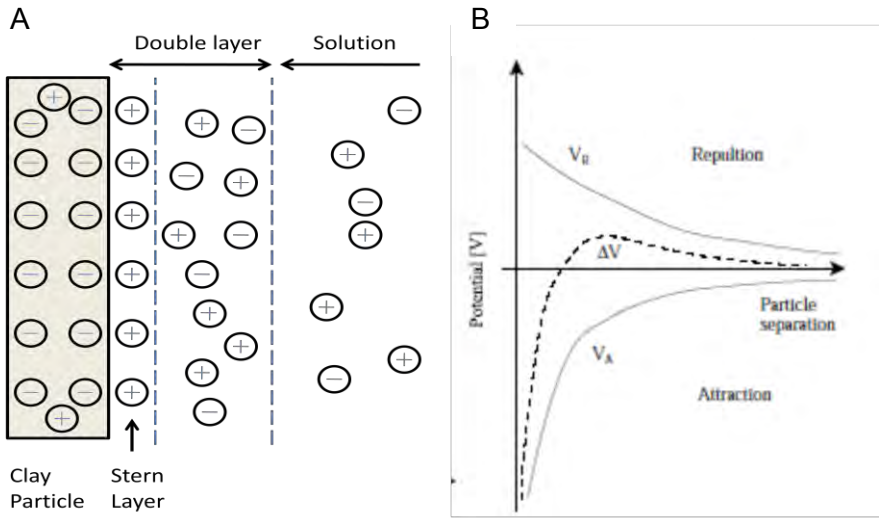

Figure 2-1: A: Schematic diagram of the double layer of a clay particle. B: the electrical potential energy for two interacting approaching suspended particles, source: Maggi (2006)

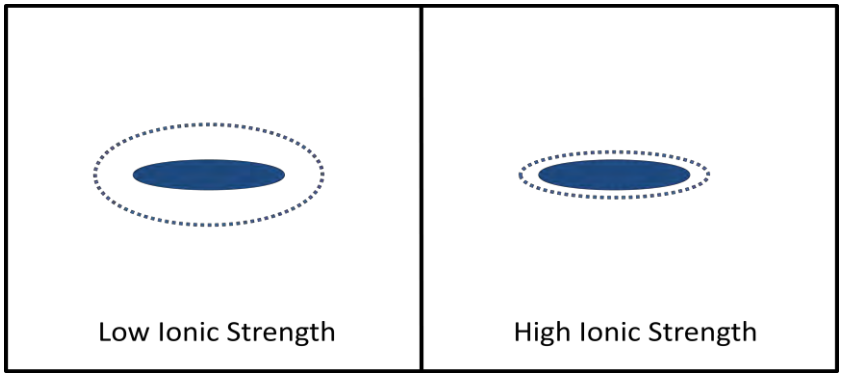

Plate 2-3: The influence of ionic strength on the size of the double layer

Salinity of an estuary varies according to different tidal conditions. A salinity gradient exists between the upper estuary and the ocean. Salinity intrusion increases the potential for large flocs to form in estuaries. These flocs do not form in freshwater systems even where other drivers may be suited to the formation of flocs. The influence of salinity on flocculation is clearly evident when comparing the behaviour of cohesive sediment in de-ionized water and saline water. The result of a comparative test is shown in plate 2-4.The test conducted using equal silt concentrations in solutions of de-ionized and saline water.

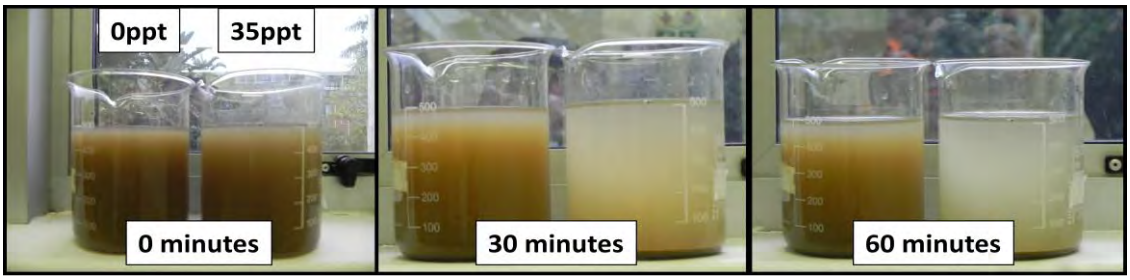

Plate 2-4: The results of a preliminary experiment where the two beakers of equal concentration and different salinities were observed over an hour.

Despite being widely investigated, very few mathematical expressions have been developed to relate salinity to the size or settling velocity of cohesive sediment. Expressions that do exist are empirical and their application is limited to the sediment investigated in the particular studies. It is widely understood that there is a threshold salinity at which coagulation occurs (Mikes et al., 2002; Mikes & Manning, 2010). Mikes & Manning (2010) suggest that this threshold salinity ranges from 0.1-20ppt. Preliminary laboratory investigations on sediments studied in this thesis indicate that this threshold is below 2.5ppt (Maine, 2010). Mikes et al. (2002) define the influence of salinity on flocculation as a three phase process, consisting of an initial stage, dynamic stage, and stabilization stage. The initial stage occurs before the threshold salinity is reached, where floc growth is limited by the available organic matter. The dynamic stage is characterized by a steep gradient of enhanced flocculation followed by a stabilization phase where the effect of salinity is reduced.

Salinity has been observed to enhance the flocculation process resulting in the formation of larger flocs (Mikes & Manning, 2010; Mikes et al, 2002; Maggi, 2006; Verney et al., 2009; Mietta et al., 2009a). Figure 2-2 clearly suggests this increase in floc size with salinity. The floc size increases with salinity up to a maximum floc size, thereafter salinity has little effect. The increase in floc size results in an increase in floc settling velocity.

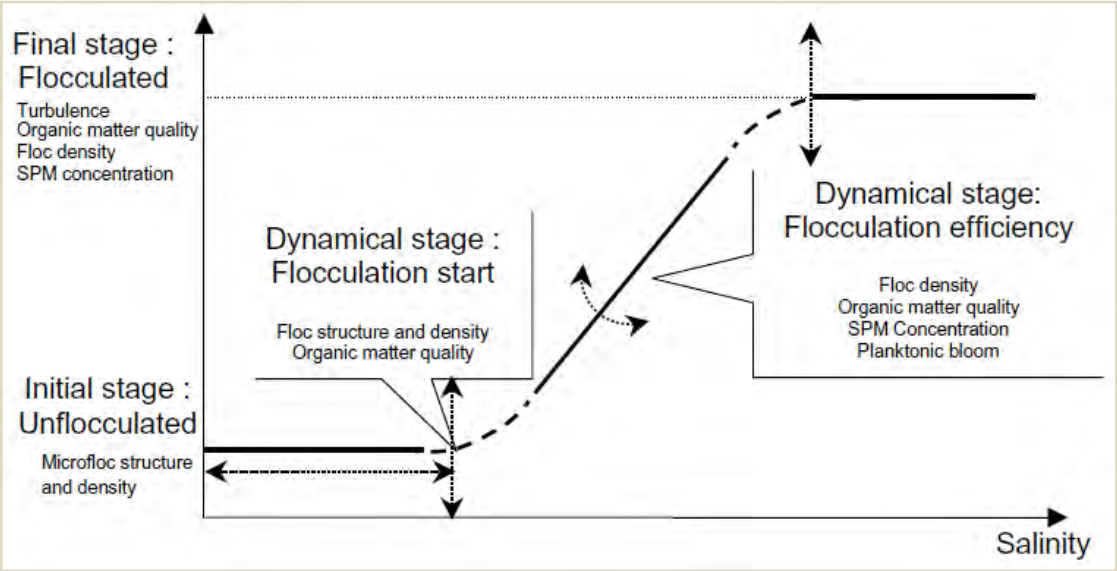

Figure 2-2: A schematic representation of the salinity influence on the process of flocculation. Source: Mikes et al., (2002)

The influence of salinity on flocculation and the threshold salinity is also dependent on the material properties of the clay and the amount of organic matter in suspension (Van Leussen, 1994). The dynamic range in which flocculation is enhanced by salinity occurs at lower salinities in illite and kaolinite clay than montmorillonite clay (Van Leussen et al., 1994).

In summary the stability of a suspension reduces with increasing ambient ionic strength. Salinity may be regarded as a driver of the flocculation process as it increases the potential for flocculation to occur.

2.4.3. Influence of pH on flocculation

Laboratory experiments by Mietta et al. (2009a) have demonstrated that pH influences the rate of flocculation and the floc size distribution. The mean floc size was observed to decrease with increasing pH (Mietta et al., 2009a; Mietta et al., 2009b). The largest flocs were observed at a pH of 2 in an agitated bowl. The enhanced growth of flocs was attributed to changes in the surface charge of particles. At low pH the surface charge of the edges became positive. This favoured the edge-face mode of flocculation and resulted in larger porous flocs forming (Mietta et al., 2009b). Changes in pH are of little concern in the estuarine context where the pH remains relatively constant between 6 and 8 (Mietta et al., 2009a). The influence of pH on floc size distribution and settling velocity in estuaries may thus be largely ignored.

2.4.4. Influence of organic matter content and biological compounds on flocculation of cohesive sediment

Organic compounds have been observed to influence the flocculation of cohesive sediment (Verney et al., 2009; Mikes & Manning, 2010; Van Leussen, 1994). Naturally occurring extra-cellular polymers such as polysaccharide chains adsorb to the surfaces of flocs and link flocs together (Van Leussen, 1994; Van Leussen, 1999). Polymers are sticky materials which are produced by microphytobenthos such as diatoms (Van Leussen, 1994; Van Leussen, 1999). The amount of organic polymers in suspension influences the number of links or bridges that can form between particles (plate 2-5). The greater the number of links, the stronger the resultant floc which forms. The amount of organic matter present influences the strength and size of flocs which form. Verney et al. (2009) found that the flocculation speed or floc growth rate was directly proportional to the total pigment concentration in the water, thus indicating that flocculation is enhanced by the presence of diatoms.

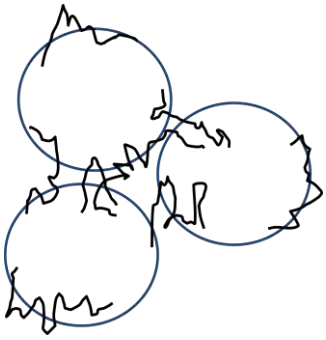

Plate 2-5: showing flocculation by the bridging of adsorbed organic polymers (adapted from Van Leussen, 1994)

The potential for polymers to bind flocs is influenced by the size of the double layer. If the double layer is large, repulsive forces prevent particles from getting close enough for a large number of links to form (Van Leussen, 1994). In solutions of high ionic strength, the energy barriers are reduced, allowing more polymers to link particles together. There is thus an interaction between the salinity and dissolved organic compounds. Plate 2-6 illustrates the influence of ionic strength on the ability of polymers to link particles.

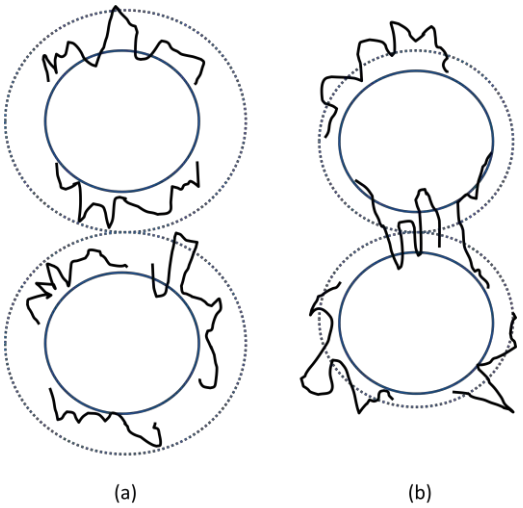

Plate 2-6(a) Polymer bridging inhibited by energy barriers at high ionic strength (b) Polymer bridging enhanced by reduced energy barriers at low ionic strength. Adapted from Van Leussen (1994).

Mietta et al. (2009a) showed that flocculation is enhanced by increasing organic matter content. In an agitated jar test where organic matter was increased from 0% to 6.52%, large largest floc sizes were observed at the highest organic matter content (figure 2-3). At low organic matter content the suspension was largely unflocculated.

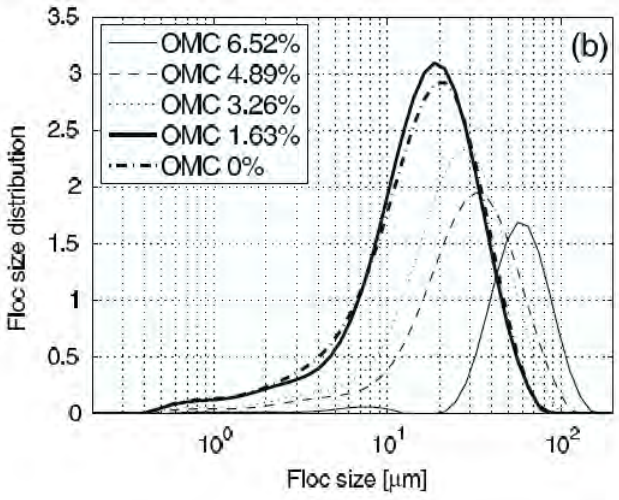

Figure 2-3: The influence of organic matter content on the floc size distribution. Source: Mietta et al. (2009a)

2.5. Kinetics of flocculation

Flocculation is characterized by two opposing processes, aggregation and fragmentation. The state of suspended particulate matter in solution is dependent on the strength of these processes. Aggregation and fragmentation rates vary according to a set of driving factors: turbulence, salinity, SPM concentration, time and material composition of SPM (Maggi, 2006; Verney et al., 2009; Mikes and Manning, 2010; Mikes et al., 2002, Van Leussen, 1994).

2.5.1. Aggregation

Aggregation is the constructive process of floc formation. Aggregation requires collisions between particles in order to occur. Thereafter it requires that particles stick together to form flocs. Aggregation occurs as a result of *effective collisions* between particles. There are three mechanisms which bring about particle collision: *turbulent shear*, *differential settling* and *Brownian motion* (Maggi, 2006; Spicer & Pratsinis, 1996; Verney et al., 2010, van Leussen, 1994, Johansen & Larsen, 1998). Each mechanism is defined by a collision frequency function, K (Van Leussen, 1994; Maggi, 2006).

Turbulent shear: $K_{SH} = \frac{(d_i+d_j)^3}{6} G$ (2.1)

Brownian motion: $K_{BM} = \frac{2kT{d_{ij}}^2}{3\mu d_i d_j}$ (2.2)

Differential Settling: $K_{DS} = \frac{\pi g}{72 \upsilon \rho_w}\left(d_i + d_j\right)^2\left(\Delta\rho_i {d_i}^2 - \Delta\rho_j {d_j}^2\right)$ (2.3)

The class of particle diameters are denoted byd_i and d_j. The shear rate is represented by G. Boltzmann's constant is represented by k. T Denotes temperature and g is the gravitational constant. The density of water and solids are ρ_w and ρ_i respectively.$\Delta\rho_i = \rho_i - \rho_w$. The combined collision diameter is d_{ij}.The dynamic and kinematic viscosities are μ and υ respectively.

Brownian motion refers to the random movement of particles in suspension. It is a mechanism sensitive to changes in temperature. An increase in temperature results in an increase in the collision frequency. The effect of Brownian motion is considered insignificant with respect to the aggregation process (Van Leussen, 1994, Maggi, 2006).

Turbulent shear induces mixing within the fluid, this leads to increased particle contact resulting in a higher rate of aggregation (Maggi, 2006; Spicer & Pratsinis, 1996, Van Leussen, 1994). Turbulent shear is characterized by a parameter G, known referred to as the *shear rate* or *root*

mean square velocity gradient. The collision frequency will be higher at higher values of G. G will be discussed in more detail later.

Differential settling describes particle collisions brought about by particles settling at different settling velocities (Van Leussen, 1994; Maggi, 2006). Faster settling flocs may collide with slower settling flocs and coalesce to form larger flocs. This mechanism is dependent on the size and effective density (Δρ) of the settling flocs.

Turbulent shear and differential settling dominate the aggregation process. Under low shear conditions differential settling is the primary mechanism of aggregation as low shear inhibits mixing (Maggi, 2006). Particle contact does not guarantee floc formation as it is necessary that particles stick together upon contact. The stability of the suspension influences the number of effective collisions that occur. Van Leussen (1994) proposed that the number of effective collisions may be expressed as:

$$N_{ij} = \alpha K(d_i d_j) n_i n_j \qquad (2.4)$$

The stability factor isα, which ranges in value from 0 to1 with 0 a stable suspension and 1 a highly unstable suspension.$K(d_i d_j)$is the collision frequency function. n_i and n_j are the number concentrations of the ith and jth particles of diameters:d_i andd_j. (Van Leussen, 1994).

The collision frequency functions are mathematical expressions which provide a conceptual understanding of particle collisions, but are impractical for use in laboratory and field studies. Laboratory and field studies generally derive empirical expressions relating floc sizes or settling velocities to the shear rate G. The use of the collision functions is limited by the ability to accurately monitor floc populations and to characterize turbulent parameters.

2.5.2. Fragmentation

Fragmentation is a destructive process whereby flocs are broken up into numerous smaller flocs. The fragmentation process is controlled by turbulent shear and particle collisions (Maggi, 2006; Spicer & Pratsinis, 1996; Verney et al., 2010, Van Leussen, 1994). Turbulent shear is composed of vortex currents. The currents induce shear stresses. Flocs are broken up when the shear stresses induced by turbulent shear exceed the internal shear strength of the floc (Maggi, 2006; Kranenburg, 1999, Van Leussen, 1994). The increase in collision frequency brought about by turbulent shear also results in flocs breakage due to violent contact between flocs at high shear rates. Breakup frequency functions have been proposed by in literature:

Shea induced breakup: $B_i^{(s)} = EG^b . L_i$ (2.5)

Collision induced breakup: $B_{i,\forall}{}^{(c)} = \sum_{j=1}^{N} k \wedge_{i,j} n_j$ (2.6)

(Maggi, 2006; Serra & Casamitjana, 1998)

E and b are empirical constants. G is the shear rate. L_i is the floc length. N is the number concentration of particles of given size. K is the probability of disaggregation by collision and $\Lambda_{i,j}$ is the collision frequency function.

The strength and size of flocs influences the rate of fragmentation. Weaker aggregates with lower shear strength are more vulnerable to breakup than more robust aggregates. Studies have shown the potential floc size to be limited by the size of the smallest energy dissipating eddies, the Kolmogorov microscale, η (Van Leussen, 1994; Spicer & Pratsinis, 1996; Manning & Dyer, 1999; Mikes et al., 2002; Verney et al., 2009). The empirical approach of investigating flocs size distribution and settling velocity in relation to the shear rate (G) and Kolmogorov microscale (η) will be discussed further on.

2.5.3. Influence of suspended particulate matter concentration on collision frequency, floc size and floc settling velocity

The frequency of collisions for all three mechanisms discussed above depends on the number of particles in suspension. The number concentrations of particles were referred to by n_i and n_j in the expression proposed by Van Leussen (1994) above. It is an intuitive conclusion that collision frequency is proportional to the concentration of suspended particulate matter (SPM). A higher concentration of flocs in suspension will increase the number of collisions that occur at a given shear rate and hence increase the frequency of aggregation (Mikes et al., 2002; Maggi, 2006; Spicer & Pratsinis, 1996). Conversely lower concentrations will yield fewer collisions. Mikes et al. (2002) summarize this by noting: “high SPM concentration enhances kinetics efficiency and floc size”.

SPM concentration is widely regarded as a controlling factor in the flocculation process (Mikes & Manning, 2010; Verney et al., 2009; Van Leussen, 1994, Maggi, 2006). Numerous studies have shown that floc size is proportional to SPM concentration (Mikes & Manning, 2010; Verney et al., 2009; Mikes et al., 2002; Spicer & Pratsinis, 1996; van Leussen, 1994; Maggi, 2006; Kumar et al., 2010). Floc size increases proportionally with concentration to an optimum concentration. Thereafter floc size is observed to decrease with increasing concentration (Maggi, 2006; Mikes & Manning, 2010). Figure 2-4 depicts a conceptual relationship between floc size and concentration. Similar relationships have been observed between SPM concentration and floc settling velocity (Verney et al, 2009; Maggi, 2006; Mikes & Manning, 2010; Van Leussen, 1994). Examples of such relationships may be viewed in figure 2-5. Floc settling velocity increases proportionally with concentration to an optimum concentration. Thereafter the high concentration hinders the settlement of flocs and decreases the settling rate. The threshold for hindered settling is widely regarded as 10g/L but may vary (Bureau of

Reclamation, 2006). SPM concentration varies over time with different hydrodynamic conditions. It is dependent on deposition and re-suspension processes and the horizontal advection of particles in flow.

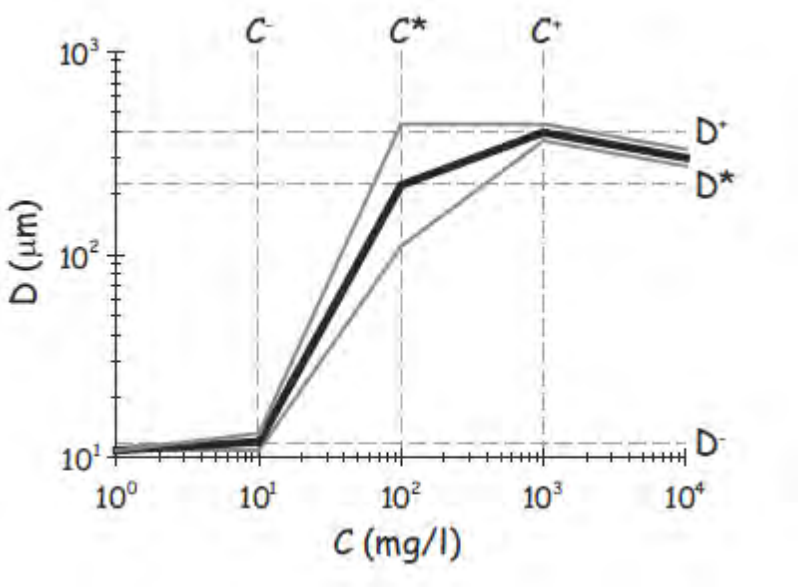

Figure 2-4: The conceptual relationship between floc size and concentration. Source: Mikes & Manning (2010)

Numerous empirical expressions have been proposed from studies investigating the influence of concentration on floc size and settling velocity. The expressions are generally expressed as a power law function such as the following proposed by Krone (1963): $w_s = KC^{\frac{4}{3}}$. In the function w_s = settling velocity, C=mass concentration and K=empirical constant

The influence of concentration needs to be considered together with turbulence. Flocculation relies on the interaction between turbulence and concentration. Considering the influence of concentration alone would suffice for investigating differential settlement in quiescent waters; however the estuarine environment is a dynamic environment where both turbulence and concentration continuously vary on tidal and seasonal scales. It is thus necessary to investigate the interaction between these two driving parameters. This will be discussed further on.

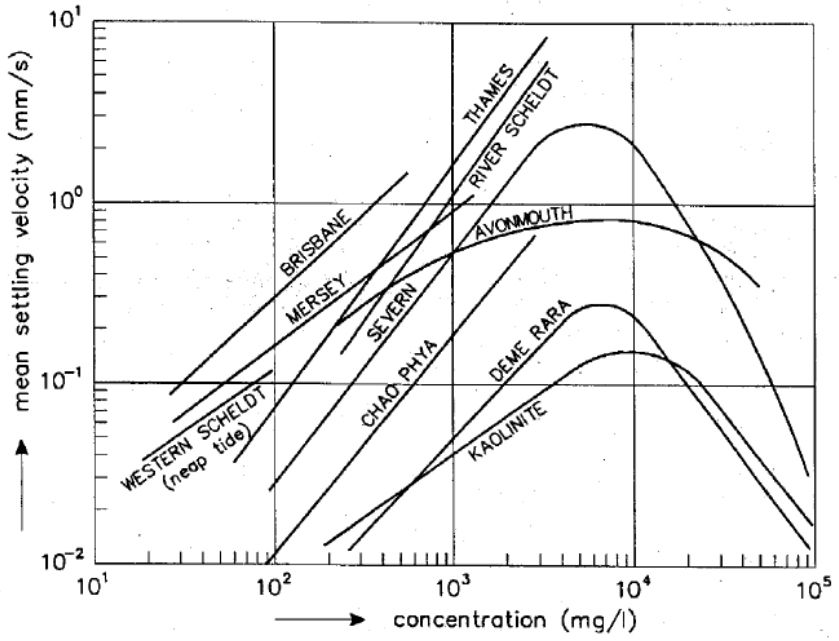

Figure 2-5: The Influence of concentration on the settling velocities of various estuaries. Van Rijn (1993) in Bureau of Reclamation (2006).

2.5.4. Parameterization of turbulent shear and its influence on flocculation

Given the focus on turbulent shear and its influence on collision frequency in all but quiescent conditions, it is necessary to parameterize turbulence in order to understand its strength as a driver of flocculation.

2.5.5. Characterization of turbulence

Turbulence is a primary driver of the flocculation process (Van Leussen, 1994; Spicer & Pratsinis, 1996; Dyer & Manning, 1999; Mikes et al., 2002; Maggi, 2006; Verney et al., 2009; Mikes & Manning, 2010; Verney et al., 2010). Turbulence may stimulate, inhibit or limit the growth of estuarine flocs. The term 'turbulence' describes a type of fluid flow characterized by irregular diffusive vortex fluctuations whereby kinetic energy is dissipated (Tennekes & Lumley, 1972). Turbulence is attributed to the unstable nature of flow at high Reynold's numbers. Vortex currents or Eddies form in the flow. The vortices are characterized by length (l), velocity (u) and time scales (t), where the length scale defines the size of the vortex and the velocity scale defines the speed at which the vortex rotates. Vortices are also defined by wave number, k.$k = \frac{2\pi}{L}$ and is expressed as the number of wavelengths per circumference of unit radius.

Large vortices will be expressed as a small wave number. Turbulence is detected and measured by velocity fluctuations around a background mean flow field. The fluctuations in velocity detected are the vortices that have formed. The turbulent kinetic energy (TKE) is determined by the mean square of the velocity fluctuations in each plane:

$$TKE = 0.5\left(\overline{u'^2} + \overline{v'^2} + \overline{w'^2}\right) \qquad (2.7)$$

Velocity fluctuations in the x, y and, z Cartesian planes are represented by *u'*, *v'* and *w'*.

The turbulent kinetic energy decays as energy is dissipated. There is a range of scales of motion that form in turbulent flow. Energy is transferred and dissipated from large eddies to progressively smaller eddies, thus forming the inertial subrange over which energy is dissipated (Tennekes & Lumley, 1972). The smallest eddies are limited in size by the viscosity of the fluid, which dissipates small eddies in the form of heat. *Kolmogorov's universal theory of the small scale structure* proposes that the smallest scales of motion are controlled by the energy dissipation rate (ε) and the kinematic viscosity of the fluid (ν) (Tennekes & Lumley, 1972). The smallest eddies are therefore defined by the *Kolmogorov* length (η), time (τ) and velocity (υ) scales. The Kolmogorov length scale defines the size of the smallest eddies and is expressed as $\eta = \left(\frac{\upsilon^3}{\epsilon}\right)^{\frac{1}{4}}$.

The Kolmogorov microscale is thus smaller at higher energy dissipation rates or more turbulent conditions. This parameter is popularly used in literature to define turbulence scales in laboratory and field studies (van Leussen, 1994;Spicer & Pratsinis, 1996; Dyer & Manning, 1999; Mikes et al., 2002;Maggi, 2006; Verney, 2006; Verney et al., 2009; Mikes & Manning, 2010; Verney et al, 2010;).

Turbulence is popularly parameterized by the *shear rate* or *root mean square velocity gradient*, G (van Leussen, 1994; Maggi, 2006; Mikes et al.; 2002; Verney et al., 2010; Spicer & Pratsinis, 1996; Milligan & Hill, 1998; Dyer, 1989). G (s^{-1}) is expressed as a function of the energy dissipation rate and kinematic viscosity: $G = \left(\frac{\varepsilon}{\upsilon}\right)^{\frac{1}{2}}$. The energy dissipation rate is ε (m^2s^{-3}) and the kinematic viscosity is υ(m^2s^{-1}).

2.5.6. Influence of turbulent structures on flocs

Turbulent shear influences the frequency and intensity of particle collisions in a floc population by causing mixing (Maggi, 2006). This may enhance the aggregation process or the fragmentation process. Shear stresses associated with turbulent structures increase the rate of floc fragmentation. Numerous studies have shown that the Kolmogorov microscale (η) controls

the maximum size of flocs that develop (Mikes et al., 2002; Verney et al., 2009; Mikes & Manning, 2010; Spicer & Pratsinis, 1996; Dyer & Manning, 1999). Floc larger than the Kolmogorov microscale are broken up due to high shear associated with the small scale eddies. Figure 2-6 of Verney et al. (2009) shows the compilation of results from multiple studies where the maximum floc size was limited by the Kolmogorov microscale. The Kolmogorov microscale is by definition inversely proportional to the energy dissipation rate or turbulence. These studies therefore show that floc size is inversely proportional to the ambient turbulence.

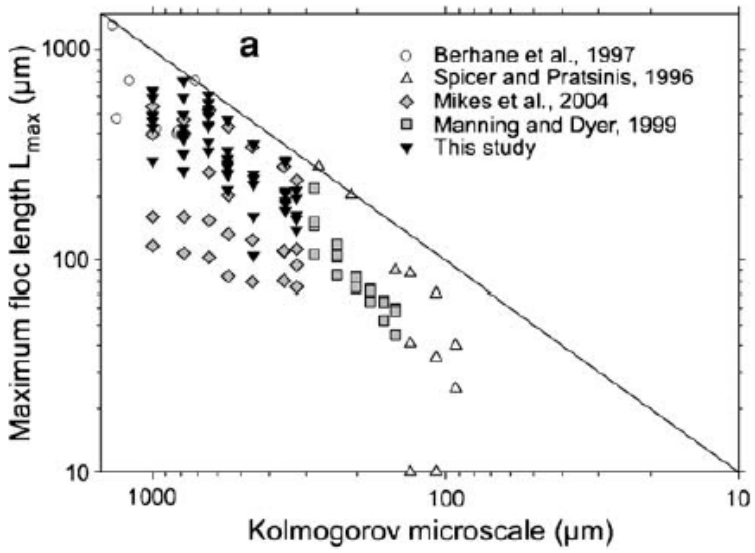

Figure 2-6: The limiting influence of the Kolmogorov microscale on maximum floc size. Source: Verney et al. (2009)

Empirical relationships between floc size and shear rate show floc sizes to increase proportionally with shear rate, peak at an optimum shear rate, and thereafter decrease when the shear rate is further increased (Maggi, 2006; Mikes & Manning, 2010; Verney et al., 2009; Spicer & Pratsinis, 1996). Figure 2-7 in Maggi (2006) shows the influence of shear rate on flocculation. The figure distinguishes two phases of the aggregation process: coagulation and flocculation. Coagulation here is considered the process by which primary particles form small aggregates or microflocs. Microflocs are robust aggregates which are highly resistant to breakup by turbulent shear. Thereafter further increases in the shear rate result in the process of flocculation where larger flocs are formed. Floc growth is limited by high shear stresses associated with high shear rates floc size is observed to decrease after an optimum floc size is achieved at a specific shear rate.

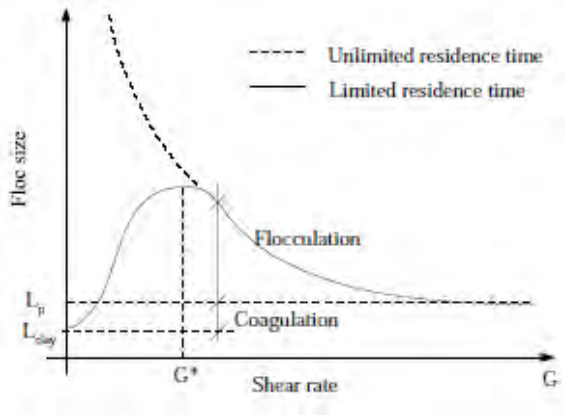

Figure 2-7: The influence of shear rate of floc size and floc growth. Source: Winterwerp (1999) in Maggi (2006)

2.5.7. Interaction between SPM concentration and turbulent shear

Three major drivers of the flocculation process have been discussed: turbulence, SPM concentration and the stability of the solution. The stability of the solution is primarily influenced by salinity, but also influenced by organic and biological content of the system. The stability plays a chemical role in the flocculation process. The other two drivers play a physical role. The process of aggregation relies on the interaction between both SPM and turbulence. Figure 2-8 of Dyer (1989) illustrates the combined influence of shear stress and concentration on the floc modal diameter. It indicates that the largest modal floc diameters are obtained at a low shear stress and high concentration. Aggregation is generally favoured at lower shear stresses where the fragmentation rate is lower (Van Leussen, 1994; Maggi, 2006; Spicer & Pratsinis, 1996). It may however be limited at low concentrations, where the probability of effective collisions is reduced. The influence of high shear stresses on fragmentation by collision may also be limited at lower concentration.

It is evident from the conceptual illustration of Dyer (1989) that any attempt to model the kinetics of flocculation should consider the influence of both turbulence and concentration.

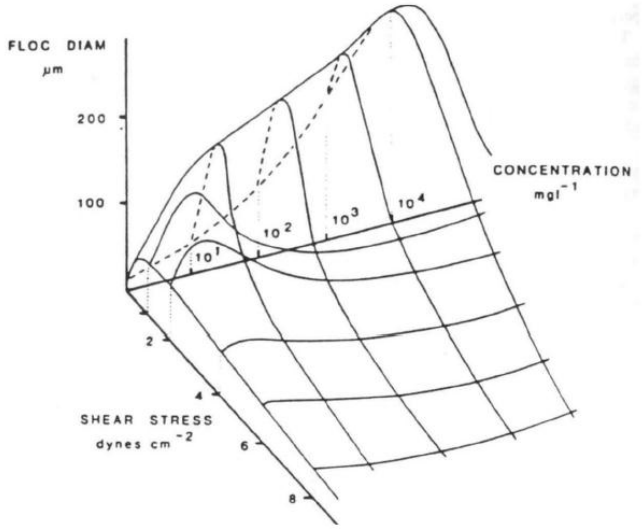

Figure 2-8: Floc diameter as a function of concentration and shear stress. Source: Dyer (1989) in Maggi (2006)

2.5.8. Time scales of flocculation

Floc residence time is regarded as an important parameter influencing the development of aggregates (Mikes & Manning, 2010; Maggi, 2006; Van Leussen, 1994). Suspended matter is required to mix and collide in order to form aggregates. The rate at which this occurs is dependent on the shear rate, concentration and stability of the suspension. The suspension may settle out before flocs are fully developed. This is an important consideration for laboratory simulations of flocculation, particularly in quiescent conditions where settlement is not hindered by bottom shear stresses. The residence time of a floc population is dependent on the height of the water column and the settling velocity of the floc population (which varies with concentration, shear rate and stability). Time scales of the process can be defined as follows (Van Leussen, 1994):

Residence time of flocs: $T_r = \frac{H}{w_s}$ (2.8)

Flocculation time: $T_F = \frac{2.3026\pi}{4\alpha\varphi(10+G)}$ (2.9)

Mixing time scale: $T_\varepsilon = \frac{H^2}{\varepsilon_z}$ (2.10)

Breakup time scale: $T_B = \frac{H^2}{\beta\varepsilon_z}$ (2.11)

The symbols present in the time scales above are elaborated as follows: where$H$=water depth; w_s=settling velocity; G=shear rate; α=stability factor (collision efficiency); φ=floc volume; ε_z=eddy diffusivity (turbulent exchange coefficient); β= breakup efficiency factor.

The derivation of flocculation and mixing time scales may be followed in Van Leussen (1994). The scales provide a useful tool to determine whether laboratory apparatus adequately simulates the estuarine time scales and whether the residence time is sufficient for flocculation to occur. The settling velocity is an important parameter that influences residence time.

2.5.9. Quasi-Steady Equilibrium

The floc size distribution and floc population of a system varies according to the rates of aggregation and fragmentation. The system reaches a quasi-steady equilibrium floc size distribution when the rate of aggregation is equivalent to the rate of fragmentation (Spicer & Pratsinis, 1996). This is dependent on the ambient shear rate of the system and the suspended sediment concentration. At low shear rates the process of aggregation is favoured while at high shear rates fragmentation is favoured (Spicer & Pratsinis, 1996; Verney et al, 2010; Maggi, 2006). Low shear rates induce gentle mixing which increases contact between particles and leads to the development of flocs. High shear rates are characterized by violent collisions between particles and high shear stresses and strains (Dyer & Manning, 1999). At very low shear rates, aggregation is dominated by differential settling and deposition occurs rapidly (Verney et al., 2010).

Differences in aggregation and fragmentation time scales (T_f and T_B) have been observed by Verney et al. (2010) in Figure 2-9. The influence of shear rate on floc size was characterized by a hysteresis loop where the fragmentation time scale was smaller than the aggregation time scale. Fragmentation reacted instantaneously to increases in shear rate while aggregation reacted slowly to decreases in shear rate.

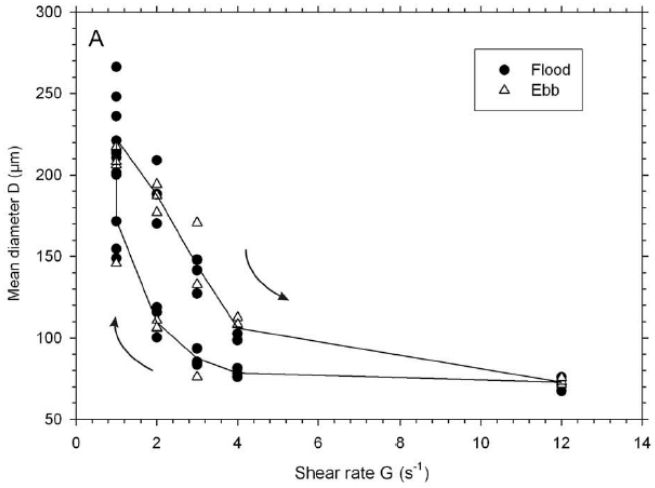

Figure 2-9: The hysteresis loop of the aggregation and fragmentation processes. Source: Verney et al. (2010)

A quasi-steady equilibrium floc size distribution or floc population is only attainable under conditions whereby the driving parameters remain constant for a sufficient period of time to allow flocculation to occur.

2.5.10. Conclusions

Flocculation is a complex dynamic process in which the driving factors interact with each other over time resulting in the formation of a population of flocs with a particular set of size, density, strength, and settling characteristics.

The influence of the driving parameters discussed above may be summarized:

- Turbulent shear enhances aggregation until associated shear stresses and violent collisions cause flocs to break up
- Aggregation is enhanced when the availability of SPM increases, due to an increased probability of collisions between particles
- Floc sizes are limited to the Kolmogorov microscale
- The floc size characteristics of a floc population vary with time, and only fully develop over the flocculation time scale

2.6. Floc settling velocity

Suspended aggregates settle due to gravitational forces. The settling velocity of solid spherical particles in a fluid is determined using Stoke's law (Van Leussen, 1994; Fennessey & Dyer, 1996; Mantovanelli & Ridd, 2006; Verney et al., 2009 ;). Stokes Law is expressed by the following formula:

$$w_s = \frac{gd^2(\rho_f - \rho_w)}{18\mu} \qquad (2.12)$$

The symbols present are: gravitational acceleration (g), particle diameter (d), dynamic viscosity (μ), particle density (ρ_f) and the density of water (ρ_w).

Stoke's law expresses floc settling rate as a function of floc diameter, density, the gravitational constant and the dynamic viscosity of the ambient fluid. This may be used to accurately define the settling rate of granular, non-cohesive sediments but its application to cohesive suspensions is limited. It relies on an accurate estimate of floc density which is difficult to determine. Floc density changes with floc size and organic content (Mikes & Manning, 2010). Larger flocs typically have lower densities than smaller flocs (Manning & Dyer, 1999; Eisma et al., 1996; Fennessey & Dyer, 1996). Expressions for estimating floc density are present in literature (Kranenburg, 1994). The method proposed by Kranenburg (1994) relies on fractal analysis of floc images. The effective floc density (ρ_f) is estimated by $\rho_f = \rho_w + (\rho_s - \rho_w)\left(\frac{D_p}{D_a}\right)^{3-n_f}$. The densities of water and sediment are ρ_w and ρ_s respectively. D_p is the diameter of primary particles and D_a is the average surface diameter of flocs. n_f represents the fractal dimension of flocs. Further detail is provided in Kranenburg (1994).

Reasonable estimates of settling velocity have been found by approximating flocs of irregular shape to spheres (Fennessey & Dyer, 1996). However difficulties in obtaining accurate estimates of floc density limit this approach.

Settling velocities are most often estimated empirically using field and laboratory techniques, typically making use of settling columns or video techniques (Van Leussen, 1994; Maggi, 2006; Larsen & Johannsen, 1998; Kumar et al., 2010; Wolanksi et al., 1992; Mantovanelli & Ridd, 2006; Van Leussen, 1996; Dyer et al., 1996; Eisma et al., 1996; Dearnaley, 1996; Manning et al, 2007). Methods of determining floc settling velocity will be discussed in chapter 3. Estimates from laboratory and field studies vary between a few mm/s for macroflocs to 10^{-3}mm/s for microflocs (Van Leussen, 1994; Manning & Dyer, 1999; Mikes & Manning, 2010). Large flocs generally have higher settling velocities than smaller flocs, and dominate the vertical settling flux (Larsen, 2002; Maggi, 2006).

The dynamic behaviour of floc populations with respect to changes in ambient conditions make high resolution estimates of floc size and settling velocity difficult. The approach is thus to obtain an average settling velocity as a function of one or more of the ambient drivers of flocculation. Van Leussen (1994) expressed floc settling velocity as a function of both concentration and shear rate: $w_s = KC_s^{\,n}\frac{1+aG}{1+bG^2}$. ($w_s$ =settling velocity; C_s=concentration; G=shear rate; K, a, b, n=empirical constants).

Estimates of floc settling velocity are important for sediment transport modelling. The settling mass flux is a product of the concentration and settling velocity (Fennessey & Dyer, 1999). This is a feature of the sediment continuity equation used to model sediment transport:

$$\frac{dC}{dt} + \frac{d(uC)}{dx} + w_s\frac{dC}{dZ} - \frac{d}{dz}\left(A_z\frac{dC}{dZ}\right) = 0 \qquad (2.13)$$

(u=mean channel velocity; w_s =settling velocity; A_z = eddy diffusivity. Source: Fugate & Friedrich, 2002).

2.7. Flocculation in an estuarine context

Flocculation in estuaries is sensitive to hydrodynamic conditions. Estuaries are characterized by varying salinity, shear rate and suspended sediment concentration. Variations in salinity occur as a result of tidal flow. Saline water is driven up into the estuary during flood tide and driven out during ebb tide. Periods of low velocity occur during the changing of tides. Shear rates are low during this time.

Shear rates and bed shear stresses vary during tidal cycles (Verney, 2006; Van Leussen, 1994; Verney et al., 2010; Verney et al, 2009). Shear rates are typically lower during slack tides (Verney et al., 2010; Verney et al., 2009). Flocculation and deposition are favoured during slack tides, particularly low slack. Turbulent shear is generated by tidal flow, waves, wind-induced waves, and boat traffic (Verney et al., 2006). During tidal flow, turbulent shear is generated in boundary layers. Most turbulent kinetic energy is generated and dissipated in the region near the bed. This is a region of high shear stress where flocs are subject to breakup (Van Leussen, 1994). This region makes up 10-20% of the water depth (Van Leussen, 1994). Regions farther from the bed are characterized by lower shear stresses. Plate 2-7 illustrates the typical velocity profile and layers of turbulent flow. The natural range of shear rates observed in situ is 1-50s^{-}

[1](Kumar et al., 2010). Values of the kolmogorov microscale observed in situ ranges from 300µm to 1000µm (Verney et al., 2009).

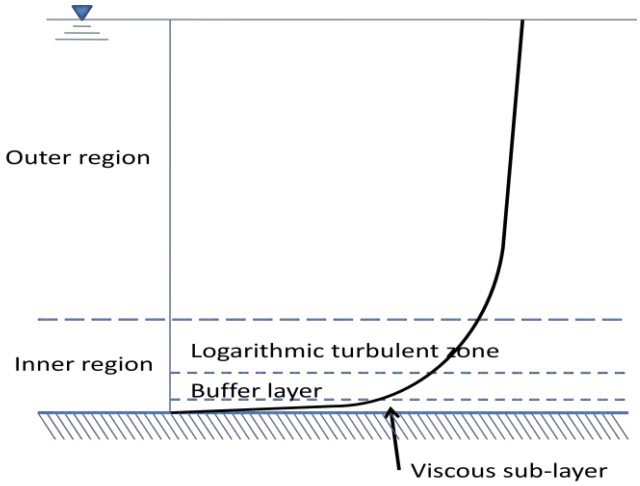

Plate 2-7: Typical velocity profile and layers of turbulent flow (adapted from Van Leussen, 1994)

SPM concentration varies on tidal and seasonal scales. Suspended cohesive sediment is the result of soil erosion in river catchments. Marine sediment also enters and leaves estuaries. This is influenced by littoral processes and wave action. Sediment yield in catchments varies seasonally. During periods of high rainfall, higher sediment runoff results in more turbid fluvial systems the concentration of suspended sediment entering an estuary may vary significantly between seasons. This is particularly the case for rivers with highly variable runoff (e.g. Grenfell & Ellery, 2009). Concentrations vary over tidal cycles due to deposition, erosion, and dilution in the marine zones of estuaries due to mixing with intruding saline water.

Suspended sediment concentrations of estuaries in literature vary considerably between estuaries. Concentrations may vary between a few mg/L to 10g/L in highly turbid estuaries (Wolanski et al., 1993; Grenfell & Ellery, 2009). The composition of SPM may also vary seasonally (Verney et al., 2009).

Erosion and Deposition

Flocs are eroded or deposited depending on the hydrodynamic conditions. Flocs formed during the process of aggregation settle towards the bed. Flocs are deposited on the bed when the bed shear stress is less than the *critical shear stress for deposition*, τ_d (Bureau of Reclamation, 1996). If the shear stresses near the bed are too high, flocs are broken up and re-circulated in the water column. In flume experiments Krone (1962, in Bureau of Reclamation, 2006) found τ_d to range between 0.06 and 0.078 N/m^2.

Erosion occurs when the shear stress at the bed exceeds the critical shear stress for erosion, τ_c (Bureau of Reclamation, 2006; Verney, 2006). The critical shear stress is the resistance of the bed to erosion, it is a function of the bed consolidation, proportion of silt, surface roughness, and biological activity in the benthic layer (Verney, 2006).

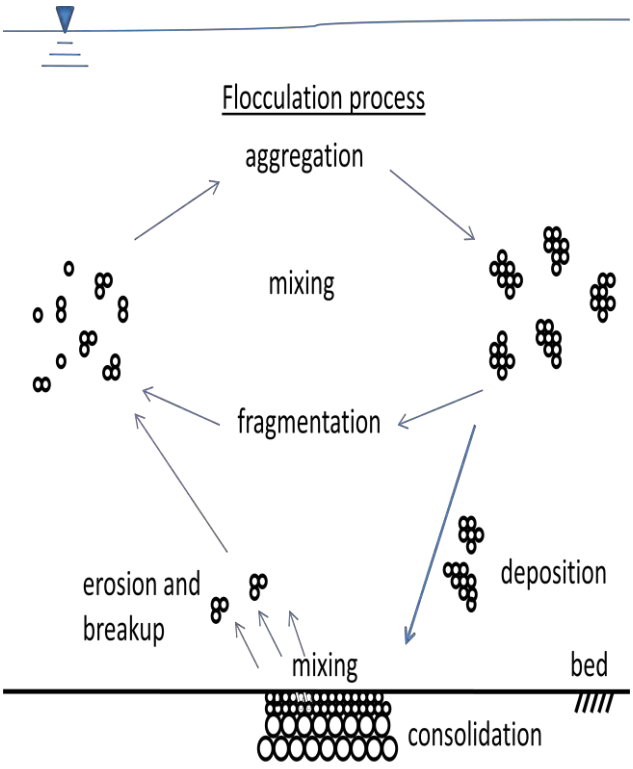

Plate 2-8: The flocculation process in the water column with erosion and deposition processes. (Adapted from Maggi, 2006)

Continuous erosion and deposition cycles occur in the estuarine turbidity maximum, where the highest suspended sediment concentrations are observed (Van Leussen, 1994). Many estuaries are characterized by erosion-deposition cycles (Fugate & Friedrichs, 2002; Wolanski & Gibbs, 1995). Plate 2-8illustrates the flocculation process in the water column.

Mixing and Stratification

It is common for stratification to occur in estuaries; whereby two distinct layers form in the water column, one of freshwater and another of saline water. Stratification inhibits mixing between layers, thus influencing flocculation. Other estuaries are well mixed with no stratification .In most estuaries there is a region of high turbidity which occurs due to mixing, this is known as the *estuarine turbidity maximum*.

2.8. Summary

Flocculation is the dynamic process which controls the behaviour of suspended cohesive sediment. The process is characterized by the formation and breakup of sediment flocs. Flocculation influences the transport of cohesive sediment. It is stimulated and controlled by a set of drivers. There are three primary drivers of the process – (1) turbulence, a physical driver; (2) SPM concentration, a physical and statistical driver; and (3) salinity, a chemical driver. There are numerous other drivers of lesser importance which influence flocculation such as organic matter content, clay mineral content, pH and temperature. The primary drivers have been extensively studied while fewer studies have focussed on the influence of the secondary drivers. Studies on flocculation have been conducted both in situ and in laboratories. Quantitative results from such studies are mostly empirical and express the settling velocity or floc size as functions of one or more of the primary drivers. The application of quantitative empirical results is limited to particular estuaries or silt types. It is thus necessary to formulate a controlled method to study the flocculation characteristics of a particular estuary or silt type. Such a method should minimize disruption to flocs given their fragile nature. Qualitative observations in literature of the influence of each driver on flocculation provide an indication of the likely outcome of future studies on flocculation.

2.9. Study Area

2.9.1. Introduction

The study focuses on sediments from the St Lucia and Mfolozi estuaries situated on the east coast of South Africa. The estuaries are situated approximately 300km north of the port city of Durban in the province of Kwa-Zulu Natal. The region has a subtropical climate with a mean annual precipitation of 890mm/annum (Lawrie & Stretch, 2011). The Mfolozi catchment is hilly with a large flat floodplain at the lower catchment. The St Lucia catchment is smaller with a large estuarine lake in a flat basin surrounded by low hills. A simple map of the estuaries is presented in plate 2-9 below.

The St Lucia estuary is the largest estuarine system in Southern Africa and an area of ecological importance (Whitfield & Taylor, 2009; Lawrie & Stretch & Stretch, 2011).The St Lucia and Mfolozi estuaries are the site of the iSimangaliso Wetland Park (formerly Greater St Lucia Wetland Park). It is an important conservation area. It is a World Heritage site and Ramsar Wetland of international importance (Lawrie & Stretch, 2011; Whitfield & Taylor, 2009). The park is an important tourist destination and provides a major source of income to the region (Whitfield & Taylor, 2009). Forestry and sugar cane farming are important industries in the region. The region has a poor rural population.

Plate 2-9: Satellite images showing the St Lucia and Mfolozi estuaries.

Anthropogenic activities over the past half century have threatened the ecology of the St Lucia estuary. The most significant impacts are associated with freshwater deprivation resulting from the separation of the Mfolozi river from a previously combined St Lucia–Mfolozi estuary in 1952 (Whitfield & Taylor; Lawrie & Stretch & Stretch, 2011). The study focuses on investigating the flocculation of silt from the Mfolozi estuary and to a lesser extent flocculation in areas of the St Lucia estuary. This section briefly describes the characteristics of the St Lucia and Mfolozi estuaries and provides historical information further motivating this study.

2.9.2. St Lucia Estuary

It St Lucia estuary is a temporary open-closed estuary consisting of a large shallow water lake linked to the ocean by a narrow winding channel aptly known as the *St Lucia Narrows*. Freshwater is supplied to the lake by five tributaries, direct precipitation and groundwater seepage from its eastern shores (Lawrie & Stretch, 2011). The lake has a surface area of 328km^2 and average water depth of 1m. The five tributaries to the lake are the Mkhuze, Mzinene, Hluhluwe, Nyalazi and Mphate rivers. A map of the St Lucia estuary is provided in plate 2-10. The shallow nature of the lake and large surface area make it vulnerable to water loss by evaporation. The mean annual precipitation and mean annual evaporation are 890mm and 1470mm respectively, as summarized in table 2-2 below.

Table 2-2: Summary of catchment data of St Lucia system, adapted from (Lawrie & Stretch, 2011).

Item and description	**Value**
Average lake surface area	328km^2
Average lake volume	322Mm^3
Mean annual Precipitation	890mm
Mean annual Evaporation	1470mm
Total Catchment area	7575km^2
Mean Annual Runoff	295Mm^3

The estuary is closed 88% of the time and open 12% of the time (Stretch & Lawrie, 2008). The mouth of the estuary has been closed since 2002. It was briefly opened by the ocean in 2007 due to a tropical cyclone (Whitfield & Taylor, 2009).Salinities in the estuary are typically high,

particularly in the northern regions of the lake where hyposaline conditions have frequently occurred during droughts. The volume of the lake has been significantly reduced during recent droughts. In December 2003 only 25% of the lake area was covered in water as a result of a drought (Whitfield & Taylor, 2009). Recent studies have shown that there is insufficient freshwater to supply the lake system (Stretch & Lawrie, 2008). The Mfolozi previously supplied the lake with 40% of its freshwater requirements prior to separation in 1952.

The estuary is dominated by predominantly muddy substrata (Cyrus & Blaber, 1988). The bed composition does vary spatially, with some regions having sandy substrata. Fine sediment is frequently re-suspended in the lake by wind induced waves (Cyrus and Blaber, 1988). Turbidities in excess of 1000ntu have been recorded in the Southern lake during strong North-Easterly and South Westerly gales. The St Lucia estuary is a microtidal estuary. The mean turbidity of the St Lucia narrows 84.2ntu (Cyrus and Blaber, 1988).

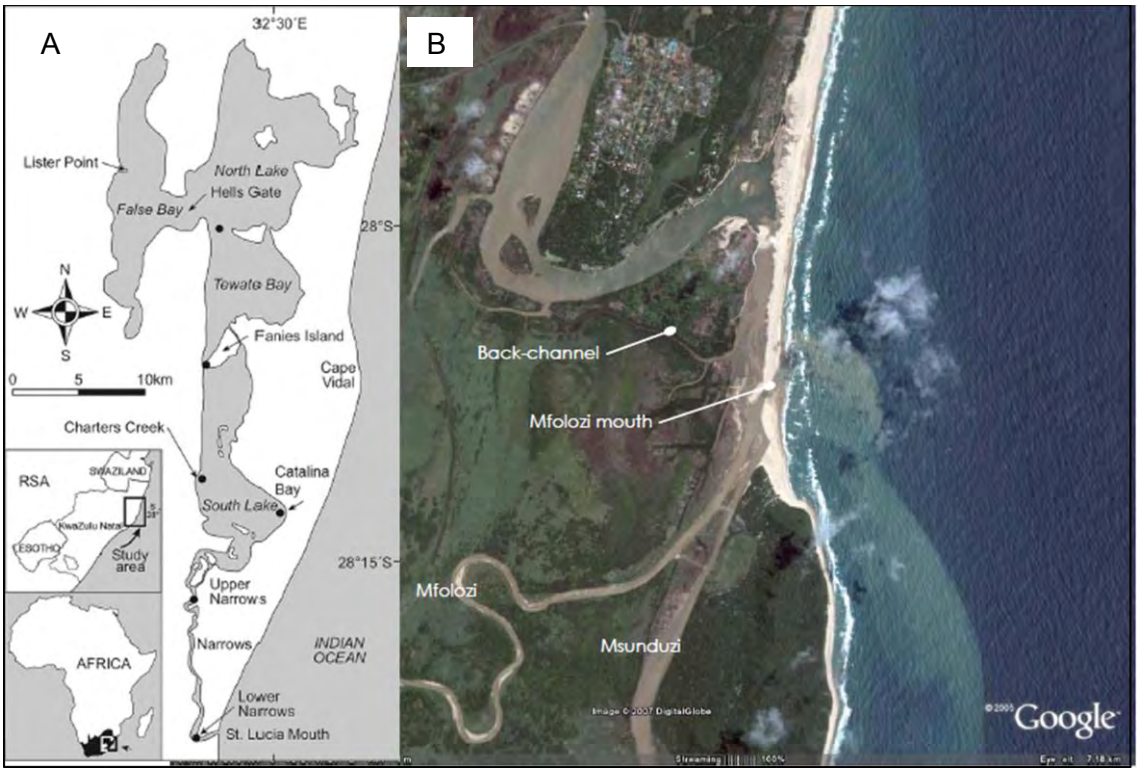

Plate 2-10: A: Simple map of the St Lucia system (source: Cyrus et al., 2010). B: Satellite map of the Mfolozi estuary (source: Stretch & Lawrie, 2008).

2.9.3. Mfolozi Estuary

The Mfolozi estuary is a temporary open-closed microtidal estuary situated south of the St Lucia estuary as displayed in figure 2-10 (Stretch & Lawrie, 2008). The estuary is mouth of both the Mfolozi and Msunduzi rivers. Catchment information is shown in the table 2-3 below.

Table 2-3: Mfolozi catchment information. (Adapted from Lawrie & Stretch, 2011)

Item and description	Value
Mean annual Precipitation	890mm
Mean annual Evaporation	1470mm
Mfolozi catchment area	10085km^2
Msunduzi catchment area	559km^2
Mfolozi mean annual runoff	729Mm^3
Msunduzi mean annual runoff	89km^2

The mean water depth of the estuary was estimated at 1.5m by Lindsay et al., (1996) with a tidal range of 1.1m at the mouth and 0.3-0.64m at the mid estuary depending on the prevailing wind conditions. Sediment transport in the estuary is ebb dominated during conditions of high river discharge, with the highest bed shear stresses of 0.8N/m^2 being recorded during ebb tide at current velocities of 0.8m/s (Lindsay et al., 1996). This is however not the case during low river discharge when the system may close due to flood dominance in the sediment transport. Resuspension events typically occur during ebb tide. The estuarine turbidity maximum is situated approximately 2.5-3.5km from the mouth of the estuary and the position varies with river flow. The Mfolozi estuary is significantly more turbid than the St Lucia estuary. An average monthly sediment load of 1400mg/L was recorded in the Mfolozi between 1973 and 1976. Suspended sediment concentrations vary seasonally and frequently exceed 2g/L during summer floods (Grenfell & Ellery, 2009). Suspended sediment concentrations as high as 6g/L have been recorded at the mouth (Lindsay et al., 1996). The bed of the lower part of the estuary is dominated by fine silt with an average particle size of 0.0052mm (Grenfell & Ellery, 2009). Suspended sediment samples at the mouth were taken by Lindsay et al., (1996). Particle size measurements indicated the suspended load is dominated by silt-sized particles.

2.9.4. Historical developments

The St Lucia and Mfolozi systems were historically combined. Prior to catchment development the combined estuary had a significantly larger tidal prism (Whitfield & Taylor, 2009). During the 20th century the sediment loads into the system increased. High sediment loads were the result of historically poor catchment management (Whitfield & Taylor, 2009). The Mfolozi flood plain

previously contained a large swamp which acted as a sediment filter. The swamp was drained and sugar cane plantations were developed in the early 20th century. Levees were constructed to protect farmland from flooding. The draining of the swamps resulted in higher sediment loads reaching the mouth of the estuary due to the channeling of the river. Periods of drought in the 1950's resulted in the closure of the combined St Lucia-Mfolozi mouth (Whitfield & Taylor, 2009). Fears of back flooding onto farmland and siltation in the St Lucia estuary resulted in the management decision to create a separate Mfolozi river mouth in 1952. The separate mouth configuration has been maintained ever since. There are concerns about the influence of high sediment loads on the estuarine ecosystem.

Lake St Lucia was deprived of a significant proportion of its freshwater supply when the Mfolozi River was diverted (Lawrie & Stretch, 2011). The estuary became predominantly closed. Water levels in the lake were maintained by artificially opening the St Lucia mouth. This significantly increased the salinity of the lake. This practice was recently discontinued. It resulted in the lake becoming saline.

Recent freshwater supply problems in the St Lucia estuary have led to an interest in re-establishing the historical combined mouth configuration. This would result in the combined estuary remaining open 70% of the time, maintaining lake levels and diluting lake salinities (Lawrie &Stretch, 2011). Fears of siltation in the St Lucia system due to high Mfolozi sediment loading have prevented efforts to restore the combined configuration. The harmful effects of high turbidities on the ecosystem have also discouraged park management from re-establishing the combined system.

High sediment loads reduce light penetration into the water column, thus reducing the macrophyte population, to an extent favouring phytoplankton dominance in the ecosystem. High sediment loads inhibit the activity of fish which are visual hunters, favouring turbid hunters which use filter feeding mechanisms. Fine sediment may clog the gills of fish and other small organisms (Berry et al., 2003). High volumes of deposited fine sediment may bury eggs and reduce the probability of hatching (Berry et al., 2003). This may lead to the degradation of the estuary as a breeding area.

2.9.5. Relevance to study

There is a need to determine the feasibility of re-establishing the combined St Lucia – Mfolozi link. This needs to address the concerns over high Mfolozi sediment loads. It is therefore necessary to investigate the transport and fate of Mfolozi sediment in the St Lucia-Mfolozi estuarine complex. This requires an understanding of the flocculation and settling behaviour of cohesive Mfolozi sediment in response to changing hydrodynamic conditions (tidal flow, SPM variation, salinity variation). The study therefore seeks to understand the flocculation and settling characteristics of Mfolozi sediment as a basis for sediment transport modelling

The study is also applicable to understanding the influence of high energy events on the settling behaviour of sediment in Lake St Lucia, particularly Charters Creek. By investigating the equilibrium floc size and settling velocity of lake sediment in response to turbulence, it may be possible to predict the mass settling flux of the lake after high energy events. This has applications in bio-physical models where the period of time during which the lake remains turbid influences the productivity of the ecosystem. The study therefore investigates the flocculation and settling behaviour of lake sediment (from Charters Creek) for possible application in lake models.

CHAPTER 3

METHODOLOGY

The chapter on methodology describes in detail the approach to the laboratory investigation. A short discussion is presented on available laboratory techniques employed to investigate flocculation and settlement of cohesive sediment. The key advantages and disadvantages of each are discussed. Thereafter a detailed description of the chosen laboratory approach is presented. The description covers the apparatus used, sampling methods, calibrations and the processing of laboratory results.

3.1. Review of laboratory techniques

3.1.1. Introduction

Flocculation and sedimentation processes have been investigated in the field by various in situ tests and in the laboratory by means of carefully designed apparatus to produce a controlled environment. In situ testing is the most popular approach observed in literature. The application of a well-designed field technique will provide the most accurate account of the behaviour of estuarine sediments. The estuarine environment is a dynamic environment where conditions vary temporally and spatially. The shear rate, suspended sediment concentration (SSC) and salinity vary with tidal cycles, river discharge and wind. The SPM concentration, mineral, biological and organic compositions vary seasonally with the regional climate. There is no control over the conditions that occur during a field test. A wide spectrum of conditions may only be observed over a seasonal time scale. It may thus take a significant amount of time to obtain the full spectrum of desired conditions.

Laboratory techniques attempt to simulate the estuarine flocculation process. Fewer laboratory based studies have been observed in literature than field based studies. The main limitation of laboratory studies is the difficulty in simulating natural estuarine processes (Van Leussen, 1994). Despite this, laboratory studies allow greater control over the range of conditions that

may occur. Particular parameters may be isolated and varied while other parameters may be kept constant. It is important to design a laboratory experiment in order to give an accurate reflection of in situ settling rates and floc size distributions.

3.1.2. Short description of laboratory techniques

Laboratory techniques attempt to simulate natural estuarine flocculation processes in a controlled environment where particular parameters may be isolated and observed in a manner not possible in the field. The different techniques reviewed vary in size and complexity. The type of technique employed is dependent on the aspects of sediment behaviour being studied. There are several parameters that can be used to indicate sediment behaviour: particle size distribution, particle settling velocity, particle structure, turbidity and suspended sediment concentration (in settling tests). The indicators are used to study the behaviour of interest and should suit the technique employed.

Three commonly used laboratory techniques have been considered for use in the planned study: the jar test technique, laboratory settling columns and annular flumes. This section gives a brief description of each of these techniques.

3.1.2.1. Jar test technique

The jar test technique is perhaps the most commonly used laboratory technique for investigating flocculation (Alldredge et al., 1994; Spicer & Pratsinis 1996; Spicer et al., 1996; Wolanski & Gibbs, 1995; Serra et al, 2007; Mikes et al., 2004; Verney, 2006; Verney et al., 2009; Mietta et al., 2009a; Mietta et al., 2009b; Mikes & Manning, 2010; Verney et al., 2010; Kumar et al., 2010). The technique is popularly used in the field of wastewater engineering but has also been applied to studies of cohesive sediment flocculation. The classic jar test approach involves an agitated beaker filled with a suspension. The agitator is used to mix the suspension. The shear rate can be varied by changing the speed of the agitator. The test is used in waste water treatment to measure the influence of coagulants on the settlement of suspensions. This approach has been adapted study to cohesive sediment flocculation (Wolanski & Gibbs, 1995; Mikes et al., 2004; Verney, 2006; Verney et al., 2009; Mietta et al., 2009a; Mietta et al., 2009b; Mikes & Manning, 2010; Verney et al., 2010; Kumar et al., 2010). Plate 3-1A below shows the typical jar test apparatus. Plate 3-1B shows the jar test apparatus used by Verney et al., (2009).

The jar test is typically performed on small volumes of 1-3L of solutions (Spicer et al., 1996; Mikes et al., 2002; Serra et al., 2007; Mietta et al., 2009a; Mietta et al., 2009b; Kumar et al., 2010). The jar test technique allows easy variation of the three primary driving parameters of

flocculation. Other parameters may also be varied. Solutions of different salinity and suspended sediment concentration may be prepared for use in the jar test. The turbulence is varied using the agitator. The nature of the turbulence developed in the jar is sensitive to the rate of agitation and the type of mixer (Spicer et al., 1996). Methods of mixing include radial flow impellors, axial flow impellors, rectangular paddles and oscillating grids (Spicer et al., 1996; Serra et al., 2007).

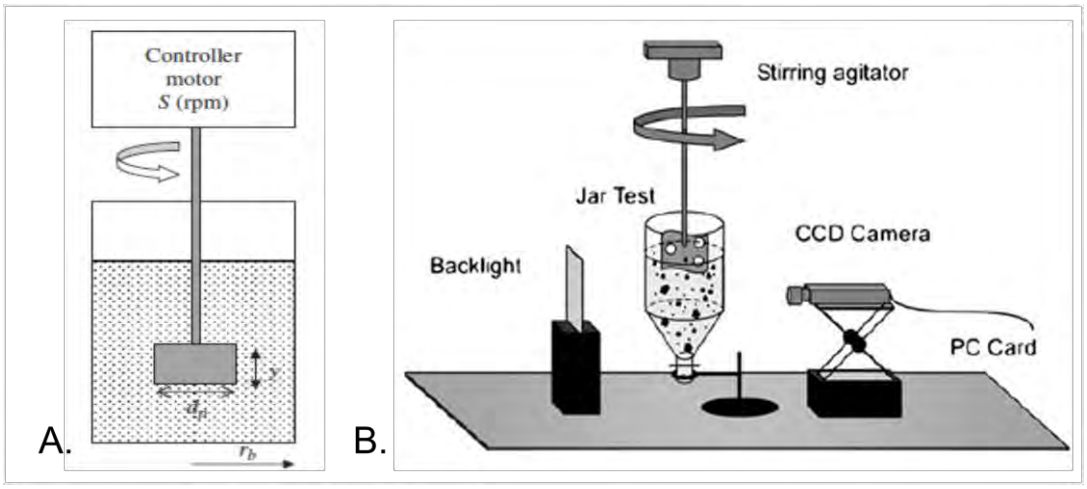

Plate 3-1: A: The typical jar test apparatus used in flocculation studies (Serra et al., 2007). B: The jar test and video-in-lab system of Verney et al., (2009).

The turbulent field generated by paddle mixers is generally not homogeneous (Kumar et al., 2010; Spicer et al., 1996; Nagata, 1975; Bouyer et al., 2005). Paddle mixers are characterized by a high shear zone around the impellor with decreasing shear away from the impellor. The flow pattern involves particle circulation around the jar. Spicer et al. (1996) found that axial flow impellors had shorter circulation times than radial flow impellors, resulting in higher exposure to the high shear zone around the impellor and thus greater susceptibility to breakup. The type of impellor used influences the growth and breakup of flocs in the jar. While using a paddle mixer, Bouyer et al., (2005) found that the mean flow induced by the impellor is weakly dissipative and that most of the organized motion within the jar is transferred to turbulent motion.

Mietta et al. (2009b) found that the jar test is unsuitable for use at shear rates below $35s^{-1}$ where settlement was observed to occur, thus reducing floc residence time. It was found that $35s^{-1}$ was the minimum shear rate at which clay particles were eroded from the bottom of the jar. Results from other literature and from preliminary lab tests disagree with this observation and indicate that settlement does not occur at the low shear rates suggested by Mietta et al., (2009b). Results to be displayed later indicate that settlement occurs in the jar at shear rates less than $10s^{-1}$.

3.1.2.2. Laboratory settling columns

Laboratory settling columns are designed to investigate floc settling velocities (Wolanksi et al., 1992; Van Leussen, 1994; Larsen & Johansen, 1998; Maggi, 2006). Settling columns in literature are typically 1-4m high cylindrical plexiglass flumes 0.1-0.3m in diameter. Columns are designed with re-circulating systems in order to maintain uniform suspended sediment concentrations. Turbulence is generated inside the column by oscillating metal grids. Certain studies employed side withdrawal pipettes to calculate floc settling velocity by measuring the concentration of regularly extracted samples along the length of the column. Other studies employed particle tracking velocimetry (PTV) systems to monitor floc size and settling velocity (Maggi, 2006).

The large size of settling columns make them vulnerable to temperature variations over their height. This potential problem may be prevented by maintaining a constant laboratory temperature and thermally insulating the settling column (Van Leussen, 1994; Maggi, 2006). Van Leussen (1994) recommended a minimum column height of 1.2m to ensure the flocculation time scale exceeds the settling time scale. Settling columns typically require large volumes of test solution. It can be difficult and expensive to sample, move and store such volumes. The duration of the tests is significantly longer than that of jar tests. This makes the settling column less suited to high repetition testing and the variation of parameters over wide ranges.

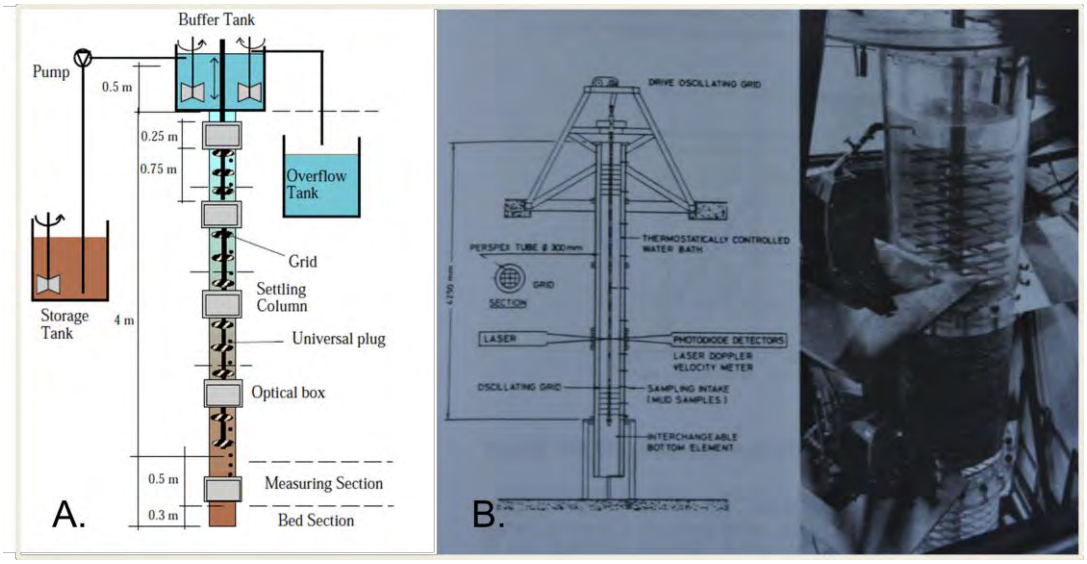

Plate 3-2: A: The settling column of Maggi (2006). B: The settling column of Van Leussen (1994)

3.1.2.3. Annular laboratory flumes

Annular flumes are a popular method of investigating the response of floc populations to changes in shear stress and also for measuring erosion and deposition thresholds (Manning et al., 2007; Graham & Manning, 2007; Ockendon, 1993; Milburn & Krishnappen, 2001; Krishnappen et al., 2003; Stone et al., 2008). The technique uses an annular flume with a floating annular ring with equally spaced paddles. The floating ring is rotated by arms extending from a motor in the centre of the flume. Flumes are typically 4-6m in diameter with channel width of 0.3m and depth 0.3m. Manning et al. (2007) employed the use of a mini-flume of diameter 0.3m and height 0.3m. The rotating annular ring and paddles generate a shear stress in the flume. The shear stress induced is proportional to the speed of rotation. The settling velocity of sediment in the flume is measured by the mass deposition rate. This is determined by withdrawal of samples through pipettes on the wall of the flume at regular time intervals or by turbidity sensors of the sidewalls of the flume. The method may be used to measure the settling velocity of suspended sediment as a function of shear stress. Floc images may be obtained either directly or by special pipette sampling techniques using a camera system once the motor is stopped.

The flume requires calibration in order to determine the shear stresses. Shear stresses may be approximated by knowing the velocity profile at a particular speed of rotation. The floating annular ring restricts the available calibration instruments to laser Doppler anemometers (Stone et al., 2008) and electromagnetic current meters (Manning et al., 2007). The flumes require large sample volumes to operate and are thus not suited to performing multiple tests where concentrations and salinities are varied over a large range. The method is better suited to monitoring the influence of varying shear stress on settling velocity.

3.1.2.4. Floc imaging techniques

Floc size distributions are commonly analysed using digital imaging techniques. Digital imaging techniques involve the use of a digital camera, optics and a lighting system to observe flocs. This may be done using either a still camera or a video camera. Floc images may be captured in the following ways:

1) Placing the imaging system at a chamber or narrow section of apparatus in which populations of flocs may be isolated and observed (Van Leussen, 1994; Maggi, 2006; Dyer & Manning, 1999). Isolation is necessary at high sediment concentrations.

2) Sampling flocs using a modified pipette (Gibbs & Konwar, 1982) and allowing them to settle in a still settling column. The floc imaging system is used to capture images of the flocs as they settle (Kumar et al., 2010; Manning et al., 2007; Manning & Graham, 2001).

3) Direct observation by the floc imaging system where the scale of the test is small enough to allow the camera to directly observe the flocs in suspension. This method has been used with the jar test (Mikes et al., 2002; Mikes et al., 2004; Verney, 2006; Verney et al, 2009; Mikes & Manning, 2010, Verney et al, 2010).

   Digital floc imaging systems typically require high resolution CCD or CMOS cameras with a macro lens to observe flocs. The quality of the image obtained depends on the resolving power of the camera, the focal length of the lens, and a backlighting or strobe light system to sufficiently illuminate the suspended particles or the background. Detailed high resolution images of flocs are possible at close range but generally at the expense of depth of field. In order to obtain a good quality high resolution image, the camera needs to be focused on a very small region of the solution. The observation of a smaller sample volume of flocs will result in a statistically poorer reflection of the population floc size distribution. The direct observation approach mentioned above is limited by the suspended sediment concentration of the fluid. At high concentrations (C>1000mg/L) floc overlap occurs and it becomes difficult for image analysis software to distinguish individual flocs (Mikes, 2011, personal communication). Mixers or agitators need to be stopped while images are captured. The camera shutter speed limits the ability of the camera to obtain clear images of moving particles at high magnification (Mikes et al., 2011, personal communication). Agitation needs to be stopped during pipette sampling to prevent floc breakage. Clearer, better quality images may be obtained using approaches 1 and 2 above. The direct observation approach (3) is the least disruptive to the floc population.

   Laser diffraction techniques:

   Floc size distributions have also been obtained using laser diffraction techniques (Aggrawal & Pottsmith, 2000; Mietta et al., 2009a; Mietta et al., 2009b). Such techniques require prior calibration in order to measure floc sizes. Flocs are classified into numerous discrete size classes (Agrawal & Pottsmith, 2000). This technique can provide superior resolution estimates of populations of fine particles. Laser diffraction techniques are not able to provide information on the structure of flocs.

   Microscope observation:

   Images of flocs may be obtained under a microscope. Ordinary microscope slides and cover strips are unsuitable because they disturb flocs during sampling. Preliminary investigations have indicated that clear images of flocs may be obtained at 40x magnification (see plate 3-3A). Microscope analysis requires the use of special slides with sidewalls. Preliminary investigations show that it is effective to fill the chamber with water and then place the modified pipette over the chamber, allowing the flocs to settle from the pipette through the water and

then onto the slide. The pipette needs to be moved around the chamber to prevent flocs from settling on top of each other. The extent to which this method disturbs flocs is uncertain. Microscopes are able to provide superior resolution images to any digital floc imaging system employing a still or video camera.

Plate 3-3: A: Microscope image of flocs obtained at 40x magnification. The solid bar represents 500µm. B: Image illustrating the pipette sampling technique with microscope slide. C: Inverted microscope

3.1.2.5. Methods to analyze floc settling velocities

Three approaches to determining floc settling velocity have been identified in literature for application in this study:

1) Floc settling velocity is calculated by measuring the mass concentration flux over the height of a water column over a length of time (Wolanski et al., 1992; Ockendon, 1993; Van Leussen, 1994; Larsen & Johansen, 1998; Stone et al., 2008;). The change in mass concentration is measured directly by the gravimetric analysis of samples withdrawn from pipettes or indirectly using pre-calibrated optical backscatter sensors. This gives a mass settling flux ($\frac{dM}{dt}$) which may be converted to a settling velocity by $\frac{dM}{dt} = w_s \frac{dC}{dZ}$. In field experiments using settling columns it is customary to use the settling velocity at which 50% of the mass is settled (w_{50}) as the floc settling velocity (Mantovanelli & Ridd, 2006).

2) Settling velocity can be directly measured by video analysis of settling flocs using a PTV system (Maggi, 2006; Manning et al., 2007; Mietta et al., 2009a; Kumar et al., 2010). The settling velocity is calculated by measuring the distance travelled by flocs between consecutive frames separated by a discrete time interval. This technique requires the identification and tracking of individual flocs. This can be done manually or using PTV software. Plate 3-4 illustrates this technique.

3) Settling velocity can be calculated indirectly with Stokes law by using floc diameters and an effective floc density (Verney et al., 2009). Floc diameters are obtained from image analysis of flocs. The effective density of flocs is calculated by the method of Kranenburg (1994) which relies on image analysis. The average floc size and effective density of the flocs are inserted into Stokes law to find a settling velocity.

The three methods are each suited to specific laboratory techniques mentioned above. The method of obtaining settling velocity using the mass concentration flux is suitable for settling columns and annular flumes but unsuitable for the jar test technique where flocs are constantly maintained in suspension, preventing settlement. The reliability of approach 3 is uncertain as it is an indirect method and sensitive to changes in the fractal dimension of flocs (Verney et al., 2009). Approach 2 is preferred as it obtains direct measurements of floc settling velocity and also provides information of the floc size distribution. Its limitation is its computationally demanding nature. It requires the development of sophisticated particle tracking velocimetry scripts and frame grabbing techniques for video output. Manually tracking settling particles is also time consuming.

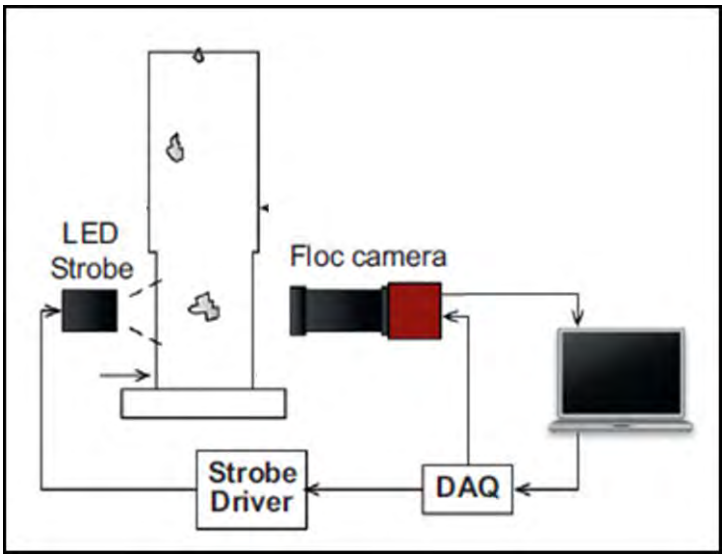

Plate 3-4: The concept of settling velocity observation using a PTV system and a still settling column. Source: Kumar et al., (2010)

3.1.2.6. The most feasible approach

The planned study required a feasible laboratory technique to measure floc settling velocities and size while varying suspended sediment concentration, turbulence, and salinity. It is necessary to perform many tests. The techniques discussed above were compared from technical and economic perspectives. The following criteria were kept in mind when comparing the techniques:

- The technical suitability of the technique to investigating the parameters and behaviour outlined in the aim of the study.
- The extent to which the technique has been used in previous studies.
- The financial and time costs that the development of the technique will require.

- The simplicity of the technique

Annular flumes, settling columns and the jar test are all suitable techniques for performing the study. All the techniques discussed have been used in previous studies on flocculation. Each may be used to obtain floc size information and settling velocities. Settling columns and annular flumes are however more complex and expensive to construct. These techniques require large sample volumes which are difficult and uneconomical to sample, transport, and store. They are also unsuitable for repetitive testing and the extensive variation of conditions due to the time consuming nature of the tests. By contrast the jar test technique is a simpler test performed at a smaller scale. The jar test technique is observed to be a more popular technique used in previous studies. It has been extensively used in studies involving coagulation. There is much literature available to set up and calibrate the jar test (Nagata, 1975; Spicer & Pratsinis, 1996; Spicer et al., 1996; Bouyer et al., 2005; Coufort et al., 2005; Serra et al., 2007; Mietta et al., 2009a). There is less literature available on settling columns and annular flumes. The availability of literature provides guidance for the design of laboratory tests and provides previous results for comparison and possible validation. The jar test technique is a more economic test to develop and perform. The small sample volume (1-3L) makes it suitable for repetitive testing. It has been selected as the most feasible technique to perform the investigation.

3.2. Laboratory Investigation

It was established that the jar test technique is the most feasible laboratory technique in which to simulate flocculation and to monitor floc size distributions as well as settling velocities. The jar test technique is the chosen approach for this study. The main reasons for this are as follows:

1. There is extensive literature available on the technique. The concepts of mixing in agitated vessels have been researched. The literature provides a useful guide on the optimal method of conducting flocculation experiments.

2. Results may be validated by comparison with results obtained in previous studies.

3. The technique is easily repeatable for future testing and validation.

4. The technique is suitable for repetitive testing where the flocculation drivers may be varied over the full spectrum of possible conditions.

5. The technique is economically feasible.

3.2.1. Description of apparatus

The technique employs an agitated glass beaker in which flocculation is simulated and a small plexiglass settling column in which to observe settling flocs. Plate 3-5 shows the jar test equipment used in the laboratory investigation.

The following brief description of the apparatus refers to plates 3-5 and 3-6.

A 1L solution at a specific concentration and salinity was prepared and placed into the 2L glass beaker (5). The beaker was placed on the steel frame (1) and the motor and agitator were lowered. The fine particles in the solution were illuminated using a backlight concentrated (8) on a clear white plastic sheet. The backlighting was provided by the beam of an overhead projector placed behind the beaker (8). The paddle agitator was driven by a 3-phase AC motor (9) and frequency controller. A Nikon D7000 with a 60mm AF-S 60mm NIKKOR macro lens (7) was placed in front of the beaker. Images were captured when the agitator was stopped. The scale was checked by capturing an image of a scale rule in the beaker.

Settling velocities were measured in the settling column (12) after agitation. The settling column is shown in plate 3-6. Sampling was performed with a glass pipette of 5mm internal diameter. Settling flocs were captured using the continuous interval timing feature on the Nikon D7000 above. The settling column was illuminated using the beam of another overhead projector (11). The pipette was held in place with a clamp (10).

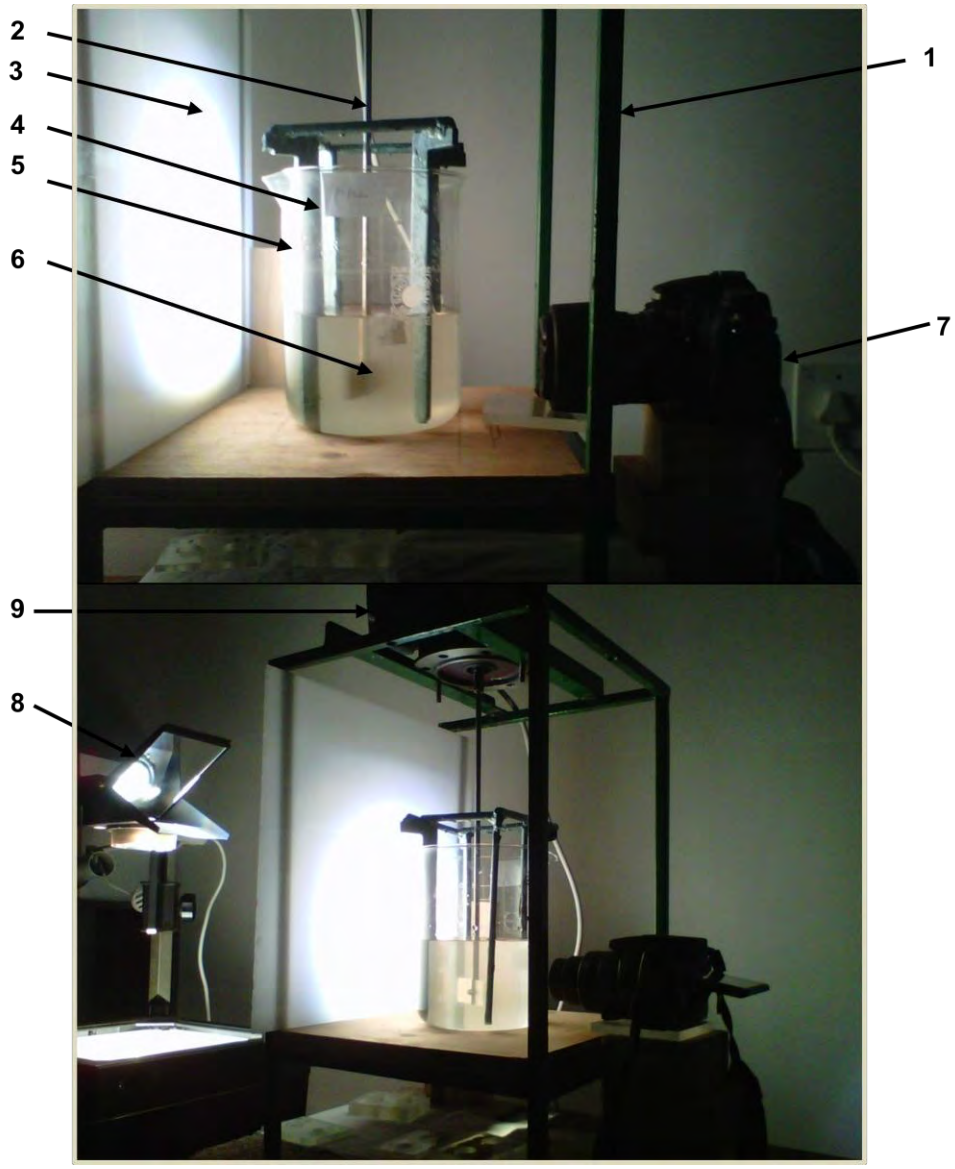

Plate 3-5**:**Jar test apparatus and floc imaging technique The numbered items are (1) Steel framework supporting the motor, (2) Stainless steel shaft, (3) White plastic sheet, (4) 4 x 12mm baffles, (5) Standard 2L glass beaker of 0.275m internal diameter, (6) 2 blade stainless-steel 65mm x 24.5mm paddle agitator, (7) Nikon D7000 camera with 60mm AF-S Nikkor macro lens (note that another camera is shown the second photograph), (8) Overhead projector (light source); (9) 3-phase AC motor.

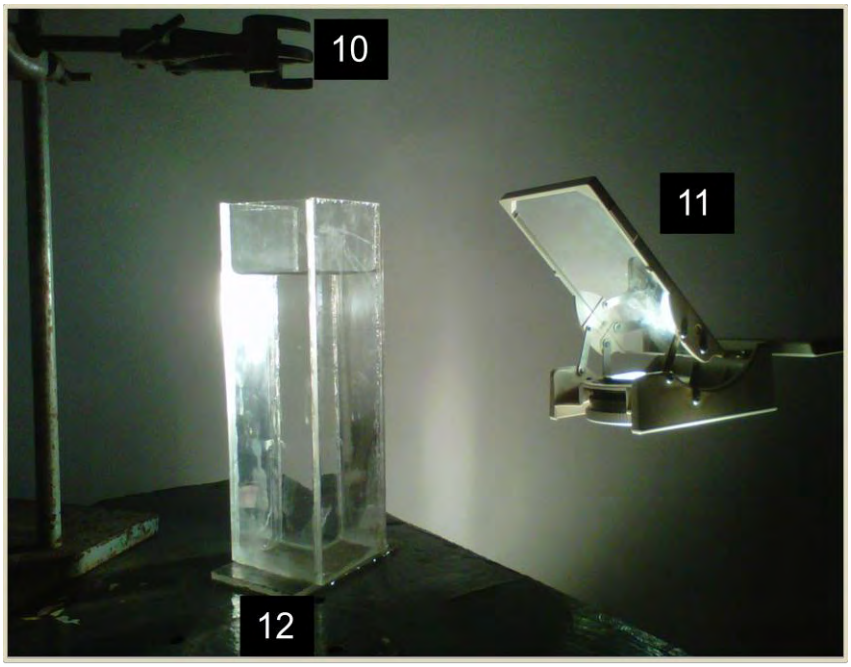

Plate 3-6: Image of the still settling column. Numbered items are (10) Clamp for fixing pipette in place (this was also aided by softer materials not shown), (11) Overhead projector (light source), (12) Still plexiglass settling column.

3.2.2. Laboratory Procedure

The laboratory procedure was guided by similar tests performed in literature and perfected by extensive preliminary testing. The duration of one test was approximately 1.5 hours. The multistep procedure following the preparation of sediment solutions is summarized below:

1. The prepared 1L solution of known concentration and salinity was placed into the 2L glass beaker. The baffles were placed into the beaker. The backlight was turned on. A scale rule with millimeter graduations was inserted into the beaker along the wall and an image of it was captured. The scale was verified using this image. The digital camera was operated on manual focus. The lens was adjusted to obtain a 1:1 ratio of image to object. An image of approximately 23.6x15.8mm was captured.

2. The solution was subject to high shear for 5 minutes in order to break up any flocs that were initially present. (see plate 3-7: 1) For this the motor speed was set to50hz.

3. After 5 minutes the agitator was stopped and lifted out of the jar. Once the large currents in the jar had dispersed, images of the particles present in solution were captured. A minimum of 4 pictures were taken. (See plate 3-7: images 2,3,4)

Aggregation tests

4. The agitator was lowered into the solution. The solution was then agitated at a particular shear rate for 70 minutes. (See section 3.2.5 for details on the shear rate calibration)

5. Floc images were captured at the following time intervals during the test: 5, 10, 15, 30, 50, 70 minutes. At each time interval the agitator was stopped and lifted for a brief period of time. During this time, images of the solution were captured. The purpose of the frequent imaging was to observe the development of flocs during the test.

6. At 70 minutes agitation was stopped. Images were captured. Images at 70minutes were assumed to represent the steady state floc size distribution of the solution. A sample was removed for microscope analysis using the pipette of 5mm internal diameter. Pipette sampling is discussed in section 3.2.6. The optimum time for flocculation (70 minutes) is discussed in section 4.2.

Settling column tests

7. A sample was then removed for the still settling column analysis using the pipette. The pipette was carefully moved from the beaker to the settling column. The tip of the pipette

was placed at the water surface of the column. Flocs were allowed to settle through the pipe into the settling column. The camera was configured to capture images continuously at a 2 second intervals. Images of settling flocs were captured for 5-10 minutes. Pipette sampling is shown in plate 3-7, image 6.

Deflocculating tests

8. While the settling column test was performed, the shear rate within the jar was increased. The solution within the jar was subject to a deflocculating test in order to understand how it behaves in response to increased turbulence. The shear rate was incrementally increased in $10s^{-1}$ steps to $50s^{-1}$ over 5 minute intervals. Agitation was stopped after each step and images were captured. Deflocculating testing was not performed on solutions subject to $50s^{-1}$ during the aggregation test. Preliminary testing indicated that 5 minute intervals provided sufficient time for deflocculating to occur.

Purpose of tests:

Aggregation tests were performed to investigate the influence of different combinations of concentration, salinity and shear rate on floc growth. This is discussed in detail in section 4-2.

Deflocculating tests were performed to investigate the influence of increasing shear rate on floc breakup.

Settling column tests were performed to investigate the settling velocities and effective densities of flocs formed during the aggregation tests.

Note on the duration of aggregation tests:

The aggregation tests were conducted for a period of 70 minutes each. This period was derived from preliminary investigations where numerous aggregation tests were performed for at least 120 minutes. After a series of tests were performed it was clear that floc growth did not occur after 70 minutes. The median and d_{90} floc sizes remained approximately constant with minor fluctuations after 70 minutes. This applied to both Mfolozi and Charters Creek sediments. This result is illustrated in section 4-2. Refere to this section for further details. The floc size statistics present at 70 minutes were regarded as the steady-state floc size distribution.

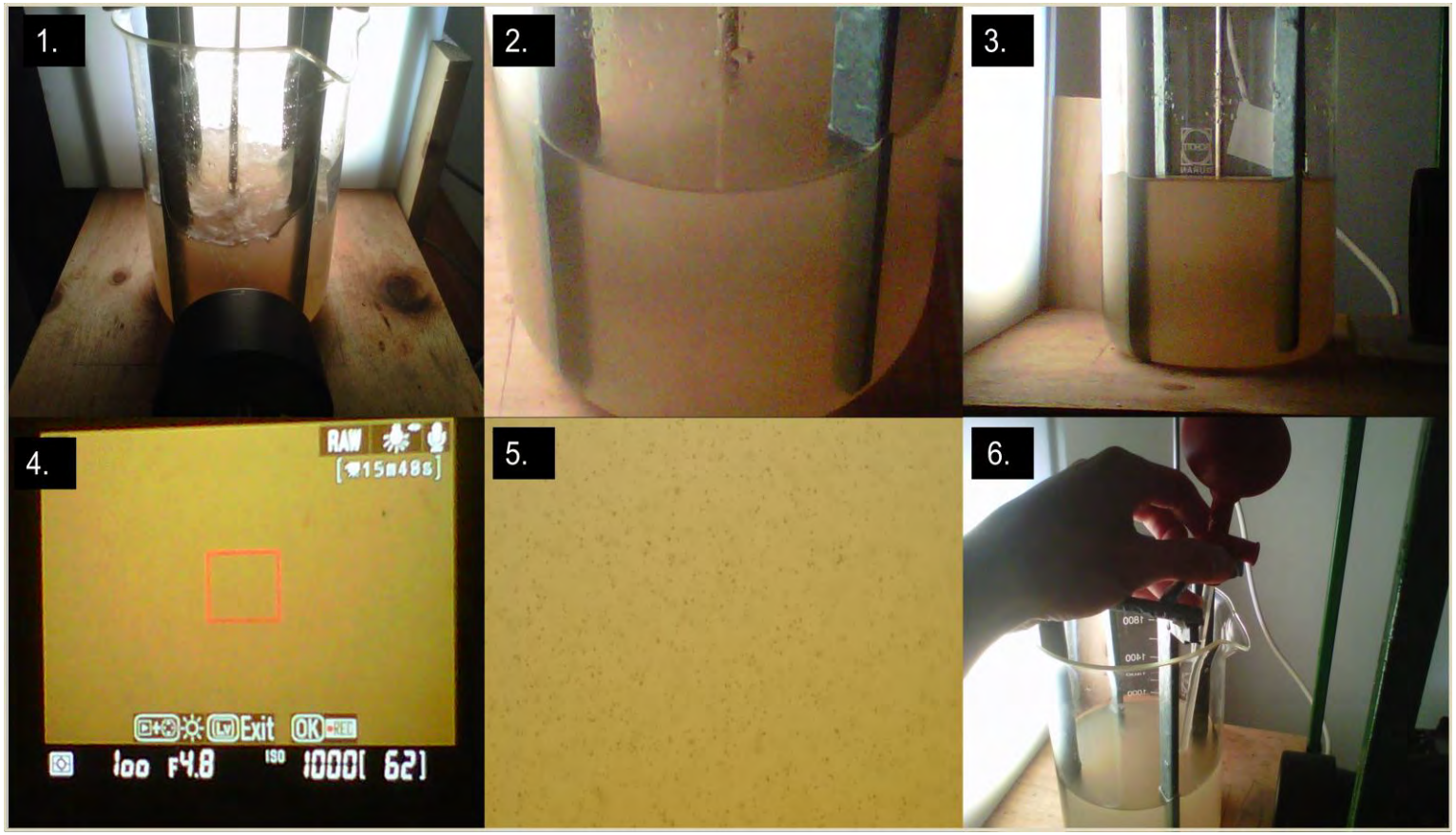

Plate 3-7: 1: The initial 5 minutes of deflocculation to break up flocs. 2: Still solution after deflocculating for 5minutes. 3: Still solution after deflocculation for 5 minutes. 4: Image capturing using the digital camera. 5: Image of Mfolozi sediments in solution (not the image in 4). 6: Floc sampling using the 5mm diameter glass pipette.

3.2.3. Sampling and preparation of sediment solutions

Suspended sediment samples were taken from Lake St Lucia and the Mfolozi River. Sampling of suspended sediment was preferred to the sampling of bed sediment. Bed sediment may be contaminated by large quartz particles and benthic matter, which are not present in suspension. The behaviour of a solution prepared using bed sediment may be different. Bulk samples of suspended sediment were collected in 20L drums. The samples were collected on a field trip during the second week of June 2011 during the dry season. The drums were transported back to the laboratory where they were stored in cool conditions until they were used for testing.

Mfolozi sediment was collected at a bridge near the town of Mthubathuba; 30km upstream of the Mfolozi mouth (see plate 3-8). The site was chosen because it was easily accessible by road and the water was fresh, with no influence of salinity. The samples were contained unflocculated sediments. Plate 3-9 shows sampling at the Mfolozi River. The suspended sediment concentration at sampling was approximately 200mg/L. The salinity was checked using a refractometer and confirmed to be zero.

The suspended sediment concentration varies with river discharge. During the wet season November – April), sediment concentrations are higher (Grenfell & Ellery, 2009). Time and financial constraints did not permit sampling throughout the year in both wet and dry seasons. It is anticipated that the composition of the sediment may change depending on the season and the part of the catchment in flood. The Mfolozi catchment is a large catchment (10,000 km^2). Monitoring the changes in sediment composition that occur within the catchment runoff is beyond the scope of this work. Hence it was assumed that the sampes taken in June are a reasonable representation of suspended Mfolozi sediment.

Sediment from Lake St Lucia was collected in a region of the lake known as Charters Creek. The suspended sediment concentration of the lake varies with wind conditions. Samples were collected on a windy day when the turbidity of the lake was high. Samples were collected at Charters Creek because it is the most accessible part of the lake. Furthermore strong North-Easterly wind on the day of sampling led to higher suspended sediment concentrations at the shores of Charters Creek. The water at Charters Creek was saline. It was not possible to obtain a fresh solution. Note that wild animals (crocodile and hippopotamus) made sampling in the shallow lake hazardous. The salinity was checked using an optical refractometer. The salinity ranged from 10 to 15ppt depending on region of the lake. The sediment concentration was approximately 600mg/L. The composition of sediment is not anticipated to change seasonally within the lake.

Purpose of sampling:

Recall that the purpose of collecting Mfolozi sediment was to study its flocculation properties and settling behaviour. This is in line with the objectives of the study (section 1.2).

The purpose of collecting sediment from Charters Creek in Lake St Lucia was to investigate its flocculation properties and settling behaviour to gain understanding of still settling behaviour after high energy events. It also provided a comparison for Mfolozi sediment behaviour. This is in line with the objectives of the study (section 1.2).

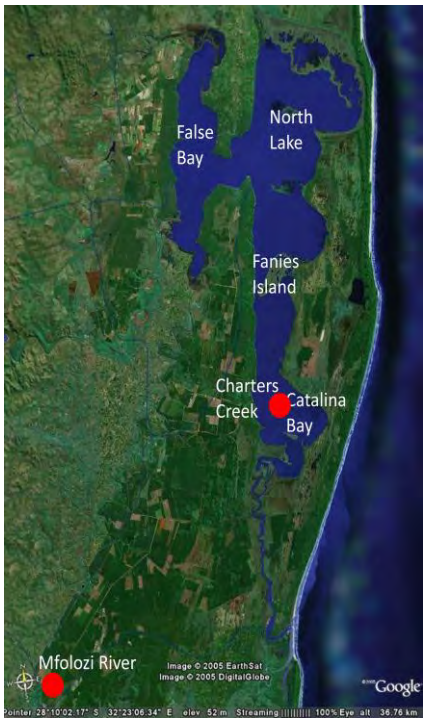

Plate 3-8: Satellite image showing sampling locations at the Mfolozi river and Charters Creek

Plate 3-9: The collection of water samples from a bridge in the Mfolozi river

Preparation of sediment solutions

The suspended sediment concentration of the samples was obtained by filtration. Filtration tests were performed according to standard procedure using 100ml samples and 0.63µm glass fibre filters (GFF). Once the concentrations of the samples were obtained, the subsamples were removed in order to prepare specific concentrations for testing. The concentrations prepared for testing were 50, 100, 200, 500, 1000, and 2000mg/L. Where the required concentration was lower than the sample concentration, it was diluted with de-ionized water. Thereafter a 100ml subsample was removed for filtration to verify the concentration. Where the concentration was higher than the sample concentration, a 1.2L subsample was removed and allowed to settle out for 2 days. Water was extracted until the required concentration was reached. This was verified by one filtration test.

The size and type of filters was sufficient for the filtration tests required. Clogging was only experienced for 1000mg/L and 2000mg/L verification tests. However this only lengthened the period of the filtration test and had no other effects. The apparent silt-dominance of the soil (refer to 4.1.1) prevented the filters from becoming clogged with finer materials.

The salinity of the samples was measured using an *Atago Optical Refractometer*. Solutions of specific salinity were prepared according to test requirements (see 3.2.4). Salinity was reduced by replacing sample water with distilled water. Salinity was increased by replacing sample water with seawater at 35ppt. The solution was first allowed to settle out before the salinity was adjusted. The new salinities were verified using an optical refractometer. It was not possible to prepare a 0ppt solution for Charters Creek sediment.

3.2.4. Conditions simulated during testing:

The laboratory study investigated the flocculation induced response of cohesive sediment to changes in the drivers of flocculation. The drivers varied are shear rate (G), suspended sediment concentration (C), and salinity (S). The study required that the drivers are varied over their full in situ range. Shear rates in estuaries vary between $1s^{-1}$ and $50s^{-1}$ (Kumar et al., 2010). The concentration of Mfolozi water may vary from clear seawater (a few mg/L) to 5g/L during a flood (Lindsay et al., 1996). The salinity varies between 35ppt in the marine zone of the estuary to 0ppt in the fluvial zone of the estuary. Drivers vary relative to each other. The approach is therefore to determine the quasi-steady state floc size distribution and settling velocity of Mfolozi silt under the following conditions:

Table 3-1: Intended conditions to be varied during testing

Parameter	Conditions varied
Salinity (S) in ppt	0, 5, 10, 15, 20
Sediment Concentration (C) in mg/L	50, 100, 200, 500, 1000, 2000
Shear Rate (G) in s^{-1}	5, 10, 20, 30, 50

The same conditions will be used for Mfolozi and Charters Creek solutions where possible. The above variations in conditions were used during extensive preliminary tests. There were a few problems encountered during preliminary tests. The test conditions were revised for the following reasons, and are elaborated in the *results and discussion* chapter.

- The extensive variation in parameters was time consuming and did not allow the repetition of tests. The performance of a single test per varied parameter does not provide a confident set of results. It was therefore decided to reduce the number of variations of parameters and repeat each test.

- The imaging technique did not permit the accurate observation of sediment flocs at concentrations of 500mg/L and above.

Table 3-2: Revised conditions varied during flocculation tests.

Parameter :	Conditions varied:
Salinity (S) in ppt	0, 10
Sediment Concentration (C) in mg/L	50, 200
Shear Rate (G) in s^{-1}	10, 50, Deflocculation tests: 20, 30, 50s^{-1}

Choice of salinity conditions:

Two salinity values, 0ppt and 10ppt were selected. Previous investigations have shown that the variation of salinity above a certain threshold has little influence on the floc size and settling velocity of the solution. The threshold is estimated to range between 0 and 1ppt for Mfolozi and St Lucia sediments (Maine, 2010). Therefore flocculation potential was not expected to differ

noticeably in the range of 5 to 35ppt (Maine, 2010). In the absence of an apparent optimum salinity, 10ppt was chosen. This salinity was easier to obtain by adding seawater to fresh solutions. Had 5ppt or 15ppt been selected, it would not have made a difference.

Choice of sediment concentration conditions:

Concentrations of 50mg/L and 200mg/ L were selected. Visibility was poor at concentrations above 200mg/L. This is illustrated in section 4.3. The performance of the digital camera was poor above 200mg/L despite any attempts to improve the backlighting. A second concentration selected to investigate the influence of varying concentration on the floc size distribution. In order to show distinction between flocculation behaviour at lower and higher concentrations, 50mg/L was selected as the low concentration. If the concentration is too low (say 20mg/L) it becomes difficult to detect floc in suspensions, particularly in conditions where flocs are fine. Furthermore the flocculation time scale increases at very low concentrations due to a lack of effective collisions.

Shear rates of $10s^{-1}$ and $50s^{-1}$ were selected to provide contrast between the influence of high and low shear on floc growth. Floc settlement was observed at shear rates lower than $10s^{-1}$. This is shown in section 4.2.3. The other shear rates were investigated in deflocculation experiments.

3.2.5. Calibration of turbulent agitator

Turbulent shear produced by the agitator is measured by the shear rate (G). The shear rate produced varies with the speed at which the agitator is rotated. There are several ways by which the shear rate may be calibrated as a function of motor speed. In this study the motor has been calibrated using the empirical methods of Nagata (1975). The shear rate (G) is expressed as a function of the energy dissipation rate (ε) and kinematic viscosity (ν):$G = \sqrt{\frac{\varepsilon}{\nu}}$.

The energy dissipation rate (per unit volume) in the agitated beaker is calculated using the power input of the motor: $\varepsilon = \frac{P}{V}$. P is the power input of the motor and V is the volume of the solution (m^3). It is assumed that the total energy input by the impellor is converted into turbulent kinetic energy (as defined in section 2.5.5.). Contributions to kinetic energy in the swirl and energy losses through wall friction are assumed negligible.

The power input is the product of the torque and rotational velocity of the agitator:$P = \tau \times \omega$. T is the motor torque (force*lever arm) and ω is the rotational speed of the agitator (rpm). Nagata (1975) proposed the non-dimensional power number (N_p) as an indication of the energy dissipation characteristics of the agitator:

$$N_p = \frac{P}{\rho n^3 d^5} \qquad (3.1)$$

where ρ= density of fluid (kg/m^3); n=impellor speed (s^{-1}) and d=diameter of impellor.

Manufacturers of commercially available impellors often determine the power numbers of their impellors (Spicer & Pratsinis, 1996; Spicer et al., 1996; Kumar et al., 2010). Nagata (1975) proposed an empirical method of determining the impellor power number from extensive laboratory testing, namely

$$N_p = \frac{A}{Re} + B\left(\frac{10^3+1.2Re^{0.66}}{10^3+3.2Re^{0.66}}\right)^p \left(\frac{H}{D}\right)^{(0.35+b/D)} (sin\theta)^{1.2} \qquad (3.2)$$

where the symbols are given by

$$A = 14 + (b/D)\left\{670\left(\frac{d}{D} - 0.6\right)^2 + 185\right\} \qquad (3.3)$$

$$B = 10^{\left(1.354\left(\frac{b}{D}-0.5\right)^2 - 1.14(d/D)\right)} \qquad (3.4)$$

$$p = 1.1 + 4(b/D) - 2.5\left(\frac{d}{D} - 0.5\right)^2 - 7(b/D)^4 \qquad (3.5)$$

$$Re = \frac{nd^2}{v} \qquad (3.6)$$

and with b= impellor width; H=water depth; θ=blade angle; n=motor speed (rpm) and v=kinematic viscosity.

The method is discussed in detail in Nagata (1975). It distinguishes between fully baffled, partially baffled and unbaffled conditions. The shear rate and homogeneity of the agitation may be improved by adding baffles to the beaker. The influence of baffles is determined by using the critical Reynold's number (R_c). The calibration of the agitator is presented in detail in an appendix of this report. Figure 3-1 below shows the calibration of the agitator for the planned study.

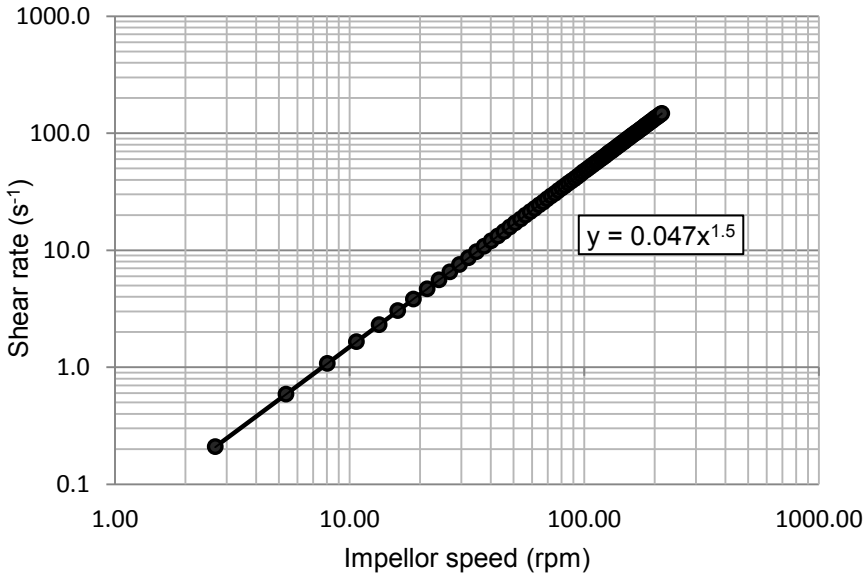

Figure 3-1: Calibration curve of the turbulent agitator for partially baffled conditions.

The calibration yields a power law relationship defined by:

$$G = 0.047\,(n)^{1.5} \qquad (3.7)$$

The motor is connected to a frequency controller. The speed of the motor is controlled by the frequency. These parameters are related by

$$n(rpm) = 26.8 \times frequency\ (hz) \qquad (3.8)$$

Details of the calibration are provided in appendix A. The calibration was compared to that of Mietta et al., (2009b) who used similar apparatus. The calibration is shown below. The calibrations are not expected to be the same as they used different sized beakers and mixers. Despite this, proximity of the two calibrations seems reasonable.

Mietta et al. (2009):$\log(G) = -0.849 + 1.5 \times \log 8(n)$ (3.9)

This study: $\log(G) = -1.328 + 1.5 \times \log 3(n)$ (3.10)

Note on the assumption for the calculation of G

The basis for the method of Nagata (1975) is the assumption that all energy input by the impellor goes into turbulent kinetic energy, where swirl and losses through wall friction are ignored. The accuracy of this assumption is questionable. It is anticipated to provide higher values of G because it ignores friction. In the absence of validating equipment in the form of a laser Doppler velocimeter (LDV), there is no means of effectively validating this method. However, one can rely upon the fact that this method has been published and extensively used in research involving mixing. For example: Mietta et al., (2009a, b); Spicer & Pratsinis (1996); Kumar et al., (2011). It is also the basis by which impellor manufacturers specify impellor power numbers. Furthermore in certain studies, such as Mietta et al., (2009a), the results of Nagata's method were validated using a LDV. The results were found to be consistent with LDV measurements, with a 5% error.

Calculation of the Kolmogorov Microscale

The Kolmogorov microscale defines the size of the smallest turbulent structures which form in any turbulent conditions. As discussed in chapter 2, the Kolmogorov microscale has been observed to limit the size of flocs that form in turbulent conditions. The Kolmogorov microscale is generally measured using a Laser Dopper velocimeter, or Accoustic Dopper velocimeter in certain conditions. It may also be derived from the shear rate, G. In this study the Kolmogorov microscale was calculated using the following relationship with G:

$$\eta = \sqrt{\frac{\nu}{G}} \qquad (3.11)$$

Both variables in equation 3.11 have been defined previously. The Kolmogorov microscale was calculated using the values of G obtained from the method of Nagata (1975). The accuracy of the values for η depends on the accuracy of the method defined above. The concerns associated with this method have been discussed. However, in the absence of the necessary equipment (LDV), this is the best estimate possible at this stage. It is acknowledged that the values for η are possibly overestimated.

3.2.6. Floc sampling techniques – modified pipette

Sediment flocs are fragile and easily break up when disrupted during sampling (Eisma et al., 1996; Gibbs & Konwar, 1982). This is particularly so for larger, weaker macroflocs which breakup into their constituent microflocs. The fragile nature of flocs limits the available techniques for observation. Pipettes break up larger flocs during sampling due to high shear at their narrow opening. Gibbs & Konwar (1982) recommended that a pipette with internal diameter and opening exceeding 4mm is sufficient to prevent floc breakup. This has been employed by Manning et al. (2007) and Kumar et al. (2010) who used pipettes with internal diameters of 4mm and 8mm respectively. Preliminary observations have indicated that a pipette with an internal diameter of 5mm does not result in floc breakage.

Using the pipette with the settling column

The settling column was filled with water at the same salinity and temperature as the suspension in the beaker as per recommendations by Manning et al. (2007) and Kumar et al. (2010). The pipette was held at the top of the settling column and flocs are allowed to settle through the pipette into the settling column. Preliminary testing has shown that this technique is sufficient to prevent floc breakup. The settling column is however sensitive to the formation of currents. The salinity of the solution in the settling column needs to be the same or slightly higher than that of the solution in the jar. If the salinity is lower, strong jet-density currents form and particles settle at high speed from the pipette. If the salinity is too high, flocs float to the surface and only settle later. The settling column tests were thus conducted with caution.

Using the pipette with microscope slides

Flocs may be observed under a microscope using microscope slides with 5mm sidewalls (shown in plate 3-10below). The slide is filled with a small volume of water. The pipet is held at the top of the water surface in the slide. Flocs settle through the pipet onto the bottom of the slide. It is uncertain as to whether this method results in floc breakup. Macroflocs have been observed on microscope slides. It is however possible that flocs settle on top of each other in the microscope slide.

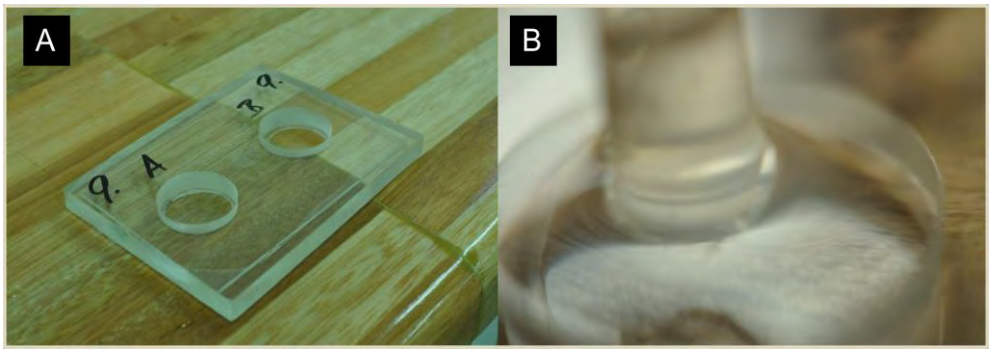

Plate 3-10: A: The microscope slide used to view flocs. B: Floc sampling procedure using a 5mm ID pipette and the microscope slide in A.

3.2.7. Calibration of digital camera for experimental use

A Nikon D7000 single lens reflex camera was used to conduct both the jar and settling column tests. A 60mm Nikkor Macro lens was fitted to the camera. The lens was manually focused to obtain a 1:1 resolution. The image was the same size as the CMOS image sensor at 23.6x15.mm. The image sensor had 16.2million effective pixels. The scale of all images captured at 1:1 was: 1 pixel=4.78µm. The actual scale was verified using a scale rule placed in the view of the camera prior to the start of a test.

Preliminary tests were performed using a Nikon P100 Coolpix camera. A resolution of 10µm per pixel was obtained when the camera was manually focused.

During periods when the D7000 was unavailable, a Nikon D90 was used with the macro lens. The Nikon D90 contained 12.3 megapixel (effective) CMOS image sensor. The dimensions of the image sensor were 23.6x15.8 mm. A resolution of 1 pixel= 5.55µm was obtained at 1:1. The scale was verified during testing

3.2.8. Material Composition tests

3.2.8.1. Organic Matter Content

The organic matter content of the Mfolozi and Charters Creek suspended sediment samples were determined by filtration. Total suspended solids was first determined by filtering 100ml samples through 0.63µm glass fibre filters. The filters were dried at 100°C in an oven. The filters were weighed once dry. The filters were then combusted at 600°C in a furnace to burn off all organic content. The organic content is calculated from the difference between the dry mass of filter and the combusted mass of the filter.

$$Dry\ sediment\ mass(g) = Dried\ filter\ weight - Original\ filter\ weight \qquad (3.12)$$

$$Organic\ Content\ (\%) = \frac{Dry\ filter\ weight - Combusted\ filter\ weight}{Dry\ sediment\ mass} \qquad (3.13)$$

3.2.8.2. Malvern Particle Size Analysis

The primary particle size of suspended sediment samples was determined using a Malvern Mastersizer 2000. The instrument uses laser diffraction to measure particle size distribution. Suspended sediment samples from Charters Creek and the Mfolozi were tested. The purpose of the particle size analysis was to classify the soil by determining the clay, silt and sand sized fractions. It was of particular interest to determine the clay fraction of both materials. It was suspected that both sediments were silt-dominant. The Malvern Mastersizer 2000 is shown in plate 3-11 below.

Plate 3-11: Image showing the Malvern Mastersizer 2000

The Mfolozi and Charters Creek sediments were tested under different conditions. Virgin suspended sediment samples were analysed. Sediment was then extracted from solution. A suspended sediment sample was taken and allowed to settle out. The liquid was removed by decanting and thereafter by evaporation in a warm oven. The dried sediment was broken up using a pessel and mortar. A portion of this sediment was mixed into de-ionized water and analysed. The remainder was combusted in a furnace at 600°c to remove organic matter. This sample was then mixed into de-ionized water and analysed. Samples of virgin, dried, and combusted Mfolozi sediments were thus analysed. Virgin samples were tested to determine the influence of organic content on the size of the clay fraction. The results are presented and discussed in chapter 4.

3.3. Data Processing

3.3.1. Processing of jar test observations

The techniques used to process the images obtained from the aggregation and deflocculation tests have been summarized in key points below:

1. Captured images from the jar test were transferred from the camera to a computer. The images were in RAW format. The Nikon ViewNX2 software package was used to convert the images into TIFF format for further processing. The imported images were then catalogued and stored.

2. An image was imported into MATLAB where it was converted into a binary image at a particular threshold. The threshold was selected by trial and error to produce a binary image where the sizes of the flocs in the original image are best preserved. The threshold was generally applicable to all images taken at a particular concentration and shear rate.

3. The images were exposed to more light near the top of the jar. This was unavoidable and resulted in an intensity gradient across the binary image. The top of the image was white while the bottom was black. Depending on the value of the threshold, there was a band across the central region of the image where the floc shapes and sizes were preserved. This area was cropped and saved as a new image for further processing. The original image was approximately 24x15 mm in size. The cropped image was typically approximately 15x4mm^2 in size. (refer to plates 3-12 and 3-13 below) Two to three images were processed to improve the statistical reliability of the results.

4. The cropped binary images were processed using the same Matlab script. The script measures the area, equivalent diameter and major axis length of all objects in the binary image. A description of the digital imaging parameters is given in section 3.3.3. The script calculated the 25th, 50th, 75thand 90th percentiles of the floc areas measured. It also output the mean and maximum floc sizes. All particles present in the binary imageless than 20µm were filtered out. The percentiles were recalculated based on the population above 20µm. In order to improve the accuracy of the processed data it was necessary to apply a 20µm filter. This was done to remove noise associated with the thresh-holding and creation of binary image. This is discussed in greater detail in chapter 4.

5. The output from the image processing script was entered into an excel spread sheet. An html file containing all the input and output data, as well as the Matlab script was produced using Matlab. Tabulated output is presented in the appendices. The html output file has been included in appendix E.

Development of the image processing script in Matlab

The script used to process the images obtained was developed using the Matlab image processing toolbox. The html file in appendix E includes the script. The script was developed by the student using introductory books on Matlab for assistance. It is not a complex script. The processing of images was however time consuming.

Images are created and recognised as true-color images, which are the superposition of three indexed images: a blue, green and red image. Each indexed image is a matrix of numbers associated with a color map. The superposition of the three matrices produces a full colour image. Once the images were imported into matlab they converted into binary images (as mentioned above). A binary image is a matrix of 1's and 0's, where every colourscale below a stipulated threshold becomes a 1, and every colourscale above becomes a 0. The Matlab image processing toolbox has built in functions with which to analyse binary images. These are known as the *regionprops* functions. These were appropriately selected by the student to output parameters such as: number of objects (groups of white pixels), the equivalent diameter of all objects (in no. of pixels), the major axis length of all objects etc. This output is given in the form of matrices. In this form, the data may be easily filtered, plotted in the form of histograms, and statistically analysed. Refere to appendix E for an example of the image processing script and its output. Graphs were created either in Matlab, or by exporting output matrices and statistical parameters into Excel and plotting graphs there.

Camera calibration to identify floc size:

In studies of this nature digital imaging systems are often calibrated using different size classes of particles. A material of known size class is added to solution (e.g. polystyrene beads of 50μm diameter). Tests are run for a few size classes. The results are analysed and compared to the known particle sizes. This indicates the accuracy of the digital imaging system. Regrettibly this form of testing could not be performed in this study. It was not possible to obtain particles such as polystyrene beads of the size range required for calibration. Such materials are not commercially available in South Africa. The study was performed without this form of calibration. During the testing a scale ruler was used to confirm the scale of the images. It was assumed that all shapes (larger than 20μm in effective diameter) present in the processed binary images were sediment flocs. The filtration of shapes less than 20μm has been discussed in detail in chapter 4, but also alluded to above. A comparison between the image characteristics of clay, silt and sand solutions was not considered necessary for this study. Note that each image processed was individually scrutinized before the results were accepted.

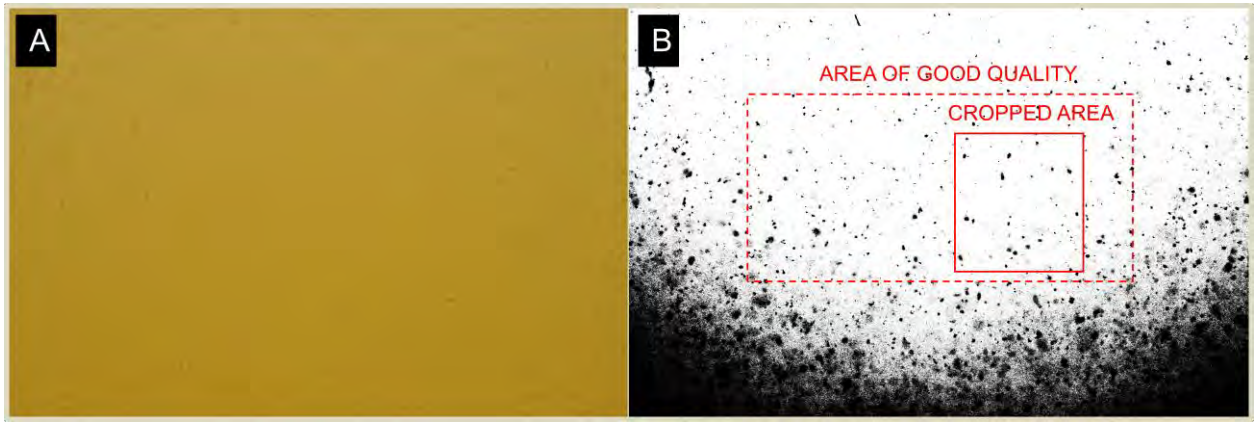

Plate 3-12: A: An Image captured during an aggregation test. B: Binary image of A.

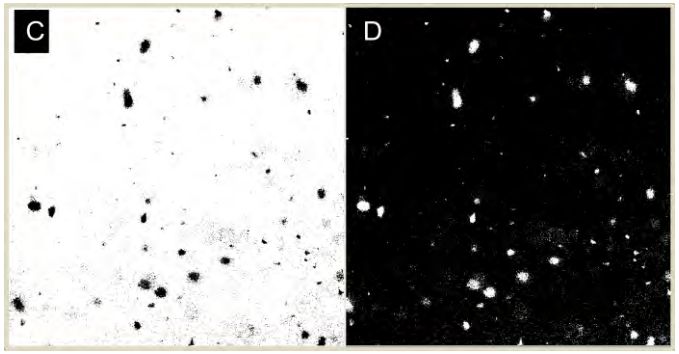

Plate 3-13: C: Crop of binary image. D: Image C altered for processing. The 20µm filter removed the 'dust' or noise from the image.

3.3.2. Processing of settling column observations

Images of settling flocs are captured at 2 second time intervals on using the Nikon D7000 and macro lens. The Nikon D90 did not have the continuous interval shooting feature of the D7000. The frame rate of the camera was measured while observing the column. This was done repeatedly. Images spaced 10 frames apart were used. The time interval between 10 images did not vary. This is shown in the appendix D. Images were captured as JPEG files. This was done to reduce the amount of storage space needed. RAW and TIFF file formats require a lot of space. Individual flocs were manually tracked using the procedure summarized by the points below:

1. Captured images are imported onto the computer and catalogued.
2. The images were browsed for a series of suitable images of settling flocs. The first and last images where a group of flocs was clearly visible were generally chosen. Sufficient images were chosen in order to get a sample of at least 20 settling flocs of different sizes.
3. The selected pairs of images were imported into Matlab. A threshold was suitably selected and the images were converted to binary images.
4. The two images (each pair) were analysed using a Matlab script. The script measured the area and centroid (pixel co-ordinate) of each object in the image.
5. A floc or floc group moving between the two images was identified and cropped in each binary image.
6. The two cropped images were analysed using a Matlab script. The script measured the area, equivalent diameter, major axis length, minor axis length and perimeter of the flocs in the image. These results were recorded in a spreadsheet. (See appendix D).
7. Flocs in the two cropped images were tracked by finding their pixel co-ordinates in the two parent images (analysed above). Each floc was tracked by using its area to find its pixel-co-ordinates in the parent image. This method worked well because of the low population of settling flocs. If more than one match was located, discretion was used to identify the correct pixel co-ordinates.
8. The pixel co-ordinates of the floc in each image are recorded in a spreadsheet.
9. The floc settling velocity was calculated in the spreadsheet.

Floc settling velocity calculation

- The vertical pixel co-ordinate of the floc in image 1 was subtracted from its vertical pixel co-ordinate in image 2 to find the pixel value of the settled distance. This value was multiplied by the scale of the images to find the settled distance. The settling time between the two images was known from the frame rate and number of intervals between frames. The settling velocity was then calculated.

$$w_s = \frac{H}{t} \qquad (3.14)$$

(w_s= settling velocity, H= settled distance, t=time between images)

Problems encountered during the experiment, and errors are discussed in Chapter 4.4.5.

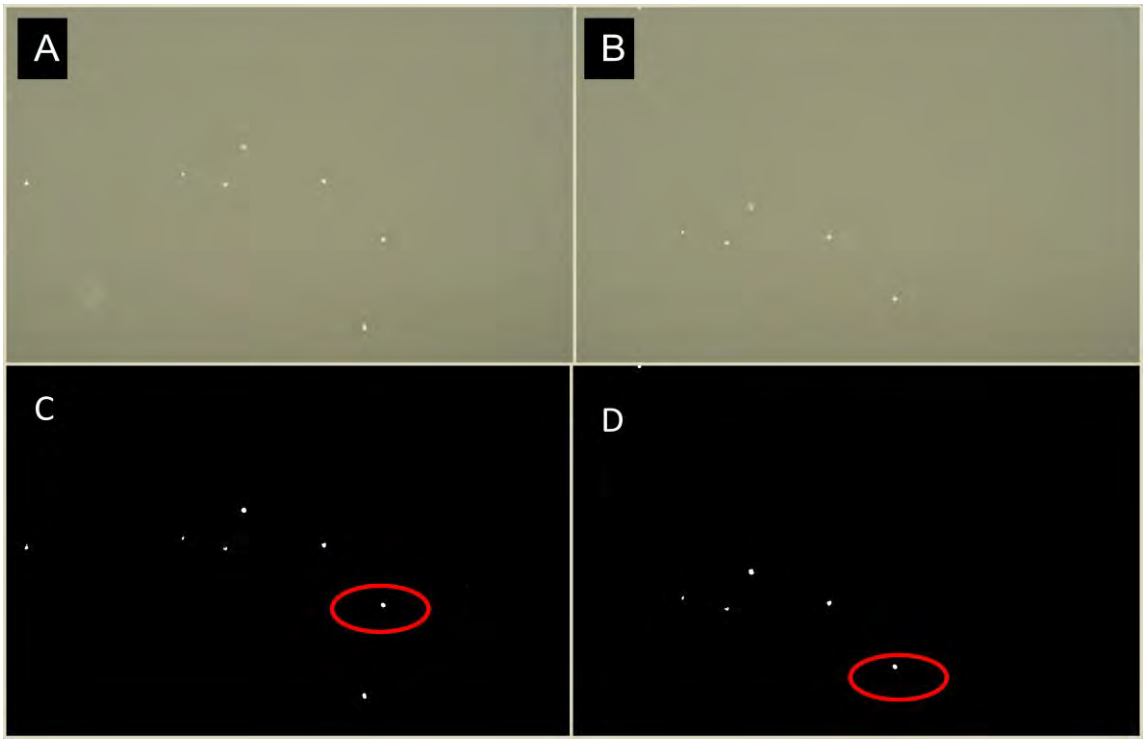

Plate 3-14: A & B: Images of settling flocs separated by a time interval. C & D: Binary images of A & B. A red ellipse is used to show the movement of a particular floc.

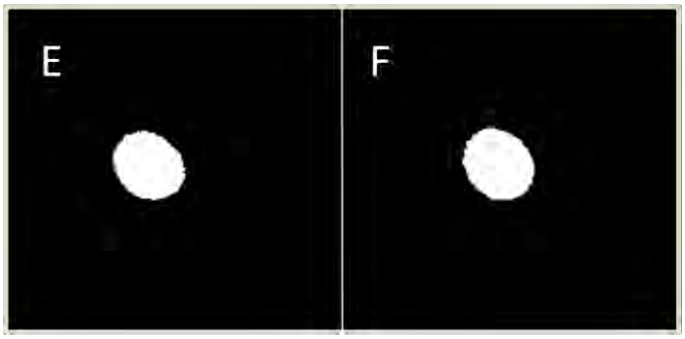

Plate 3-15: E & F: Images of the floc tracked in images C & D above.

Effective floc density

The effective density of the settling flocs was calculated using Stoke's approximation. Stoke's law expresses the settling velocity of settling particles in the following equation:

$$w_s = \frac{g(\rho_s - \rho_w)d^2}{18\mu} \quad (3.15)$$

The law may be rewritten to express the particle density (ρ_s) as a function of the settling velocity and equivalent diameter.

$$\rho_s = \rho_w + \frac{18\mu w_s}{gd^2} \quad (3.16)$$

The calculated density is an *effective density*. It is not the true density because the diameter of the particle has been approximated. The effective density was calculated each time the floc settling velocity was measured. The equivalent diameter of flocs was used because it provides a more accurate approximation of the floc mass.

3.3.3. Digital Imaging Parameters

Images during the test were captured as true-colour images. True-colour images are formed by the superposition of three intensity arrays; a red, blue and green intensity array. Images were converted to binary images during analysis. A binary image is an image composed of pixels of two intensities, black and white. Threshold intensity is defined when converting an image to a binary image. All pixels above the threshold intensity are rendered as white pixels while all pixels below the threshold intensity are rendered as black pixels. The image analysis scripts make use of the *regionprops* functions in Matlab image processing toolbox. This function counts all white objects surrounded by a black background. An object is defined by pixel connectivity '8', where objects are formed by pixels connected vertically, horizontally and diagonally. The function was used to measure various properties of each object (floc) in the image. The properties measured are listed and elaborated upon below:

- *Area*: the number of pixels in the object
- *Equivalent diameter*: the diameter of a circular disk of equivalent area to the object. This approach gives the closest approximation to the mass of the object (Verney et al., 2009). It however underestimates the size of long elongated flocs.

$$EquivalentDiameter = \sqrt{\frac{4A}{\pi}} \qquad (3.17)$$

- *Major Axis length*: the length of the major axis of an ellipse that has the same normalized second central moments as the object. This parameter provides a more reliable estimate of the size of the floc (Verney et al., 2009).
- *Minor Axis length*: the length of the minor axis of an ellipse that has the same normalized second central moments as the object.
- *Perimeter:* the sum of the distances between each adjoining pair of pixels around the object.
- *Fractal dimension:* the perimeter-based fractal dimension of an object may be used to describe its shape. The 2 dimensional perimeter based fractal dimension is given by: $logA = n_f \log(a)$.A is the area of the floc and a is the major axis length of the floc (Verney et al., 2009). The floc is a sphere when n_f=2.

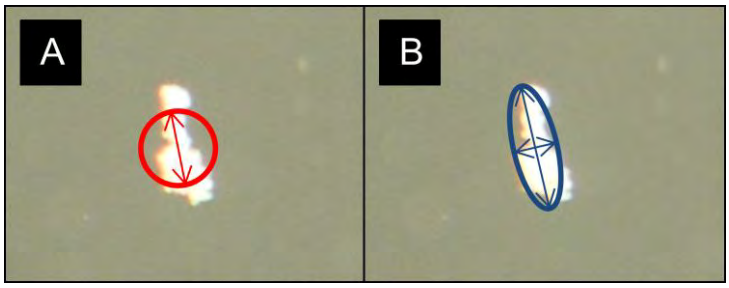

Plate 3-16: A: Depicting the equivalent floc diameter. B: Depicting the Major and minor axis lengths of an object

3.3.4. Statistical analysis of results

Jar Test Images:

The area, equivalent diameter and major axis length of all objects in the images obtained from the jar tests were measured. The mean, 25^{th}, 50^{th}, 75^{th}, 90^{th} percentiles and the maximum size were calculated for each of the parameters. The percentiles provide a way to compare different floc size distributions. Large flocs are expected to form of small portion of the floc population. It is therefore necessary to look at the 75^{th} and 90^{th} percentiles to investigate their behaviour. If the 75^{th} and 90^{th} percentiles of a certain distribution are higher than that of another distribution, it is an indication the population of larger flocs is higher in that particular test. All objects of equivalent diameter less than 20μm were filtered. Filtering small particles and noise from the results improves the ability to detect changes in the macrofloc population.

The proportion of the total population removed by the 20μm filter is significant. It is uncertain as to whether the proportion of the floc mass is significant. It is suspected that there is a large background mass of fine sediments which are undetectable by most techniques.

Volume-based distributions

Volume-based floc size distributions were obtained using the measured floc areas. All flocs were assumed to have uniform density and unit thickness. Flocs were placed into bins according to their equivalent diameter. Each bin formed a percentage of the total floc volume. This percentage was calculated. The distribution was plotted. The volume-based distribution and assumption of uniform density provided an indication of the size range over which the sediment mass was concentrated.

3.4. Key aspects of methodology

The methodology used to investigate the flocculation dynamics of cohesive sediments from the Mfolozi and St Lucia estuaries may be summarized by the following key points:

- Suitable laboratory techniques were investigated and compared
- The jar test technique was selected to be performed in conjunction with a still settling column to measure settling velocity
- The technique used digital imaging to measure changes in the floc population and to measure settling velocities.
- The concentration, salinity and shear rate of suspended sediments were be varied for different tests
- Aggregation tests were performed to measure floc growth during different conditions. This involved agitation at a constant shear rate for 70minutes. Images were captured at regular time intervals.
- Deflocculation tests were performed to measure the influence of increasing shear rate on floc breakup. This was done by incrementally increasing the shear rate in the jar. Images were captured at each increment.
- Settling tests were performed to measure the settling velocities and effective densities of flocs formed during aggregation tests. This was done by capturing images of settling flocs in the still settling column.
- Particle size analysis was performed using the Malvern Mastersizer to measure the clay-sized and silt-sized fractions of both sediment types.

CHAPTER 4

RESULTS AND DISCUSSION

Chapter 4 presents and discusses the results of the investigation. The material composition test results are shown and the sediments are classified. The flocculation potential of Mfolozi and Charters Creek sediments at different concentrations, salinities and shear rates is shown by the results of aggregation tests. The effects of increasing shear rate on floc size are shown in the results of deflocculation tests. Floc size characteristics are presented and discussed for both tests. The settling velocities and effective densities measured in settling column tests are presented and examined for trends. Test limitations and experimental error are discussed for each section. The chapter is concluded with suggestions for the application of the results obtained.

4.1. Material Composition Tests

4.1.1. Particle Size Analysis

Sediment samples were extracted from the bulk water samples collected from the Mfolozi River and Lake St Lucia for particle size analysis. Particle size analysis tests were performed to classify the sediment. The Malvern Mastersizer 2000 was used to size the primary particles present. Tests were performed on virgin water samples and on dried and combusted sediments. The results were found to differ.

Table 4-1: Malvern particle size analysis results

Sample	d5	d10	d50	d90
Virgin Mfolozi water sample	0.836	1.145	4.018	16.558
Dried Mfolozi sediment	1.240	1.781	10.523	44.129
Dried and Combusted Mfolozi Sediment	2.934	5.795	31.170	69.357
Virgin Charters Creek water sample	1.680	2.576	8.220	28.682
Dried Charters Creek sediment	1.865	2.791	14.416	40.937
Dried and Combusted Charters Creek sediment	3.001	6.229	42.453	111.908

*All figures in µm

Table 4-2: Sediment Classification

Sample	Clay % (<2µm)	Silt % (2-63µm)	Sand % (63-2000µm)
Virgin Mfolozi water sample	24.8	72.6	2.6
Dried Mfolozi sediment	12.0	84.9	3.1
Dried and Combusted Mfolozi Sediment	3.3	83.2	13.5
Virgin Charters Creek water sample	6.7	90.4	2.9
Dried Charters Creek sediment	5.7	92.1	2.2
Dried and Combusted Charters Creek sediment	3.3	65.0	31.7

The virgin water sample results of Mfolozi sediment shows a large clay fraction of 24.8%. This is not reflected in the results of the dried and combusted samples. The reduction in clay sized materials may be attributed to the high organic content of Mfolozi sediment. Both the Mfolozi and Charters Creek virgin samples in table 4-2 show a reduction in the clay fraction when dried, and a further reduction when combusted. There are two likely explanations for this behaviour:

(1) The loss of organic matter during combustion. A significant reduction in particles less 2µm with ignition suggests high organic matter content.

(2) Water samples were dried in order to remove the sediment from suspension. When sediment is dried, finer particles and organic matter adhered to each other, forming aggregates. These aggregates required separation prior to testing. This was done using a pessel and mortar. It was difficult to break down all of these small aggregates without excessive grinding which causes the particles to shear. The dried and combusted sediments were mixed into a solution of de-ionized water for the particle size analysis. It is uncertain whether all aggregates have been separated in the solution. Therefore the clay-sized fraction and the lower end of the silt fraction may be under-represented after drying and combustion. Note that these sediments remained in solution for a few days prior to testing.

The sand fraction for both sediments was observed to increase after drying and combustion. This seems reasonable in light of the decrease in organic fines and possible aggregate formation. It is likely that the sand fraction is overestimated, particularly for the Charters Creek sediment. The estimate of 31.7% seems high in comparison to images of the sediment taken during flocculation experiments, where few sand-sized particles are visible. The median sizes of Mfolozi and Charters Creek sediments were 31.17µm and 42.453µm respectively after combustion. These estimates were also higher than expected. This is perhaps an indication that aggregates that formed when the sediment was dried were still present during the test. The

particle size distributions of the virgin and combusted samples presented in figure 4-1 (A-D) show a disproportionately high increase in the sand fraction after combustion. Images of unflocculated suspended sediment show very few sand-sized particles but rather an abundance of undetectable fine particles. This supports the explanation of aggregate formation during drying.

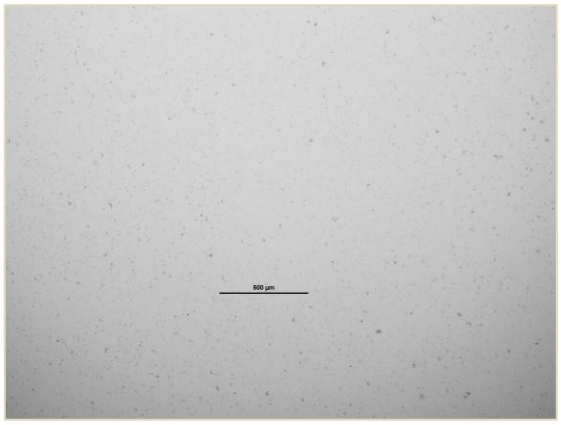

Plate 4-1: Microscope image of fine unflocculated sediment. The solid bar represents500µm.

This result was not unexpected. In a previous study similar behaviour was observed (Maine, 2010). This behaviour of dried cohesive sediment is accepted and general conclusions may still be drawn from the particle size analysis results.

General conclusions:

Mfolozi and Charters Creek sediments may be classified as silt-dominant. The virgin samples are dominated by silt-sized particles. Combusted sediment samples were silt-dominant. The clay fractions of both sediments were less than 5% after combustion. The clay fractions of the two different sediments were similar. The low clay fractions will likely limit the flocculation potential of the two sediments. The particle size analysis results also indicate that the organic matter content of Mfolozi sediments is high. This may influence its flocculation potential in comparison to Charters Creek sediments.

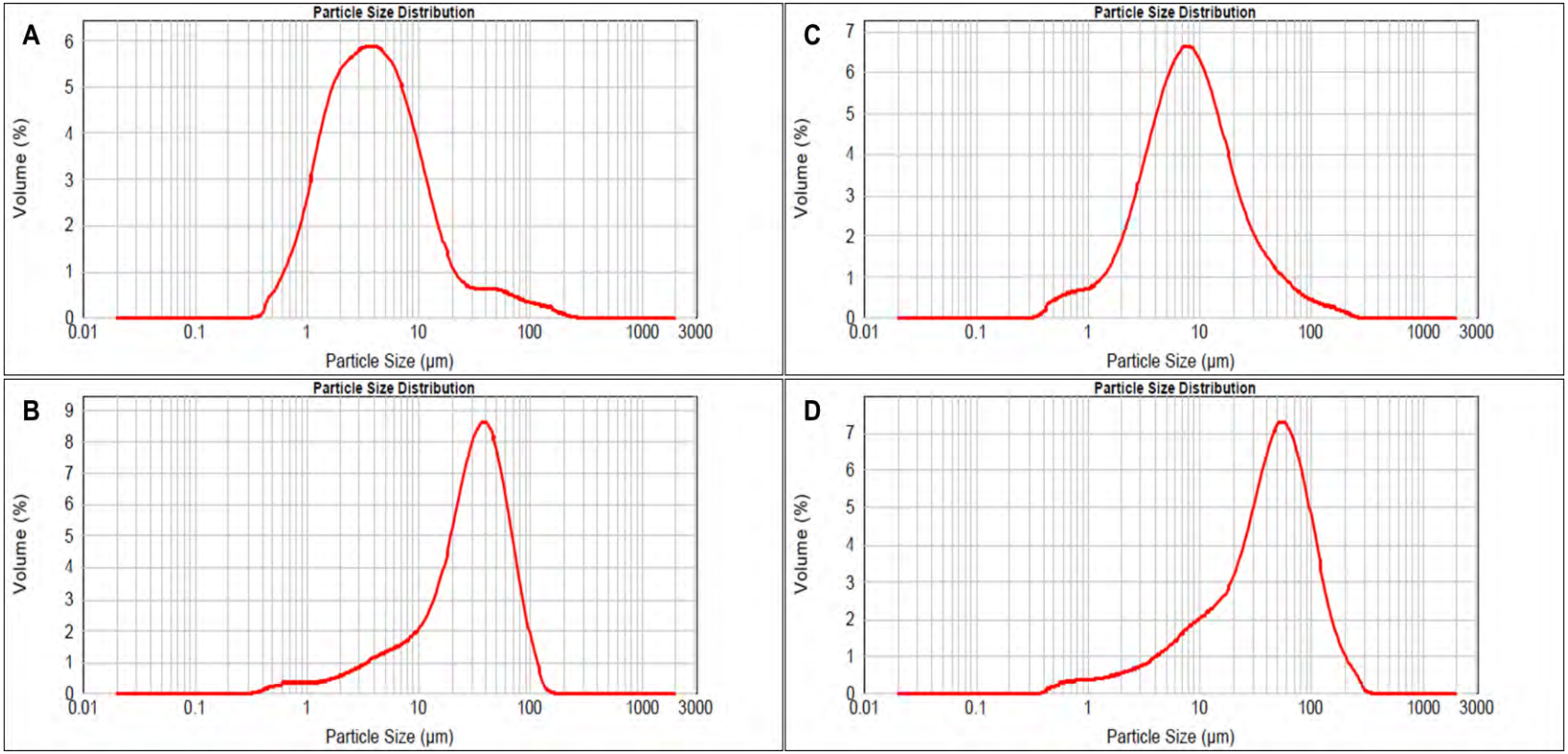

Figure 4-1: Particle size distributions for: A: virgin Mfolozi water sample. B: combusted Mfolozi sediment. C: virgin Charters Creek water sample. D: combusted Charters Creek sediment

4.1.2. Organic Matter Content

The organic matter content of the bulk water samples was measured over the period of the flocculation experiments. The OMC was also measured for the dry sediment extracted from the bulk samples. The results in table 4-3 show the average OMC for both sediments to range between 12.8-18.6%. The organic matter content was higher than expected. This may influence the flocculation potential of the sediments. The average OMC varied for the Mfolozi bulk water samples. The high OMC of the Mfolozi water and dried sediment corresponds with observations in the particle size analysis above. It is evident that the OMC of Mfolozi sediment was higher than that of Charters Creek sediment at the time of the particle size analysis tests.

Table 4-3: Organic Matter Content of sediments

Sample	Date	SSC (mg/L)	OMC (%)
Mfolozi bulk water sample (mean)	06-Oct	211	13.3
Mfolozi bulk water sample (mean)	07-Nov	174	16.1
Charters bulk water sample (mean)	31-Oct	615	14.4
Charters bulk water sample (mean)	07-Nov	638	13.3
Mfolozi dried sediment (mean)	08-Nov		18.6
Charters dried sediment	08-Nov		12.8

Reasonable steps were taken to avoid bacterial growth within the water samples. The water samples were stored in a dark laboratory and not exposed to significant temperature changes. Most organisms such as phytoplankton and zooplankton present during sampling were expected to die. It is reasonable to expect small variations of organic matter content between filtration tests considering the small sample sizes. The filtration tests were performed on 100ml samples.

For the purpose of the study it may be concluded that the organic matter content both sediment types was high, varying between 12 and 19% during the time of the flocculation tests.

4.2. Flocculation Tests

4.2.1. Aggregation tests:

The development of sediment flocs was observed for both Mfolozi and Charters Creek sediments under different conditions. Images of the solutions were captured over a 90 minute interval and analysed to determine floc size information. Each test was repeated. Both the initial test and repeated test results were combined and plotted as one set of results. The two sets of results for each set of conditions are still visible in the figures below. The tests were generally repeatable with similar floc sizes observed at each stage of the test. The behaviour of the Mfolozi and Charters Creek sediments was compared and the behaviour of the sediments was observed to differ.

Mfolozi sediments:

The results of the aggregation tests performed on Mfolozi sediments are displayed in figures 4-2 to 4-4. The median floc size and 90th percentile (D_{90}) floc size were measured. The floc size is measured as the major axis length or ellipsoidal length. When comparing the median and d_{90} floc sizes for each test, it is evident the solution populations were dominated by fine particles below 40µm. Larger flocs are only observed in the 90th percentile. Larger flocs form only a small percentage of the entire population. Note that the fraction of the population below 20µm in size was not observed. Macroflocs only formed in saline conditions at a low shear rates (figure 4-3B).

The D_{90} floc size increased over time under these conditions. The growth of the median floc size was low in comparison. In fresh water conditions and at high shear rates, no increase in the median or D_{90}floc size was observed. The growth rate decreased when the suspended sediment concentration was reduced from 200mg/L to 50mg/L.

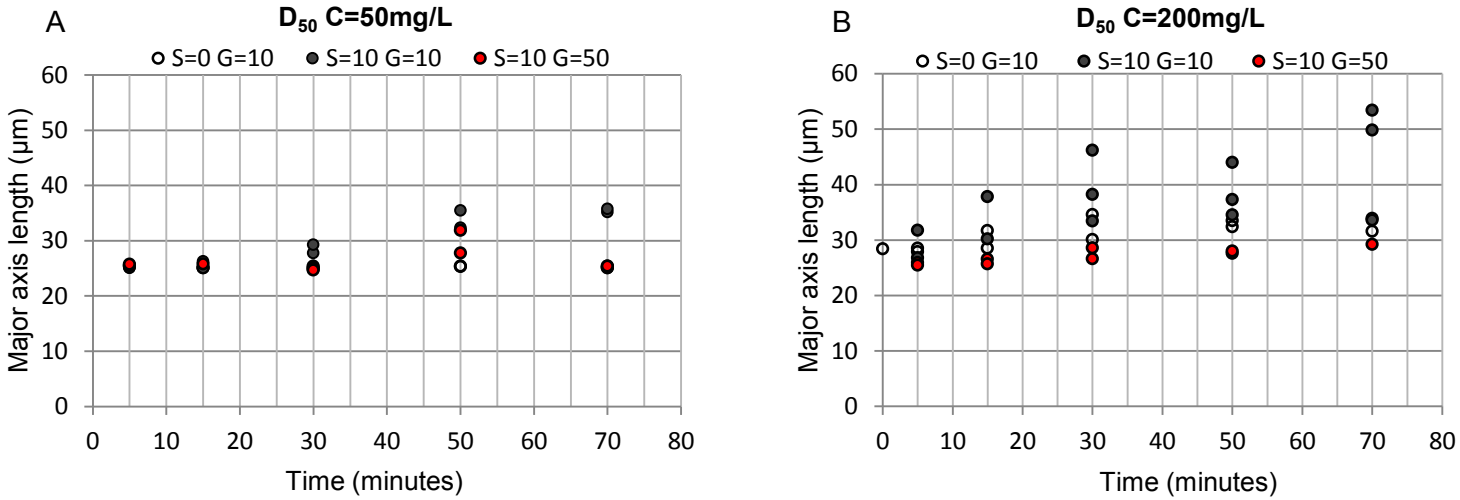

Figure 4-2: A: Growth of median aggregate size of 50mg/L Mfolozi sediment solution. B: Growth of median aggregate size of 200mg/L Mfolozi sediment solution. Key: C – suspended sediment concentration, S – salinity (ppt), G – shear rate (s^{-1}). Note that each condition represents the results of 2 tests.

Influence of salinity:

A distinct difference in floc development was observed between 0ppt and 10ppt (figure 4-2B to 4-3B). Larger floc sizes were observed at 70 minutes for the saline solutions. This trend is more significant for the D_{90} than the median floc size. This trend was stronger for the solution of higher concentration. Macroflocs did not develop at 0ppt. The flocculation potential of the sediment increased when the salinity was increased. This is consistent with expectations based on previous work reviewed in section 2.4.2.

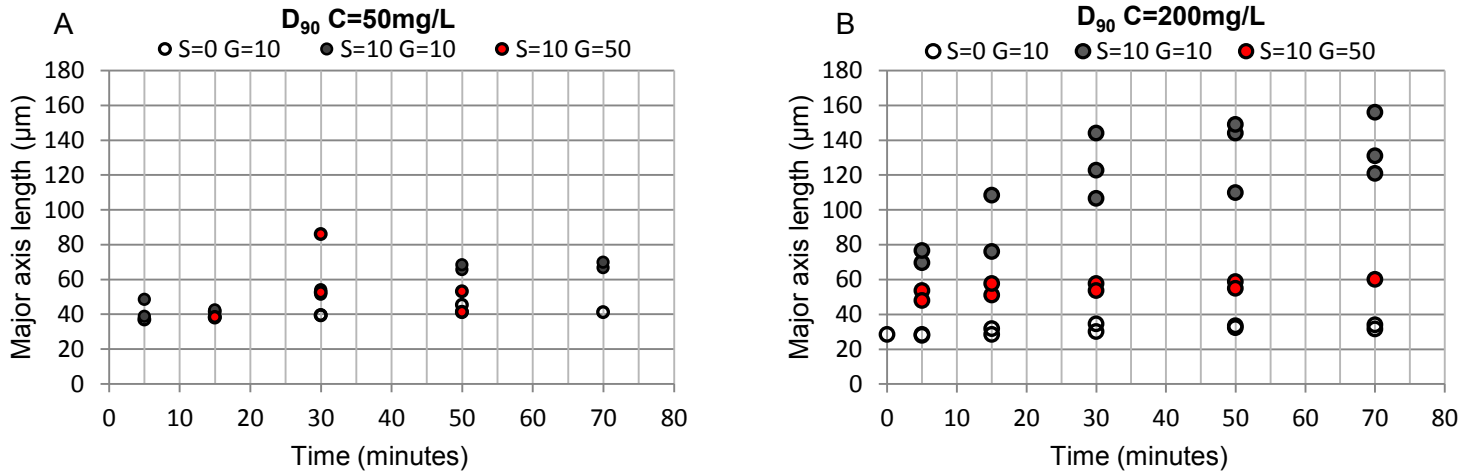

Figure 4-3:A: Growth of D_{90} aggregate size of 50mg/L Mfolozi solution. B: Growth of D_{90} aggregate size of 200mg/L Mfolozi solution. Key: C – suspended sediment concentration (mg/L), S – salinity (ppt), G – shear rate (s^{-1}). Each condition contains the results of repeated tests.

Influence of turbulence on aggregate development:

The development of aggregates was hindered at the high shear rate of $50s^{-1}$. Figure 4-3 shows that floc growth did not occur when the shear rate was increased from $10s^{-1}$ to $50s^{-1}$. The median floc size was also marginally lower when the shear rate was increased. This trend is consistent with expectations. The high shear causes any flocs that form to break apart. Only small flocs are present under such conditions. The D_{90} at 200mg/L did not exceed 60µm, and at 50mg/L did not exceed 30µm. There were some problems detecting particles under high shear conditions. It is possible that some results have been over-estimated for the 50mg/L solution due to a low population of detectable smaller flocs (elaborated in section 4.3). The results displayed in figure 4-2 and 4-3 indicate that the likely optimum shear rate for flocculation is $10s^{-1}$. Below $10s^{-1}$ the shear rate is too low to continuously resuspend sediment in the jar, as the settling time scale exceeds the flocculation time scale. Hence it is uncertain as to whether larger flocs will form below $10s^{-1}$.

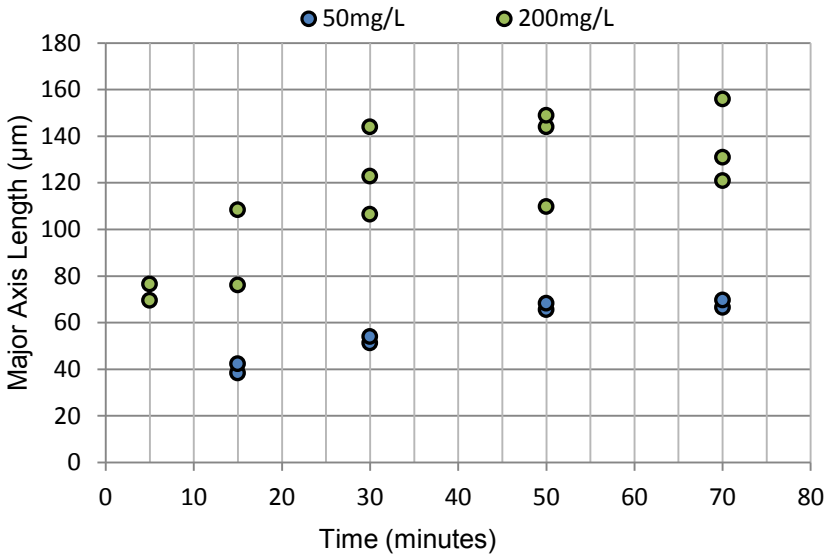

Figure 4-4: Aggregate (D_{90}) growth rate of 50mg/L and 200mg/L Mfolozi sediment solutions

Influence of suspended sediment concentration

The aggregate growth rate was higher at 200mg/L than 50mg/L in figure 4-4. In the other tests floc growth was limited chemically (by low salinity) or by high shear. Under suitable saline and turbulent conditions the floc growth is limited by the concentration. At low concentrations there is a reduced probability of effective collisions due to a lower population of suspended particles. Fewer effective collisions occur and aggregate growth is limited. Conversely, aggregate development is enhanced at high concentrations due to a higher collision frequency. The observations of Mfolozi sediment were consistent with these expectations.

It was difficult to detect particles at 50mg/L at high shear or low salinity. The particles were often too fine to detect when conditions did not allow aggregation to occur.

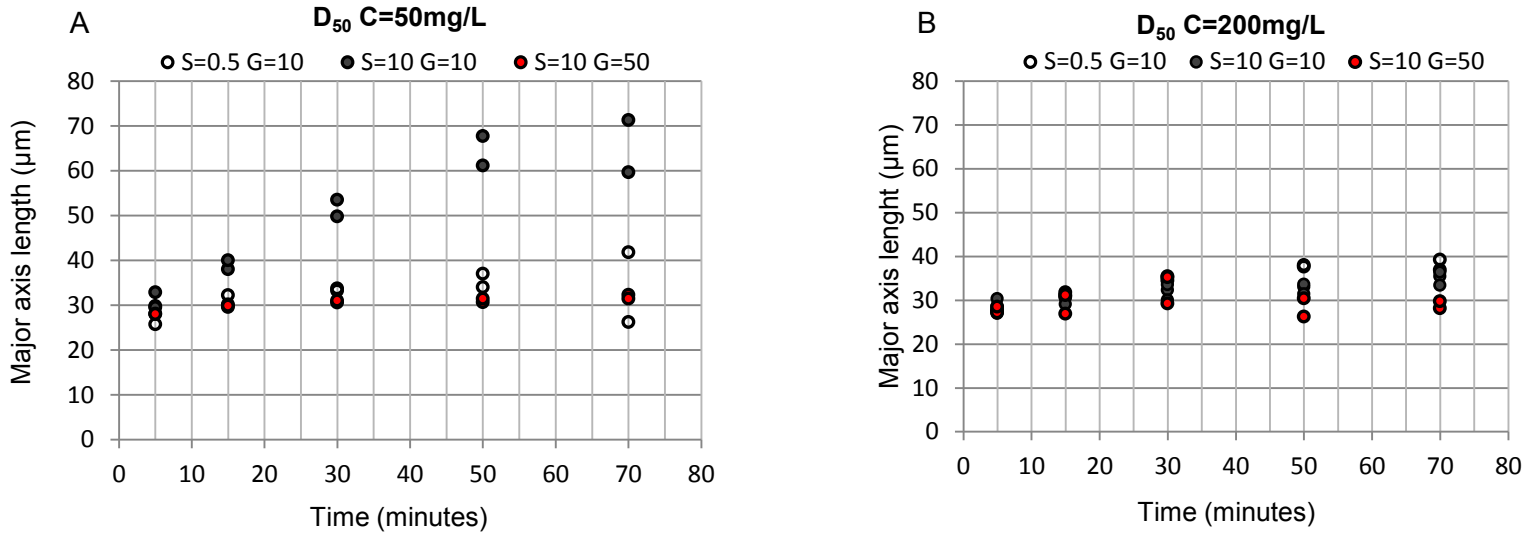

Figure 4-5: A: Growth of median aggregate size of 50mg/L Charters Creek sediment. B: Growth of median aggregate size of 200mg/L Charters Creek sediment. Key: C – suspended sediment concentration (mg/L), S- salinity (ppt), G – shear rate (s^{-1}). Each condition contains the results of two tests.

Charters Creek sediments:

The behaviour of Charters Creek sediments differed somewhat to that of Mfolozi. The sediment was dominated by fine particles while macroflocs only formed a small portion of the population. Aggregate development was hindered at high shear. The behaviour of the sediment in response to salinity and concentration increased differed to that of Mfolozi sediment. Large aggregates formed at low salinity and concentrations. Results are illustrated in figures 4-5 to 4-7.

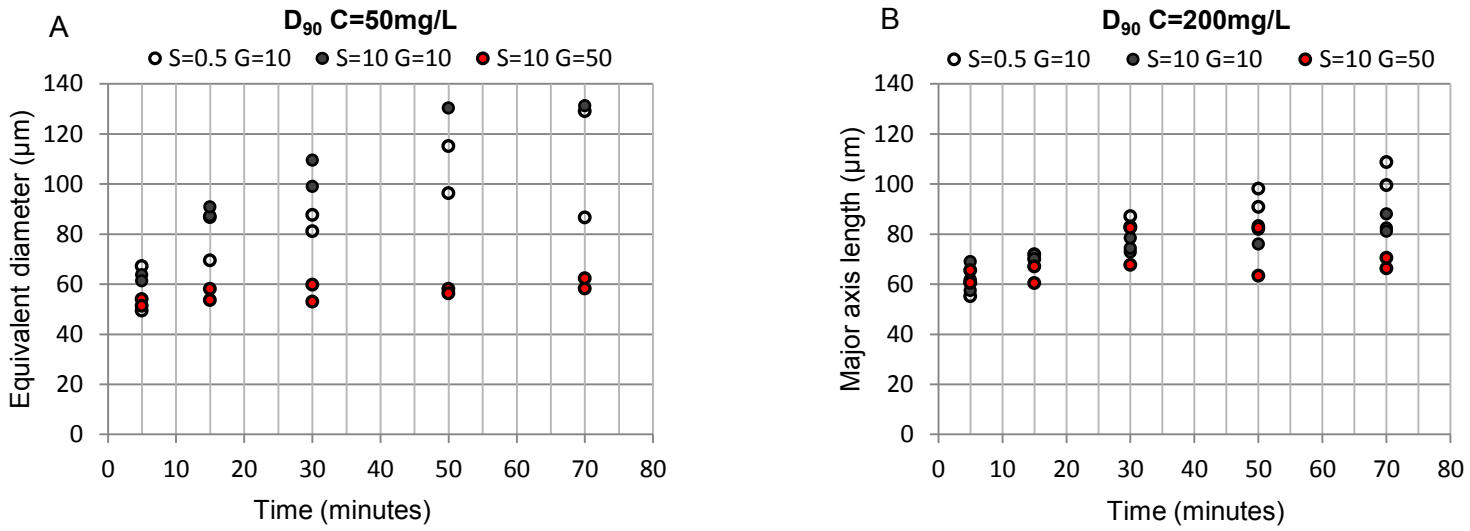

Figure 4-6: A: Growth of D_{90} aggregate size of 50mg/L Charters Creek sediment. B: Growth of D_{90} aggregate size of 200mg/L Charters Creek sediment. Key: C – suspended sediment concentration (mg/L), S – salinity (ppt), G – shear rate (s^{-1}). Note that each condition contains the results of two tests.

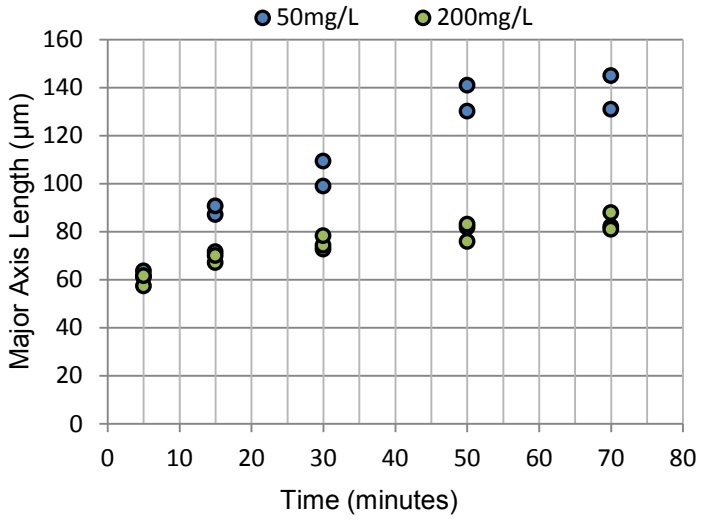

Figure 4-7: Aggregate growth rate of 50mg/L and 200mg/L Charters Creek sediments (G=10s^{-1}, S=10ppt)

Aggregate growth:

The growth of the d90 floc size generally exceeded that of the median floc size, which did not appreciate significantly. The median floc size was observed to increase significantly at 50mg/L and 10ppt in figure 4-5 A. The flocculation potential of that solution was high resulting in the flocculation of a significant portion of the population. Aggregate growth was not observed under high shear conditions. The largest flocs were observed at concentration 50mg/L, salinity 10ppt, and shear rate 10s^{-1} (figure 4-6A). After 30minutes the D_{90} was higher than 100µm. The D_{90} increased to 130µm.

Salinity:

The results of the 50mg/L concentration tests (figure 4-5 A and 4-6 A) show enhanced aggregate development with salinity. Larger flocs were formed at 10ppt than 0.5ppt. This is consistent with expectations. The 200mg/L results did not show the same behaviour. The median diameter was not influenced by changes in salinity (figure 4-5 B) but the D_{90} floc size was higher at 0.5ppt than 10ppt. Note that the Charters Creek bulk water samples were saline and it was difficult to reduce the salinity to 0ppt. The salinity was reduced to 0.5ppt as a compromise. Aggregates were generally observed to develop at 0.5ppt. The aggregate development observed at 0.5ppt indicates that it is above the threshold salinity required for flocculation to occur.

It is unclear why the 200mg/L 10ppt solution developed smaller flocs than the 0.5ppt solution. Aggregates were however not as clearly visible in the solution when imaged. Above the threshold salinity, little can be said about why the 0.5ppt (200mg/L) solution aggregated better

than the 10ppt (200mg/L) solution, or if it had at all. It is possible that the result was caused by imaging difficulties with the camera in the 200mg/L solution. The 50mg/L solution (figure 4-6 A) clearly showed an increase in flocculation potential with salinity.

Turbulence:

Aggregate growth at $50s^{-1}$ was not evident. The high shear rate prevented the development of large flocs. Figures 4-5 and 4-6 show both the median and d90 floc sizes to be smallest at $50s^{-1}$. Flocs that formed during the tests were broken up by the high shear stress.

Particles in solution at high shear were fine and difficult to detect. The results at $50s^{-1}$ were likely to have been overestimated, particularly at the beginning of the tests. This is discussed in greater detail in section 4.3 below. Floc growth was favoured when the shear rate was $10s^{-1}$. This is anticipated to be the optimum shear rate for floc growth. At lower shear ($G= 5s^{-1}$) the flocculation time scale is higher than the settling time scale (refer to 4.2.3), limiting floc development. Above $10s^{-1}$, floc size was observed to decrease (refer to deflocculation – 4.2.2).

Concentration:

Aggregates at 50mg/L were generally the same size as those at 200mg/L. In tests where aggregation was observed, larger aggregates were formed at 50mg/L than 200mg/L. This is shown in figure 4-7. At 200mg/L the d90 floc size was less than 100µm while it exceeded 140mg/L at 50mg/L. This behaviour was unexpected. Larger flocs are expected to form at higher concentrations due to higher collision frequency, as observed for Mfolozi sediments. This problem may be in part caused by imaging difficulties. Images at 200mg/L contain larger floc populations and floc overlap occurs. The flocs are not as clearly visible as those formed at 50mg/L. At 50mg/L the large particles (not all necessarily sediment flocs) are easier to see while the finer particles are still difficult to detect. The particle size distribution may be biased towards larger particles. The degree to which this influences the results is uncertain. Images of the 50mg/L and 200mg/L test are shown in plate 4-2. The 50mg/L image appears clearer and flocs are easier to distinguish than in the 200mg/L image.

The fact that this behaviour was not experience with Mfolozi sediments is a concern. Based on observations thus far it may be concluded that Mfolozi sediment behaves as expected and exhibits a higher flocculation potential at 200mg/L than Charters Creek sediment (at S=10ppt, $G=10s^{-1}$). Mfolozi flocs formed at 200mg/L were larger than Charters Creek flocs.

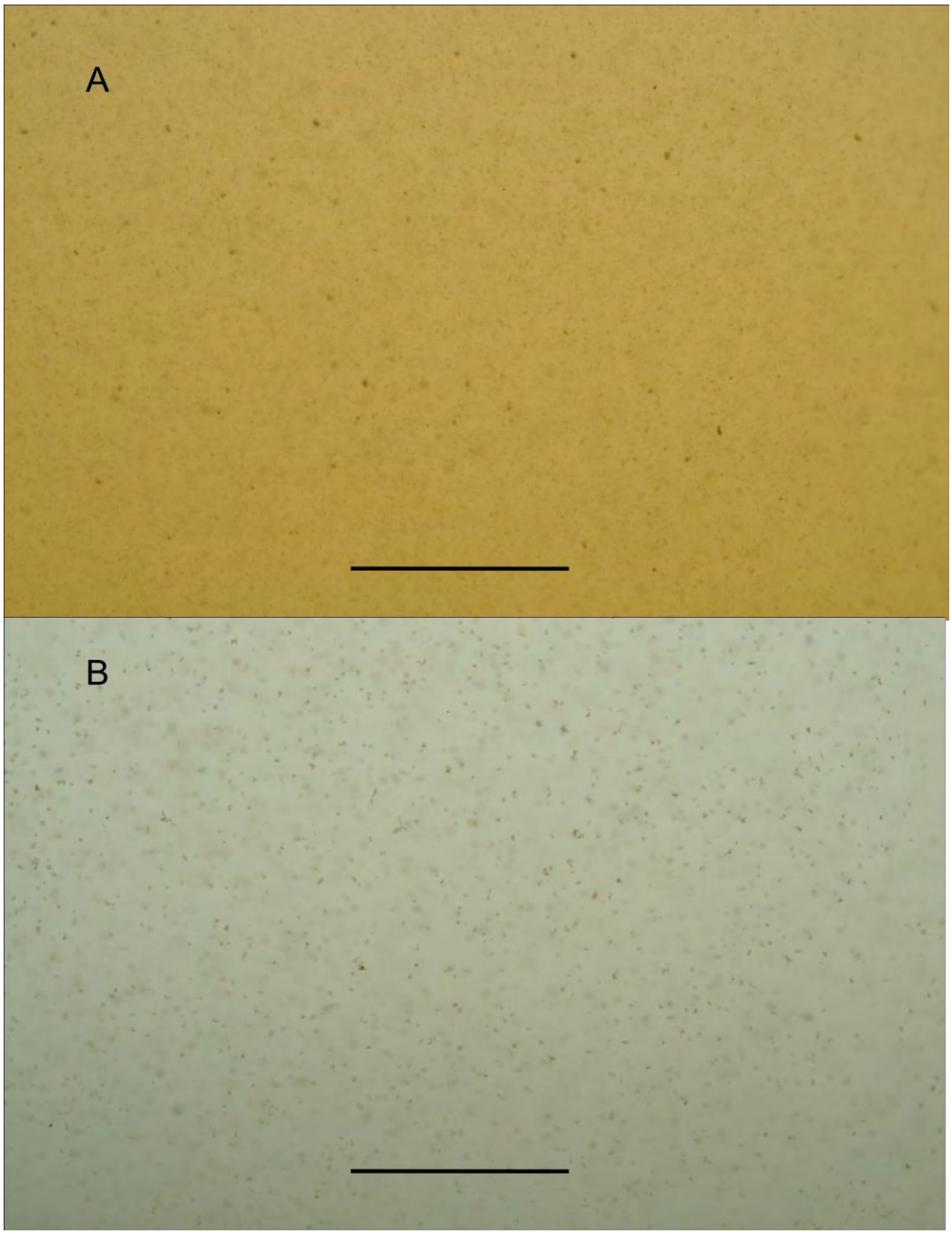

Plate 4-2: A: An image of flocculated Charters Creek sediment at 200mg/L, 10ppt, and $10s^{-1}$. B: An image of flocculated Charters Creek sediment 50mg/L, 10ppt, $10s^{-1}$. Images captured at 70minutes. The solid bar represents 5mm.

Relevance of aggregation test results

Aggregate growth was measured for both Mfolozi and Charters Creek sediments. The development of larger aggregates is favoured under certain conditions, while hindered under other conditions. Low shear and saline water promote floc growth. These results suggest that aggregates are likely to develop in the field where such conditions occur. Aggregate behaviour therefore needs to be considered in sediment transport studies regarding the Mfolozi River or Lake St Lucia.

The tests were not able to show aggregate behaviour in concentrations higher than 200mg/L due to poor floc visibility. During Mfolozi floods, suspended sediment concentrations often exceed 1000mg/L. There is a need to establish whether the aggregation behaviour at 200mg/L may be extrapolated to 1000mg/L. This is investigated in chapter 4.4.8.

The proportion of particles under 20µm is however uncertain as it is undetectable. This aspect of the behaviour is thus still unknown.

Experimental error and comparison of results:

The average difference between the results of the repeated tests were calculated and included in table 4-4. The average result for the combined data was also calculated. The table shows the error for most repeated tests to be 4-6%. The table also provides a means of comparing results obtained under different conditions.

Table 4-4: Summary of observed aggregation behaviour

Sediment	Conc (mg/L)	Shear Rate (s^{-1})	Salinity (ppt)	Average Difference in d90 results of repeated test (um)	Average d90 Result (um)	Average error (%)
Mfolozi	200	10	0	6.1	83.6	7.3
Mfolozi	200	10	10	6.6	101.1	6.5
Mfolozi	200	50	10	12.6	60.2	20.9
Mfolozi	50	10	0	11.3	49.1	23.0
Mfolozi	50	10	10	2.6	51.8	5.0
Mfolozi	50	50	10	N/A	37.3	N/A
Charters	200	10	0.5	3.1	73.2	4.2
Charters	200	10	10	1.9	66.9	2.8
Charters	200	50	10	3.9	63.2	6.2
Charters	50	10	0.5	2.5	84.1	3.0
Charters	50	10	10	4	84.3	4.7
Charters	50	50	10	2.1	48.1	4.4

The average results shown in the table have been used to support conclusions made in this section.

- For both Mfolozi concentrations, the addition of salinity resulted in larger flocs
- For the Charters Creek 200mg/L results, the addition of salinity did not result in a n increase in floc size, this is attributed to imaging difficulties
- For all concentrations of Mfolozi and Charters Creek sediments, the increase in shear from $10s^{-1}$ to $50s^{-1}$ resulted in a decrease in floc size.
- For Mfolozi sediments, the increase in concentration from 50mg/L to 200mg/L resulted in an increase in floc size. This was not observed for Charters Creek sediments, and has been attributed to experiemental error.
- The Mfolozi sediments followed the expected trends when the drivers were changed.
- The Charters Creek sediments did not.

In the absence of sufficient data, the basis of this comparison is the simple statistical calculation in table 4-4. If the sample size of available results was larger, the T-test is the preferred method.

4.2.2. Deflocculation tests

Deflocculation tests were performed on solutions immediately after the aggregation tests. The shear rate was incrementally increased and images were taken to capture the response of the floc population. The median and 90^{th} percentile of the floc population were measured. The results are presented in figures 4-8 and 4-9 below. Note that as each aggregation test was repeated, so to were the deflocculation tests. The results of both tests were combined and plotted together in figures 4-8 and 4-9.

The test results show that flocs break up when the shear rate is incrementally increased from $10s^{-1}$ to $50s^{-1}$. This breakup is significant for the d_{90} floc size (figure 4-8 B and 4-9 B). The median floc size did not respond as strongly. This indicates that the large flocs which formed during the aggregation tests are more fragile and sensitive to breakup than the rest of the population. This behaviour corresponds with observations made in literature on the fragile nature of macroflocs. (See section 2.3). The weak reduction in median floc size (4-8 A and 4-9 A) suggests that finer flocs are more robust and less prone to breakup. This corresponds with observations of the nature of microflocs in literature. In all of the results it is observed that, when the initial floc size was lower, less floc breakup occurred. This is particularly noticeable for the Mfolozi 50mg/L solutions which showed lower floc breakup in comparison to 200mg/L (figure 4-8B), but contained smaller flocs to begin with at $10s^{-1}$. The explanation for this corresponds to the one given above. The response of the floc population depended on the initial state of the flocs at $10s^{-1}$. It did not appear to be dependent on the salinity and concentration of the solutions. Furthermore similar behaviour was observed for both Mfolozi (figure 4-8) and Charters Creek (figure 4-9) solutions.

Time scales:

The time scale for floc breakup is clearly shorter than the time scale for aggregation. The aggregation tests showed that flocs require a period of 50-70minutes to fully develop. The deflocculation tests show that flocs require a period less than 5 minutes to breakup when the shear rate is increased. Similar observations were made in Verney et al (2010). Flocs breakup quickly in response to the high shear stresses associated with turbulent eddies. By contrast it takes a longer period of time for flocs to constructively interact through effective collisions.

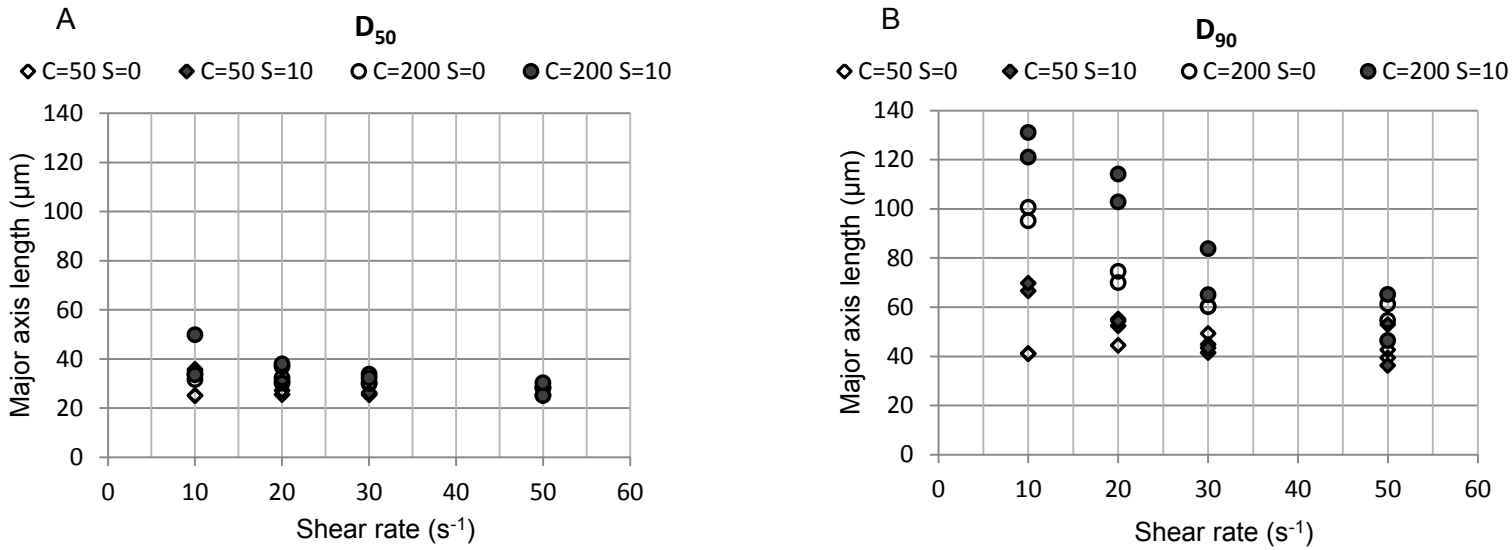

Figure 4-8: A: Response of Mfolozi D_{50} floc size to incremental increases in shear rate. B: Response of Mfolozi D_{90} floc size to incremental increases in shear rate. Key: C – suspended sediment concentration (mg/L), S – salinity (ppt), G – shear rate (s^{-1}).

Imaging difficulties at high shear rates:

There were problems detecting flocs at high shear rates and low concentrations. This problem was experienced in certain aggregation tests and has been discussed. Most tests were unaffected. It may cause certain $50s^{-1}$ shear rate results to be over-estimated. The causes of this problem are addressed in section 4.3. Despite this, the results still show the expected general trends and are acceptable. It is reasonable to assume that the floc size will continue to decrease if the shear rate is increased. This would be difficult to show in a laboratory test given the imaging difficulties experienced.

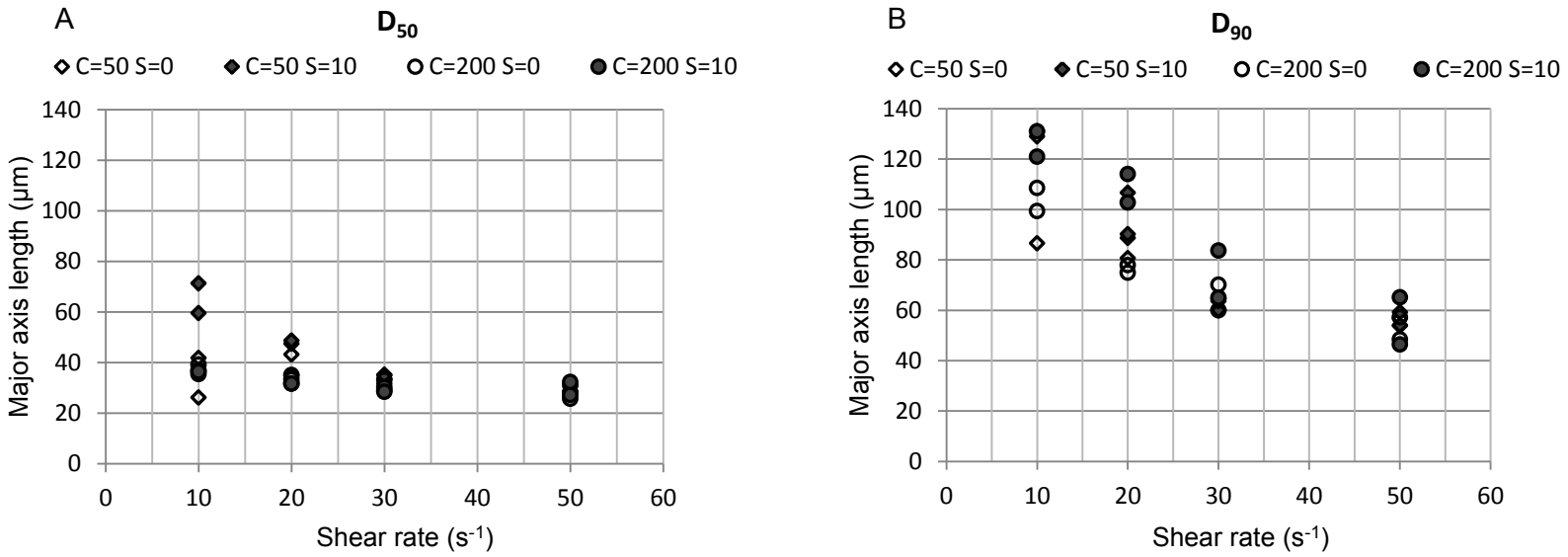

Figure 4-9: A: Response of Charters Creek D_{50} floc size to incremental increases in shear rate. B: Response of Charters Creek D_{90} floc size to incremental increases in shear rate. Key: C – suspended sediment concentration (mg/L), S – salinity (ppt), G – shear rate (s^{-1}).

Influence of Kolmogorov microscale:

The d90 floc size was compared to the Kolmogorov microscale at each shear rate. The d90 major axis length is assumed to represent the maximum floc size. The single maximum floc size measured was often a large organic particle (e.g.: a small twig) and was a poor representative of the maximum

floc size. The d90 floc size did not exceed the Kolmogorov microscale during the tests. Floc sizes were all more than 100µm lower than the Kolmogorov microscale. This is shown in figure 4-10 A.This behaviour corresponds to observations in literature shown in figure 4-10 B. It indicates that floc sizes are limited by the size of the smallest eddies present. Flocs that grow larger than this size are broken up. The K-microscale is not the only factor which limits the size of flocs. Floc growth is limited in size by the chemical flocculation potential of the sediment and the suspended sediment concentration. These effects were observed in the aggregation tests. In the absence of all other limiting factors, floc size is limited by the Kolmogorov microscale. The Mfolozi and Charters Creek sediments appear to have a limited flocculation potential. This may be attributed to silt dominance and low clay content.

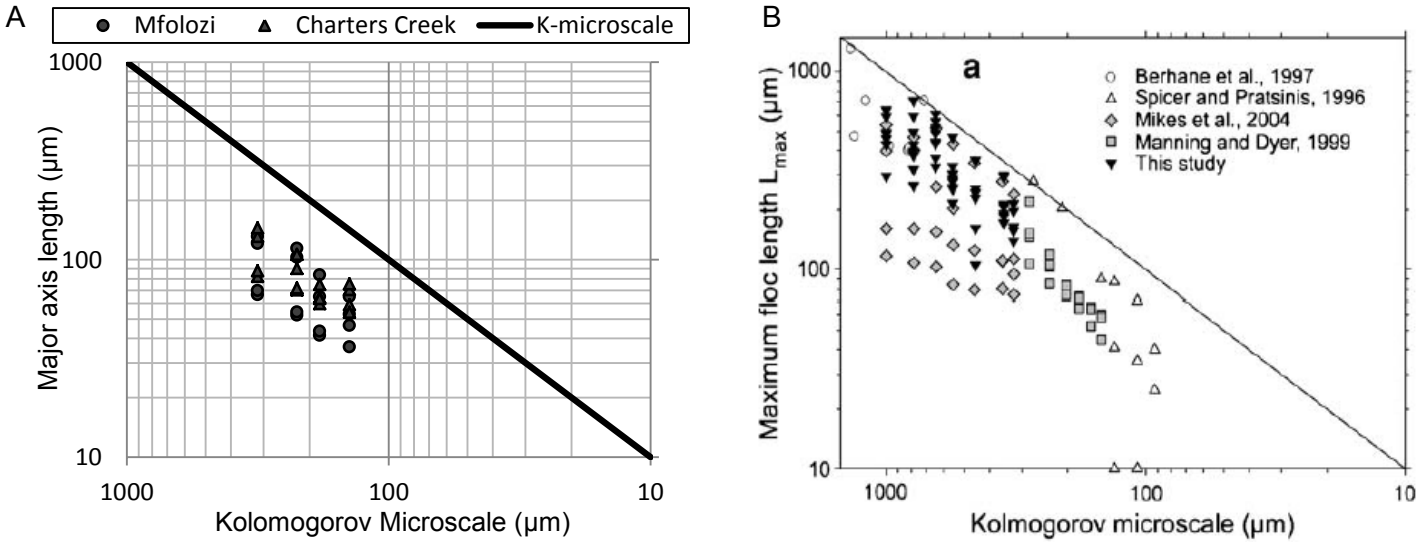

Figure 4-10: A: Comparison between the largest D_{90}Mfolozi and Charters Creek floc sizes with the Kolmogorov microscale. B: Verney et al. (2009) showing the limiting influence of the Kolmogorov microscale on maximum floc size.

Relevance of deflocculation test results

The results of the deflocculation tests have shown that flocs break apart when shear is increased. A flocculated suspension is vulnerable to destruction by turbulent shear. Therefore turbulent flow and high energy structures (such as waves) will result in floc breakup in the field. Turbulence in the Mfolozi estuary is produced by tidal flow, river flow and waves. Turbulence in Lake St Lucia is produced mainly by wind waves. In both estuaries there is significant potential for sediment resuspension and floc destruction to occur. This will likely inhibit settlement in the field. This ought to be considered in sediment transport studies.

The results validate the conclusions made in section 4.2.1. that, the optimal shear rate for flocculation is $10s^{-1}$. In the figures above it is shown that floc size progressively decreases as the shear rate is increased from $10s^{-1}$ to $50s^{-1}$. The performance at low shear is uncertain. It is investigated in the section that follows.

Repeatibility

Each deflocculation tests was repeated. The limited sample size of test results (4 results) limited the application of statistical inference tests. It was therefore decided to produce a qualitative comparison based on the figures produced from the results. This qualitative comparison is supported by simple statistics presented in table 4-5 on the following page. The table shows the average difference between each result of the repeated tests. It also provides the average d90 result. The results of the repeated tests may be followed in figures 4-8 and 4-9. The largest difference between any two test results was 20µm. The average difference was generally less that 5µm, which yields an error of 5-10% depending on the magnitude of the result. Sources of error must be considered when assessing repeatability. The precision of the results depends on the quality of the images and the image processing technique (as discussed in section 4.2.1 amd elabourated in 4.3).By comparing the results in figures 4-8 ,4-9 and table 4-5, the qualitative conclusion is that the tests are repeatable.

Table 4-5: Summary of Deflocculation behaviour

Sediment	Conc (mg/L)	Shear Rate (s^{-1})	Salinity (ppt)	Average Difference in d90 results of repeated tests (µm)	Average Result (µm)	Average error (%)
Mfolozi	200	10	0	3.7	69.6	5.3
Mfolozi	200	10	10	7.6	87.1	8.7
Mfolozi	50	10	0	8.1	55.3	14.6
Mfolozi	50	10	10	1.1	34.7	3.2
Charters	200	10	0.5	3.5	66.9	5.2
Charters	200	10	10	2.4	69.1	3.5
Charters	50	10	0.5	1.1	71.7	1.5
Charters	50	10	10	4.6	71.6	6.4

4.2.3. Aggregation at low shear rates

Certain aggregation tests were performed at a shear rate of $5s^{-1}$ in preliminary tests. Settlement occurred during the course of the test. Floc growth was observed during the initial part of the test. Thereafter the floc size and concentration decreased. There were small accumulations of settled sediment at the bottom of the jar. Figure 4-11 shows the decrease in d90 over the latter part of the aggregation test. The median floc size did not substantially decrease. Mfolozi sediment at C=200g/L, S=10ppt, and $G=5^{-1}$ was used in the test. Similar results were observed when other solutions were subject to the same shear rate. It is evident that flocs formed in the jar and settled. The result supports the notion that aggregation is favoured at low shear rates. It is not possible to determine the size of the settled flocs. The minimum shear rate at which settlement did not occur was $10s^{-1}$. The aggregation tests were performed at $10s^{-1}$ to provide comparable results. In hindsight it is noted that settlement could have been reduced by changing the shape of the jar to a conical base. Such a shape promotes sediment resuspension.

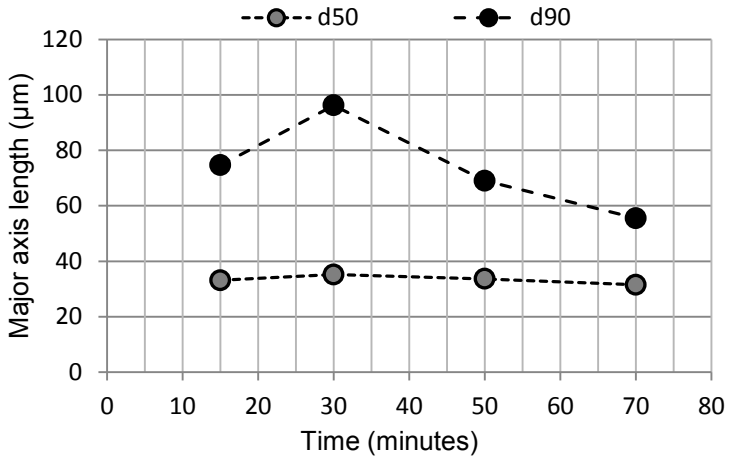

Figure 4-11: Aggregate growth of 200mg/L 10ppt Mfolozi sediment at shear rate $5s^{-1}$. d50 – 50^{th} percentile diameter, d90 – 90^{th} percentile diameter.

A deflocculation test was also performed on the solution. The results are displayed in figure 4-12. When the shear rate was increased from $5s^{-1}$ to $10s^{-1}$ both the D_{50} and D_{90} increased. The D_{90} increased by 120µm to 180µm. This increase was caused by the re-suspension of sediment which had settled during the aggregation test. These flocs were larger than those that formed during the aggregation tests at $10s^{-1}$ in figure 4-3 B. This is possibly attributed to flocs forming in collisions of deposited material. The floc size was however less than the Kolmogorov microscale (316µm).When the shear rate was further increased the floc behaviour was similar to that observed previous tests (figure 4-8B). The small increase in floc size observed at $50s^{-1}$ is the result of error induced by poor particle visibility.

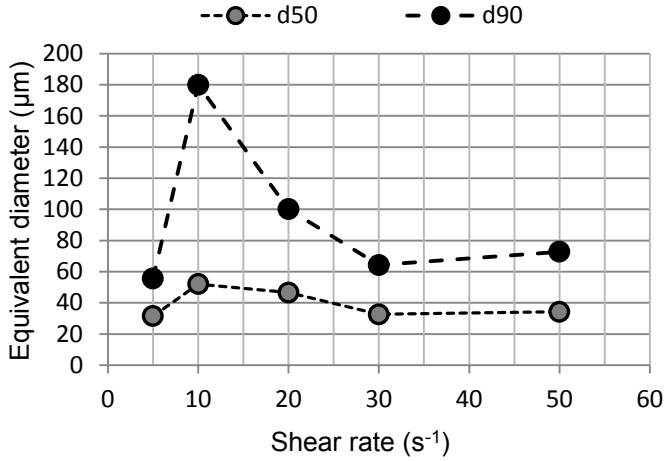

Figure 4-12: The response of 200mg/L Mfolozi sediment formed at $5s^{-1}$ to increases in shear rate. d50 – 50^{th} percentile diameter, d90 – 90^{th} percentile diameter.

4.2.4. Aggregation time scale

The aggregation timescale for both Mfolozi and Charters Creek sediment solutions was generally under 70 minutes. This was observed during preliminary tests. The results of the aggregation tests (figures 4-2 to 4-7) show that full aggregate development took 50-70 minutes. Aggregate size remains approximately constant after 70 minutes. This is illustrated in figure 4-13 below. The figure shows no change in D_{50} and small fluctuations in D_{90} after 70minutes. Aggregate growth prior to 70 minutes corresponds to that shown in figure 4-3B for 200mg/L 10ppt Mfolozi sediment at $G=10s^{-1}$. This figure supports the decision to run the aggregation tests for 70minutes.

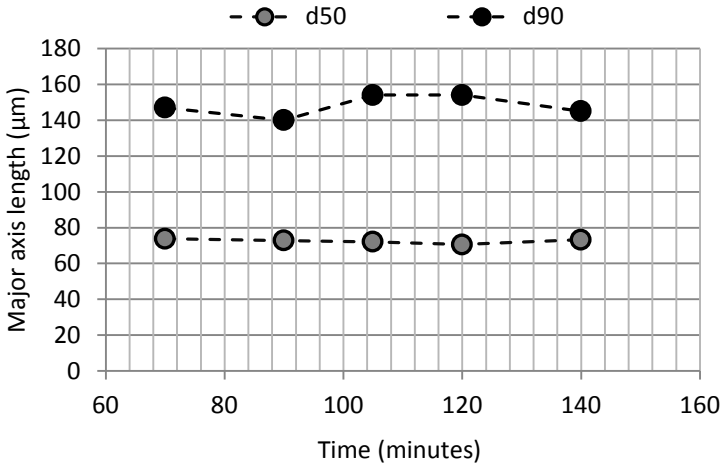

Figure 4-13: Aggregate development from 70-140 minutes for 200mg/L Mfolozi sediment at $G=10s^{-1}$.

A series of images showing aggregate development over 70min is displayed in plate 4-3 below. By 30 minutes significant flocculation had occurred.

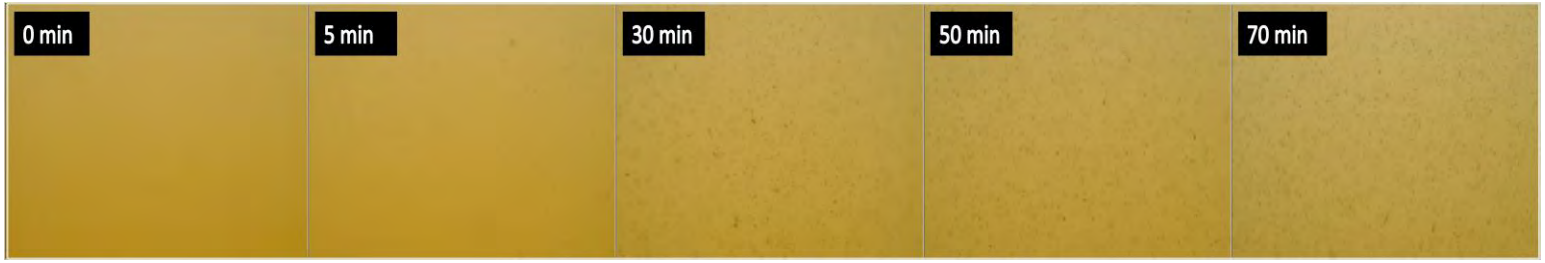

Plate 4-3: Images showing the formation of aggregates of 200mg/L Mfolozi sediment ($G=10s^{-1}$, S=10ppt)

With reference to the previous section (4.2.3 -Aggregation at low shear rates): Images showing floc destruction during the deflocculation test are shown in plate 4-4 below. The images clearly correspond with figure 4-12. Observe that the 70 minute flocs at $G=5s^{-1}$ are finer than those formed at $G=10s^{-1}$ above. This is attributed to settlement at $5s^{-1}$. The increase in floc size due to re-suspension of settled particles from $5s^{-1}$ to $10s^{-1}$ is clearly visible below. The decrease in floc size from $G=10s^{-1}$ to $G=50s^{-1}$ is clearly visible.

Plate 4-4: Images showing the deflocculation test performed on 200mg/L Mfolozi sediment (Initial $G=5s^{-1}$, S=10ppt)

4.2.5. Volume-based floc size distributions:

The image analysis results of the aggregation tests show that the floc population is dominated by finer particles. The mass and volume-base distributions do not follow the same trend as the population distribution. Floc volume distributions were calculated from the areas of flocs measured at 70 minutes during the aggregation tests. The results are shown in figures 4-14 to 4-17 below. The floc size results from the aggregation tests indicated that macrofloc population is significantly less than the microfloc population. The macrofloc population however constitutes a greater proportion of the floc mass and volume. This is evident in the figures below. The figures also show that the floc size at which the mass is concentrated changes with concentration, salinity and shear rate. For simplicity all flocs are assumed to have equal density. Floc volume and mass are therefore assumed to be linearly proportional to the area of the floc. It is acknowledged that these assumptions may be inaccurate. If the three dimensional spherical-type shape of the flocs was considered, larger flocs would constitute a greater proportion of the total mass. Measured flocs are separated into 25µm bins.

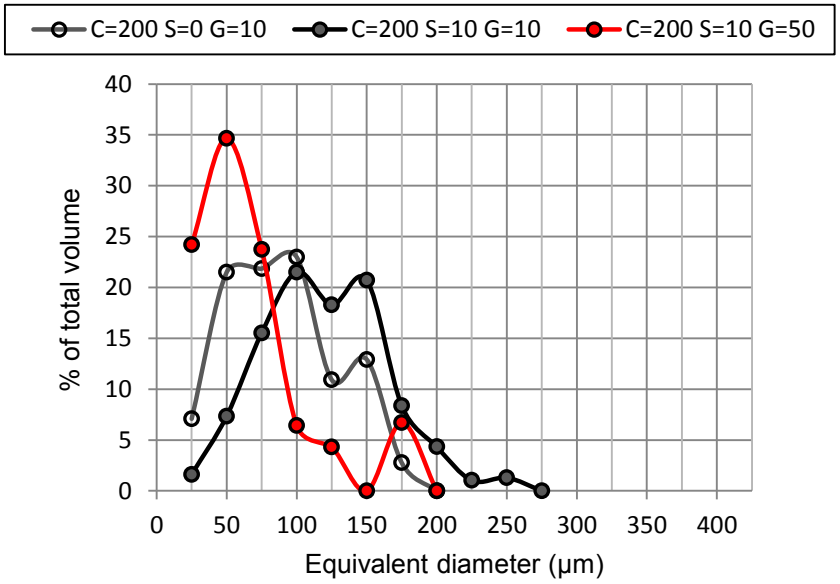

Figure 4-14: Floc volume distribution from the 200mg/L Mfolozi aggregation tests. Key: C – suspended sediment concentration (mg/L), S- salinity (ppt), G – shear rate (s^{-1}).

The volume distributions of results in figure 4-14 show the floc mass to be concentrated at different floc sizes under different conditions. At 10ppt and $10s^{-1}$ the floc mass was concentrated between 100 and 150µm. At 0ppt, the mass was concentrated between 50 and 100mg/L. The mass was concentrated at large floc sizes when the salinity was increased. This result was expected given that a higher population of large flocs was observed in the 10ppt

solution (figure 4-3 B). The floc mass of the $50s^{-1}$ solution was concentrated at lower size range than the $10s^{-1}$ solution. The mass was concentrated at 50µm. Finer flocs were formed at the high shear rate. These flocs clearly dominate the mass of the floc population. A similar result was observed for the Charters Creek 200mg/L aggregation tests shown in figure 4-15 below. The flocs formed at $50s^{-1}$ were smaller with mass concentrated at 50µm. The mass $10s^{-1}$flocs at both 0 and 10ppt was distributed over a greater range of floc sizes. There were imaging difficulties during the 200mg/L tests as previously discussed. These are likely to have affected the distributions in figure 4-15 below.

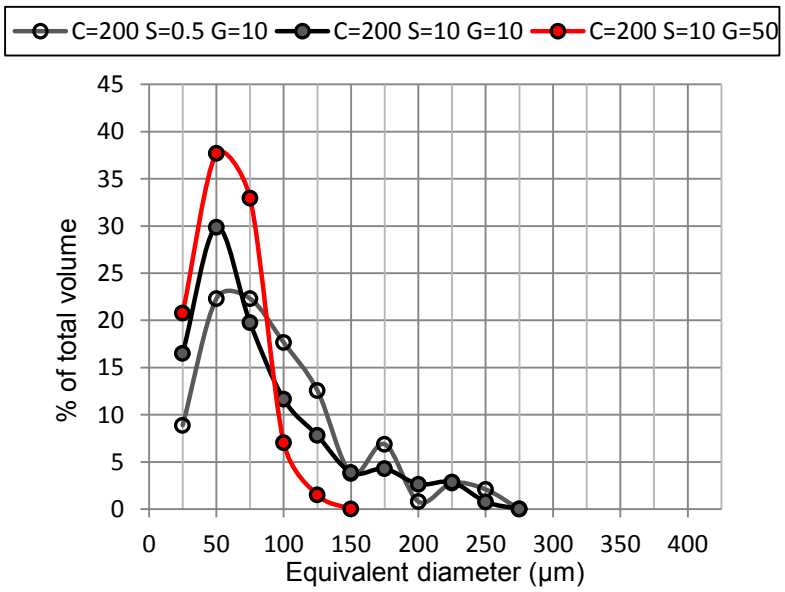

Figure 4-15: Floc volume distributions of the 200mg/L Charters Creek aggregation tests. Key: C – suspended sediment concentration (mg/L), S- salinity (ppt), G – shear rate (s^{-1}).

The influence of suspended sediment concentration on the floc mass distribution may be observed in figure 4-16 below. The floc mass of the 200mg/L sediment was concentrated at a larger floc size than the 50mg/L sediment. This is because larger flocs were able to form at 200mg/L due to a higher frequency of effective collisions between particles.

Deflocculation tests:

The volume-based distributions of flocs at each stage of the deflocculation test performed on 200mg/L Mfolozi sediment was calculated and presented in figure 4-17. During the test d_{90} floc size decreased as the shear rate was incrementally increased. The increasing shear stress caused larger flocs to break apart. Figure 4-17 shows that as the shear rate is increased, the floc mass moves from large floc sizes to smaller floc sizes. This implies that at high shear stresses, most of the sediment mass is constituted by smaller flocs. The figures above and

below all show that at a shear rate of $50s^{-1}$ the floc mass is concentrated in microflocs between 25 and 75µm while at $10s^{-1}$ it is concentrated in larger flocs (100-150µm for Mfolozi sediments).

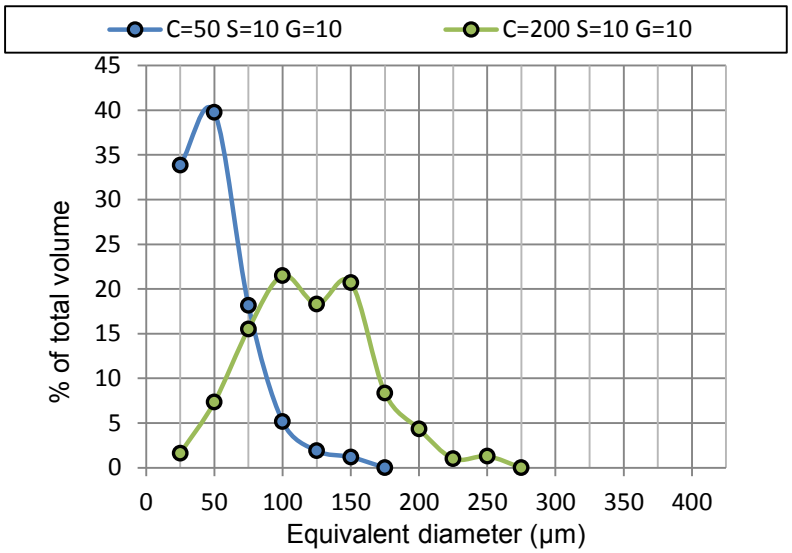

Figure 4-16: Floc volume distributions of 50mg/L and 200mg/L Mfolozi aggregation tests. Key: C – suspended sediment concentration (mg/L), S- salinity (ppt), G – shear rate (s^{-1}).

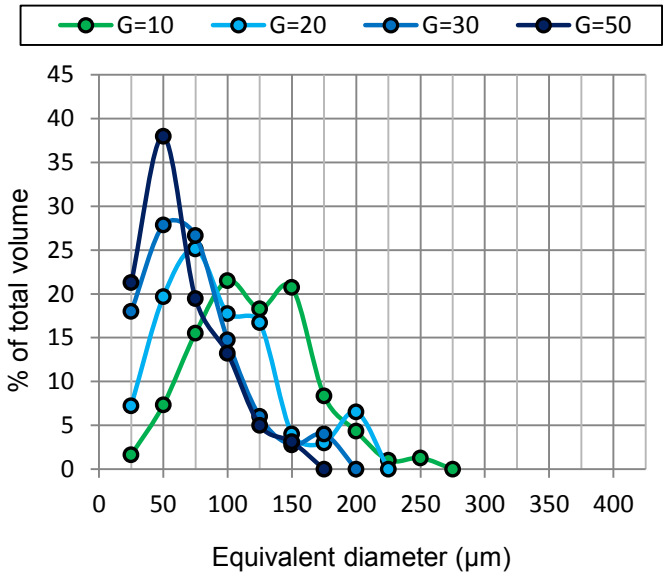

Figure 4-17: Floc volume distributions for 200mg/L Mfolozi sediment at incrementally increasing shear rates. Key: C – suspended sediment concentration (mg/L), S- salinity (ppt), G – shear rate (s^{-1}).

Relevance of volume-based distribution results

The results presented in figures 4-14 to 4-17 all have implications for sediment transport modelling. It is clear that most of the sediment mass is concentrated in particles of 50µm equivalent diameter or greater. In conditions of low shear and high concentration, the sediment mass is concentrated in macroflocs. The observation that macroflocs and large microflocs form a small percentage of the floc population is now less important. Most of the suspended mass will settle in the form of macroflocs or large microflocs. The suitable approach to estimating the mass settling flux would be to find a characteristic settling velocity for the floc size at which the sediment mass is concentrated. This is discussed in more detail later.

Figure 4-17 validates the prior mentioned conclusion that the optimal shear rate is $10s^{-1}$. The volume-based distribution for $10s^{-1}$ showed a higher proportion (>50%) of mass concentrated in macroflocs the the distributions for $20s^{-1}$, $30s^{-1}$ and $50s^{-1}$. It furthermore shows volume-based distributions concentrated at progressively low floc sizes as shear rate is increased.

Limitations of results:

The aggregation test results did not include flocs less than 20µm in diameter. The influence of these particles is uncertain. If the population of unflocculated material is significant, the volume-based distributions will be inaccurate. This may already be so for test results at $G=50s^{-1}$. If the mass of unflocculated material is significant, this needs to be considered in sediment transport studies and a characteristic settling velocity for these particles requires estimation. This issue is elaborated upon in section 4.4.8.

It is acknowledged that the distributions above are crudely based on the areas of the observed flocs. Despite this, the distributions were sufficient to demonstrate expected trends. It is incorrect to assume a uniform floc density. Floc effective density decreases when floc size increases. The effective density of smaller flocs is higher than those of larger flocs. This is shown further on in section 4.4. The difference in densities of flocs larger than 50µm is generally not significant (less than $100kg/m^3$). Correcting for varying densities is not anticipated to significantly change the observed results. It must also be remembered that the distributions are based on images of flocs. Limitations of the image processing technique will reduce the quality of the distributions. Images captured during conditions where flocs are too fine to detect will also lead to poorer quality results if used. Experimental error is discussed in section 4.3 below.

Note that the floc equivalent diameter is used instead of major axis length. The equivalent diameter provides a more accurate approximation of the mass of a floc when used. This parameter is used in the settling tests.

4.2.6. Conclusions from flocculation tests

The flocculation tests were able to show the dynamic behaviour of cohesive sediments in response to various drivers. Both before and after testing the populations of particle size distributions were dominated by microflocs. Macroflocs formed a small percentage of the total population. Under the ideal conditions of salinity and low shear both Mfolozi and Charters Creek sediments displayed a tendency to flocculate. Large flocs in excess of 100µm formed. The flocculation behaviour was best detected in the 90^{th} percentile of the floc size distribution.

At high shear rates large flocs did not form. At low shear stress, settlement occurred in the jar. The influence of turbulent shear on floc breakup was shown in deflocculation tests. As the shear rate was incrementally increased above 10ppt, flocs were observed to breakup. The largest floc sizes were smaller than the Kolmogorov microscale. The Kolmogorov microscale limited the size of flocs which formed.

Salinity was observed to increase flocculation potential. Flocs formed in freshwater or low salinity were significantly smaller than those which formed in saline conditions.

Flocculation was enhanced by increasing the suspended sediment concentration. This is attributed to increased collision frequency. This was difficult to observe in higher concentrations due to floc overlap.

Despite the floc population being dominated by fine microflocs, the flocculated mass was generally concentrated in large microflocs and macroflocs. These aggregates are anticipated to dominate the mass settling flux of the sediment. The mass was concentrated in fine particles when flocculation did not occur.

The flocculation and deflocculation tests were repeatable.

4.3. Experimental Error

Several concerns with certain results have been discussed in sections 4.1 and 4.2. It was difficult to obtain an accurate floc size distribution during conditions when most flocs were small and when the suspended sediment concentration was high. Floc size statistics were possibly overestimated when the floc population was fine. Floc sizes were possibly underestimated when the suspended sediment concentration was high. The camera resolution limited the detectable particle size to 5.27µm. The resolution was reduced when the images were processed. Under certain conditions a background light intensity gradient provided further problems.

4.3.1. Image analysis at high concentrations

The image quality reduced when the suspended concentration was increased above 200mg/L. Particles in suspension start to overlap each other and it was difficult to distinguish the boundaries of individual flocs. This problem is made worse by reduced light transmission through the jar. The contrast between flocs and the background became poorer. Fewer particles were clearly visible. An aggregation test was performed on a 400mg/L solution of Charters Creek sediment (S=10ppt, G=10s^{-1}). An image of the solution after 70minutes is presented in plate 4-5. The particle size statistics after 50 and 70minutes are displayed in table 4-6. A binary image and histogram are presented in plate 4-6 and figure 4-18.

Table 4-6: Particle size statistics of 400mg/L Charters Creek sediment after 50 and 70minutes

	50min results			**70min results**		
	Area (μm^2)	Equivalent Diameter (µm)	Major Axis Length (µm)	Area (μm^2)	Equivalent Diameter (µm)	Major Axis Length (µm)
Mean	1696	34	29	1499	34	28
d25	472	22	22	472	22	22
d50	639	25	25	722	25	25
d75	1222	34	30	1291	35	30
d90	5777	62	39	3555	57	37
Max	17914	151	251	19136	156	208

Plate 4-5: Image of Charters Creek 400mg/L solution after 70minutes of aggregation

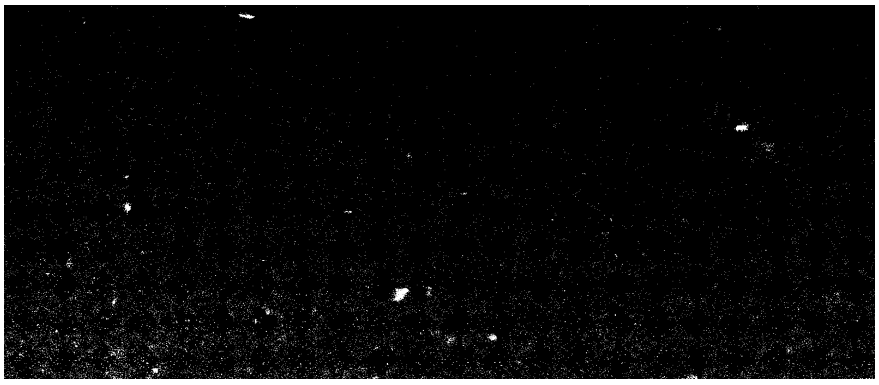

Plate 4-6: Cropped binary image of 400mg/L Charters Creek solution after 70minutes

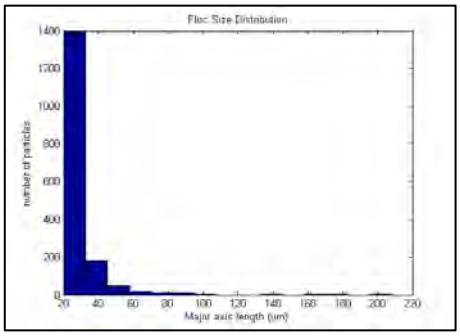

Figure 4-18: Floc size distribution of 400mg/L Charters Creek solution after 70minutes

Very few particles were visible at 400mg/L. Visible particles were usually large organic particles and not sediment aggregates. The best quality binary images were able to show these particles and high populations of very fine particles (which were not particles). The floc size distribution shown in figure 4-18 reflects this. The small particles visible are the result of noise created during the binarization process and are not aggregates. Large aggregates are expected to develop at higher concentrations due to an increased frequency of effective collisions. This result was observed for Mfolozi sediment when the concentration was increased from 50mg/L to 200mg/L and has been observed in literature. The technique is not able to show this at 400mg/L. The statistics presented in table 4-6 are significantly lower than those measured at 200mg/L (figure 4-3 B). It is concluded that the technique is unreliable at concentrations above 200mg/L.

4.3.2. Image analysis of fine suspensions

Image analysis was difficult when solutions contained very fine flocs. These particles cannot accurately be detected below 20µm despite a camera resolution of 5.27µm. This is because there is insufficient contrast between the background and fine flocs. It is often evident that the solution is predominantly composed of fine flocs. This generally occurs during the initial period of aggregation test and during tests at high shear rates. The technique is not able to quantitatively show this in the form of accurate statistics. Larger flocs are accurately detected. The number of these particles is insignificant in comparison to the population of fine particles. However only these particles will be analysed because they are the only detectable particles. There is therefore a smaller population composed of larger particles analysed. The particle size statistics are therefore over-estimated in favour of larger flocs. This is shown in table 4-5 where the 70minute results of 50mg/L Mfolozi sediment at shear rates of $10s^{-1}$ and $50s^{-1}$ are compared. The results show the expected trend where smaller flocs develop at higher shear. However the d90 floc size of the $50s^{-1}$ test was higher than that of the $10s^{-1}$ test. When two of the captured images at 70minutes (Plates 4-7 and 4-8) are compared it is obvious that this is incorrect. This substantiates the claim that floc sizes may be overestimated. It is likely that all the statistics measured may have been too over-estimated to various degrees.

Table 4-7: Comparison between the results of 50mg/L Mfolozi sediment at G=10 and G=50s^{-1}

	S=10ppt C=50mg/L G=10s^{-1} t=70min			**S=10ppt C=50mg/L G=50s^{-1} t=70min**		
	Area (μm^2)	Equivalent Diameter (μm)	Major Axis Length (μm)	Area (μm^2)	Equivalent Diameter (μm)	Major Axis Length (μm)
Mean	1384	37	42	1472	34	30
d25	611	26	26	500	22	22
d50	944	33	36	667	26	25
d75	1611	43	50	1194	34	31
d90	2666	56	70	4546	62	41
Max	24551	177	311	11165	119	306

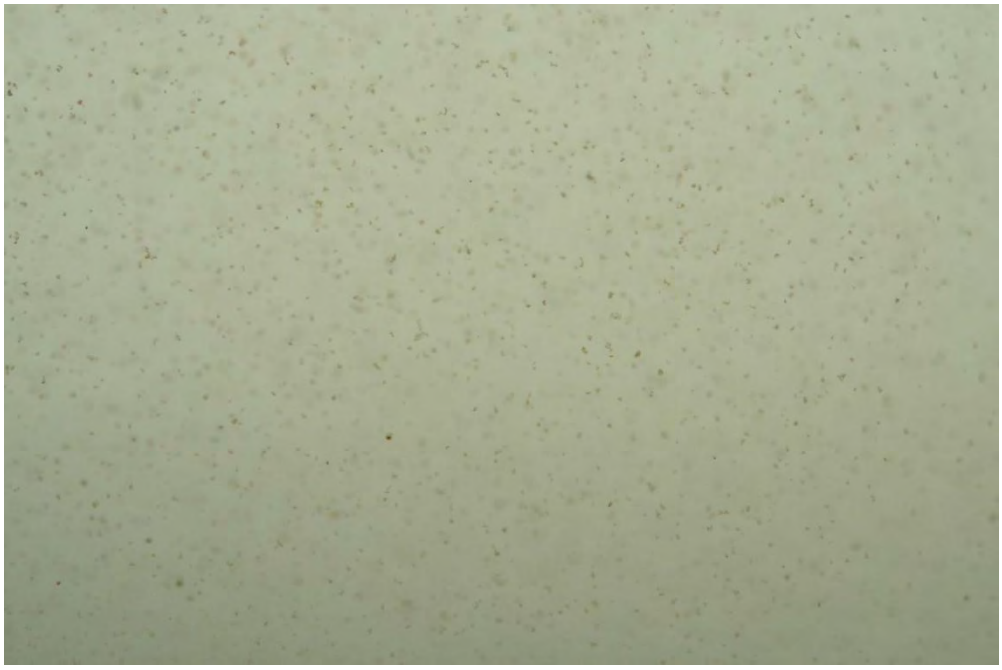

Plate 4-7: Image of 50mg/L Mfolozi sediment after 70minutes aggregation at G=10s^{-1}

Plate 4-8: Image of 50mg/L Mfolozi sediment after 70minutes aggregation at G=50s^{-1}

It must be acknowledge that all of the results are over-estimated because all particles under 20µm were filtered out. It is unreasonable to expect the technique to have the same resolution as a microscope, Coulter Counter or the Malvern Mastersizer. Furthermore most techniques in literature also have a limited resolution. The uncertainty regarding particles finer than 20µm is addressed in section 4.4.8. Despite the development of macroflocs, it is possible that volume based-distribution may contain a large proportion of particles finer than 20µm.

The ability to capture images of fine solutions can be improved. This may be done by using a different light source and by improving the camera resolution. A light sheet of greater intensity through the side of the beaker may provide better illumination and contrast between particles. The use of superior lens will increase the magnification and improve the resolution of the images. The use of a camera with superior image sensor will also improve the resolution. Lighting conditions and image resolution are not the only factors which hinder the analysis of fine particles. Aspects of the image processing procedure reduce the potential to detect smaller particles.

4.3.3. Image processing limitations

Images captured during the aggregation and deflocculation tests are converted to binary images and suitable areas are cropped for further processing. The binary threshold is selected in order to best preserve the sizes and shapes of the flocs. There is usually a background

intensity gradient which causes certain parts of the binarized image to be lighter and other parts darker. This problem is overcome by cropping an area in-between where image quality is preserved. The original and cropped-binary images are compared and scrutinized before the image is accepted. The texture of the background presents a problem when a binary image is created. Images are captured in RAW format the background has a texture which is visible when zoomed to pixel level. Certain pixels are darker and others lighter. When the darker pixels are below the selected binary threshold, they appear as black particles in the binary image. The particles are 1-2 pixels in size and possibly larger in areas of the image of lower intensity. All particles less than 20µm in size are filtered out to prevent this noise from influencing the results.

Particles within the depth of field of the lens appear clear and in focus. Particles out of focus may be problematic. Out of focus flocs appear lighter and are generally removed when the image is binarized. Sometimes the flocs are darker and visible in the binary image. Out of focus flocs may thus be larger or smaller than their actual size. This may affect the accuracy of the results when there are many out of focus flocs. The flocs may also appear as multiple smaller flocs. This will also reduce the accuracy of the floc size distribution. It is difficult to determine the influence of these problems on the accuracy of the results. However, the cropped binary images were inspected for these problems. Problematic images were rejected and re-processed at a different threshold.

4.3.4. Reproducibility of results:

The aggregation and deflocculation tests were not anticipated to yield precise results. Each test conducted under a specific set of conditions was repeated to assess the reproducibility of the results. The results of both tests have been combined and plotted in figures 4-2, 3, 4, 5, 6, 7, 8 and 9. Qualitatively, the repeated tests generally showed a common trend. The points of the two test results were generally reasonably close to eachother. However the results of certain tests varied by 30µm, creating significant error. For example, the 0ppt, 70 minute result in figure 4-6A showed a difference of 44.5 µm. This was summarized in table 4-4 (page 86) where the average difference between the results of the two tests have been compared and average errors were estimated. The average difference between the results at each stage of repeated tests was 4-6%.

It is unfortunate that the nature of the experiments limited the amount of observations that could be made. For each aggregation test, only 5 results were produced (1 floc size result for each observation, observations were made at 5, 10, 30, 50 and 70 minutes). For each deflocculation

test only 4 results were produced (G= 10, 20, 30, 50s^{-1}). The number of observations made limited the sample size for each set of results. This made a quantitative statistical inference analysis unfeasible. Had there been more results per test, a T-test would have been a suitable method of assessing the reproducibility of the results.

It must be acknowledged that the analysis of digital images is a time consuming process and that a significant quantitiy of work would be required to obtain more data. The results displayed in figures 4-2 to 4-15 and tables 4-4 to 4-5 provide sufficient evidence of reproducibility despite some errors visible.

The reproducibility of results is dependant on the precision of the tests. There are numerous factors which potentially reduce the precision of the tests, such as the following:

- The quality of the images captured (image resolution, lighting conditions, clarity, focus, the scale of the images, lens errors – abbarration,)
- The image processing procedure (thresholding, creation of binary image, cropping)
- The number of images used per test

Under the same conditions (concentration, salinity and shear rate), two tests performed should theoretically produce the same results. It is however acceptable to expect small errors due to the factors above.

An important observation from figures 4-2 to 4-9 is the proximity of independent tests performed under identical conditions. The tests have not been individually labelled. However the results of individual tests are apparent and easily identified.

The results of identical tests performed on samples from different seasons are expected to differ with the type of sediment present in suspension. Regretibly samples were not obtained from different seasons to validate this statement.

4.4. Settling Tests

4.4.1. Introduction

The settling velocities of sediments were measured in the laboratory using a still settling column. The technique appeared simple but it required careful attention to the preparation of the solution within the column and to the transfer of flocs using a pipette. There were problems with density currents during preliminary tests. The technique has been improved and the problems were largely eliminated. Tests were performed on Mfolozi and Charters Creek sediments immediately after the aggregation tests. General trends between settling velocity, equivalent diameter and effective density were observed. The variation of these relationships with other conditions such as suspended sediment concentration was also observed. Characteristic settling velocities for different particle sizes were obtained. This gives insight into the settling rate of suspensions when observed with the particle size distribution obtained in the aggregation tests.

4.4.2. Observed general trends

The settling velocity of flocs increased with their equivalent diameters. The trend was strong in certain tests and weak in other tests where scatter was observed. A correlation analysis was performed on the results of all the settling tests. The results are presented in table 4-8. In certain tests either fewer settling flocs were tracked or the size range of observed flocs was small. The correlation was poor under these conditions. A stronger trend is expected if a greater size range of settling flocs is observed. Floc settling velocity was expected to increase with equivalent diameter. Settling velocity was proportional to the square of the particle diameter in Stoke's Law. This trend is also mentioned in literature. The equivalent diameter was used instead of the major axis length as it better approximates the mass of the floc.

The effective density of flocs decreased with their equivalent diameter. This trend was strongly observed throughout the tests.This is evident in the ρ values in table 4-8, most of which exceeded -0.90, indicating strong monotonic relationships of decreasing density with diameter. The effective density of smaller flocs was significantly higher than that of larger flocs. This is particularly so for flocs less than 50µm in diameter. This behaviour was expected. The density of macroflocs was typically under 1100kg/m^3, with an excess density less than 100kg/m^3. Macroflocs were expected to have a lower effective density. The density range of macroflocs was acceptable (Verney, 2011 – Personal communication). The effective density of smaller microflocs typically exceeded 1300kg/m^3. Densities significantly higher than this were also

observed, but may be subject to some error to be discussed further on. Figures 4-20, 4-22 and 4-23 show the trends between effective density and floc size.

Table 4-8: Correlation analysis of measured settling velocities and effective densities with equivalent diameter

Mfolozi Sediments			Settling velocity – Equivalent diameter		Effective density – Equivalent diameter	
C (mg/L)	S (ppt)	G (s^{-1})	ρ	n	ρ	n
50	10	10	0.06	20	-0.87	20
50	10	50	0.78	9	-0.33	9
100	0	10	0.69	20	-0.94	20
100	5	10	0.82	20	-0.90	20
100	15	10	0.91	20	-0.99	20
200	0	10	0.54	31	-0.89	31
200	10	10	0.81	41	-0.97	41
200	10	50	0.12	23	-0.95	23
Charters Creek sediments						
50	10	10	0.74	61	-0.92	61
100	0.5	10	0.72	20	-0.63	20
100	5	10	0.53	20	-0.93	20
100	15	10	0.81	20	-0.94	20
200	0.5	10	0.38	14	-0.98	14
200	10	10	0.76	58	-0.94	58

Microflocs and macroflocs were observed in the settling tests. The settling velocity of microflocs (< 100µm for this comparison) was typically less than 0.5mm/s for Mfolozi sediments and 0.8mm/s for Charters Creek sediments. Microflocs were also observed to settle less than 0.1mm/s. Smaller microflocs settled slower than larger ones. The range of microfloc settling velocities may be observed in figures 4-19 to 4-23. It was difficult to track particles finer that 20µm (~4 pixels).

The settling velocity of macroflocs (>100µm) typically exceeded 0.4mm/s for Mfolozi sediments and 0.5mm/s for Charters Creek sediments. The settling velocities ranged from these values to 2mm/s. Larger macroflocs settled at 1mm/s and faster. Measured settling velocities varied with effective density. Settling velocities were lower when flocs were less dense. This occurred at low salinity and concentration.

The results indicate that microflocs are denser more robust aggregates with lower settling velocities. Macroflocs are large fragile, loosely-packed aggregates with higher settling velocities. These comments correspond to comments and observations of aggregates in literature.

4.4.3. Settlement velocity sensitivity to concentration, salinity and shear rate

The results of settling tests performed on Mfolozi and Charters Creek are presented in figures 4-19 to 4-23 below. The figures compared the settling behaviour under different conditions. Where possible, 95% confidence intervals have been included for the figures.

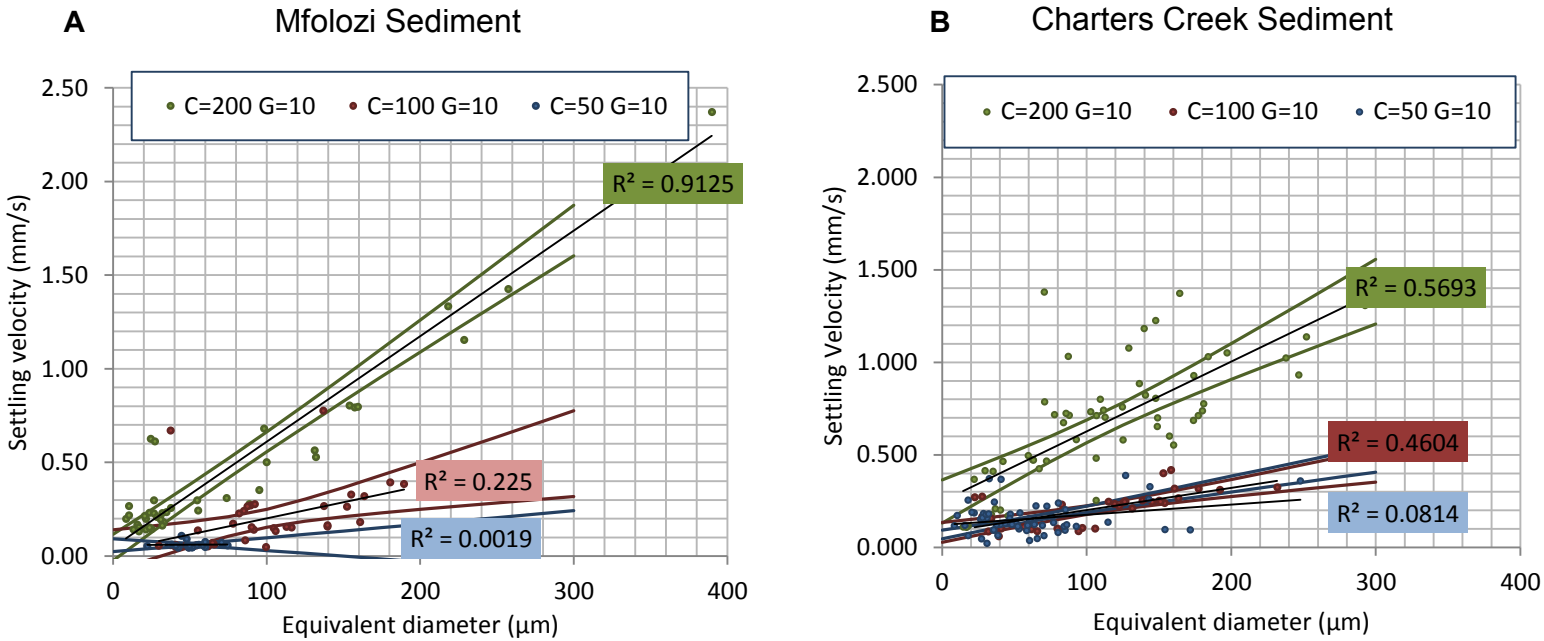

Figure 4-19: A: Settling velocity results for Mfolozi sediment at different concentrations B: Settling velocity results for Charters Creek sediment at different concentrations. Key: C – concentration (mg/L), G – shear rate (s^{-1}), all salinities 10ppt.

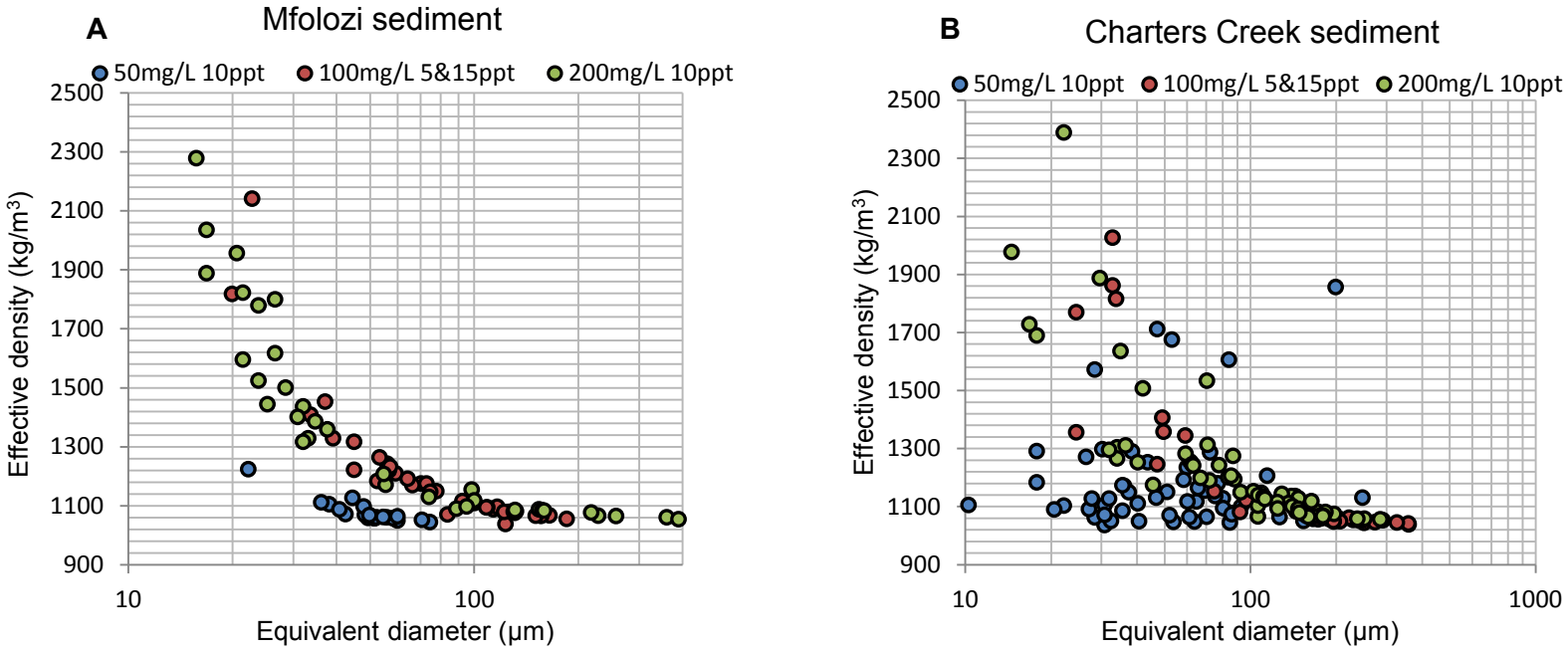

Figure 4-20: A: Effective density results for Mfolozi sediment at different concentrations. B: Effective density results for Charters Creek sediment at different concentrations.

Influence of suspended sediment concentration on settling velocity:

The settling velocity of flocs from the 100 and 200mg/L solutions were higher than those from the 50mg/L solutions. This is shown in figure 4-19 A and figure 4-19 B. The slope of the trend lines in both figures indicate that at 200mg/L, settling velocities are highest, followed by 100mg/L, where settling velocities are distinctly higher than at 50mg/L. The suspended sediment concentration influences the size of flocs that form during aggregation. Larger flocs form at higher concentrations due to an increased collision frequency. Denser flocs are expected to form under these conditions. Larger flocs and denser flocs will settle faster. The strength of certain linear relationships were poor, particularly for the 50mg/L solutions, this is attributed to high density variability in the small range of floc sizes observed in these conditions.

The effective densities of the settling flocs are shown in figures 4-20 A and 4-20 B.The results clearly show that flocs formed at 50mg/L are less dense than those formed at 100 and 200mg/L. There is no apparent trend when comparing the results at 100mg/L and 200mg/L. The outliers at 50mg/L in figure 4-20 B are assumed to be quartz particles.

In summary it is clear that smaller, less dense flocs are formed at lower concentrations while larger denser flocs are formed when the concentration is increased. This behaviour was expected and was discussed in sections 2.3 and 2.5.

Influence of salinity on settling velocity

The results of settling tests at different salinities are presented in figures 4-21 to 4-22. Figures 4-21 and 4-22 show that, at the same concentration, the settling velocities of flocs of saline solutions are higher than those of unsaline conditions. The trend lines for the saline solutions show larger slopes than those of the unsaline solutions. Furthermore a larger range of floc sizes is observed for saline conditions, suggesting the presence of aggregation. This is particularly evident in figure 4-21 B where saline flocs settled quicker than unsaline flocs of the same size. There were more large flocs observed in saline conditions. This trend was observed in the aggregation tests. The effective densities of the settling flocs are compared in figures 4-22 A and 4-22 B. The effective densities of Mfolozi flocs observed in figure 4-22 A show little sensitivity to salinity. The Charters Creek flocs in figure 4-22 B show distinctly higher effective densities in saline conditions.

In the aggregation tests it was observed that the flocculation potential of cohesive sediment increases when salinity is increased. In saline conditions larger and denser

flocs are expected to form. These flocs will have a higher settling velocity. This was observed in the settling tests. Larger flocs were observed in saline conditions. These flocs had higher settling velocities. Saline flocs were denser than unsaline flocs of the same size. The mass settling flux of a saline suspension is therefore expected to be higher than that of a freshwater suspension.

The coefficients of correlation suggested that the results displayed monotonic, yet not necessarily linear behaviour.

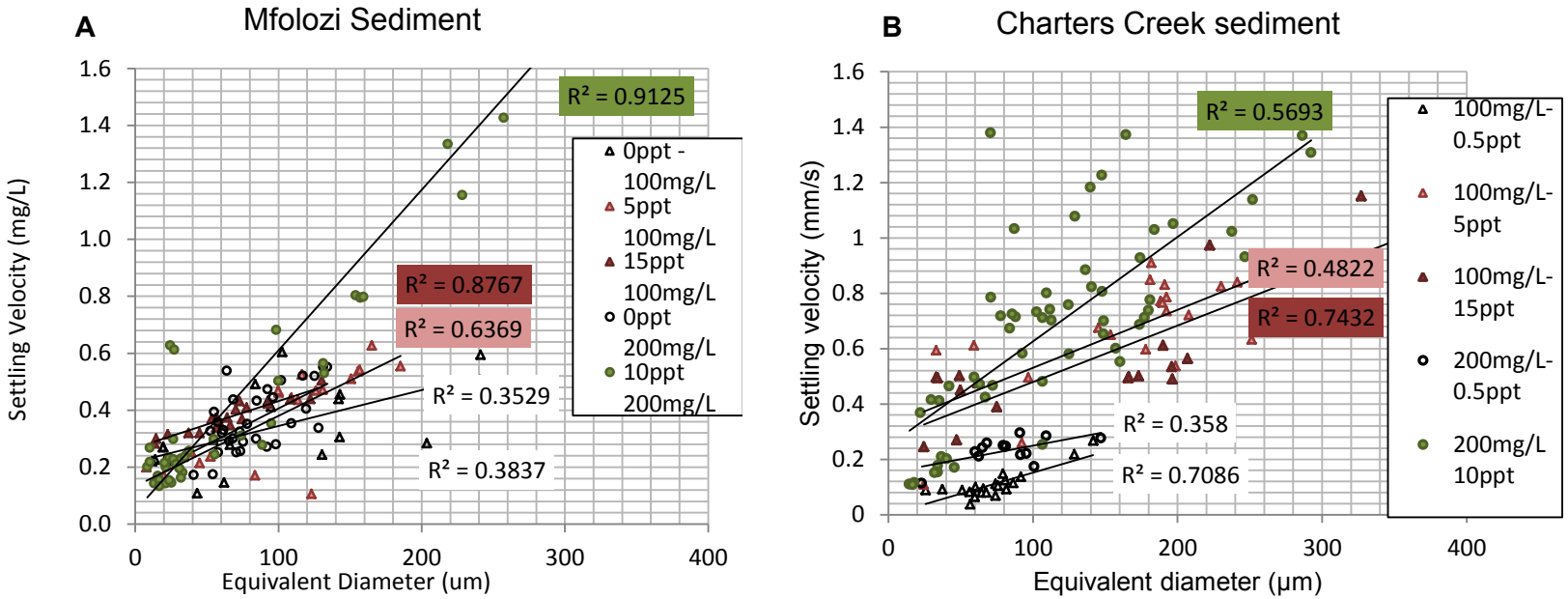

Figure 4-21: A: Settling velocity results for Mfolozi sediment at different salinities. B: Settling velocity results for Charters Creek sediment at different salinities. Key: Concentration in mg/L, shear rate in s^{-1}.

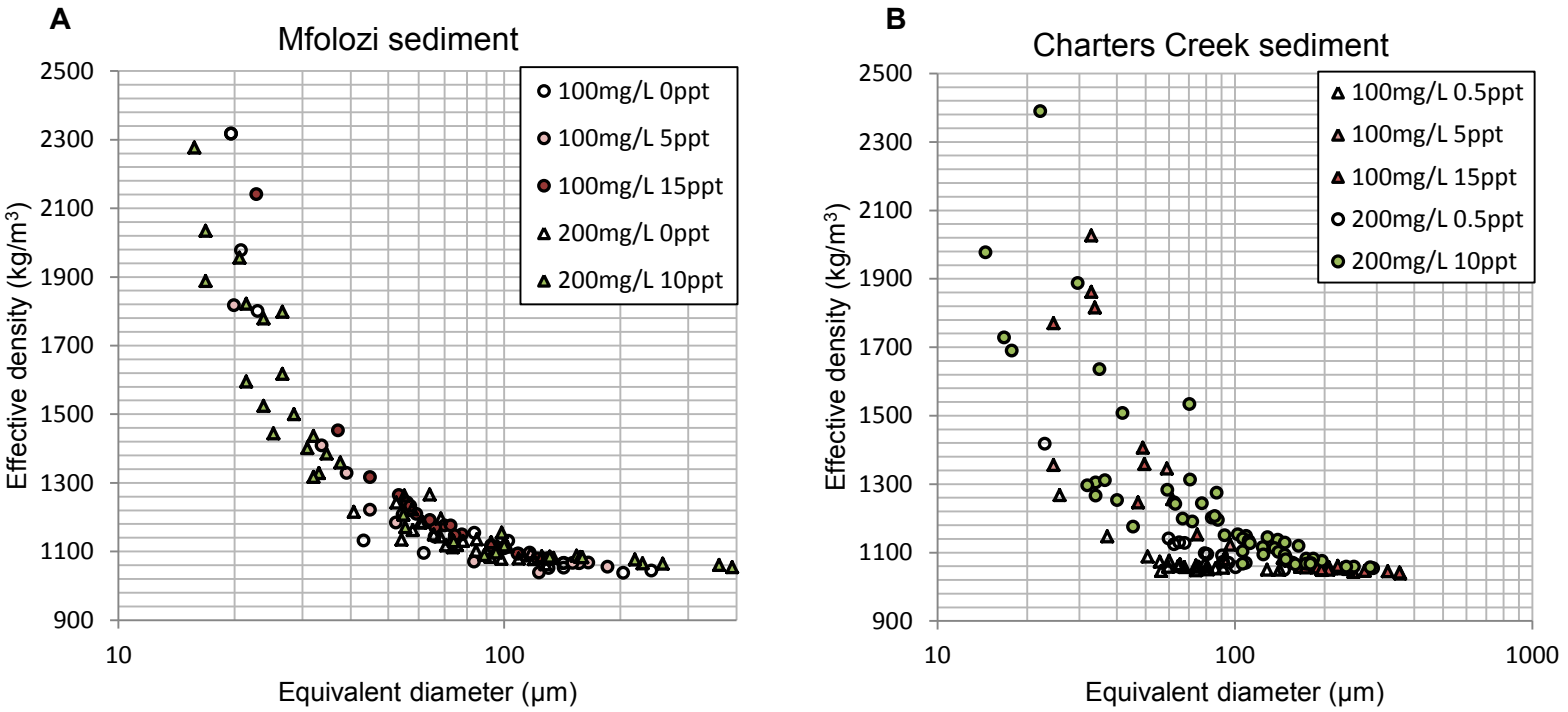

Figure 4-22: A: Effective density results for Mfolozi sediment at different salinities. B: Effective density results for Charters Creek sediment at different salinities.

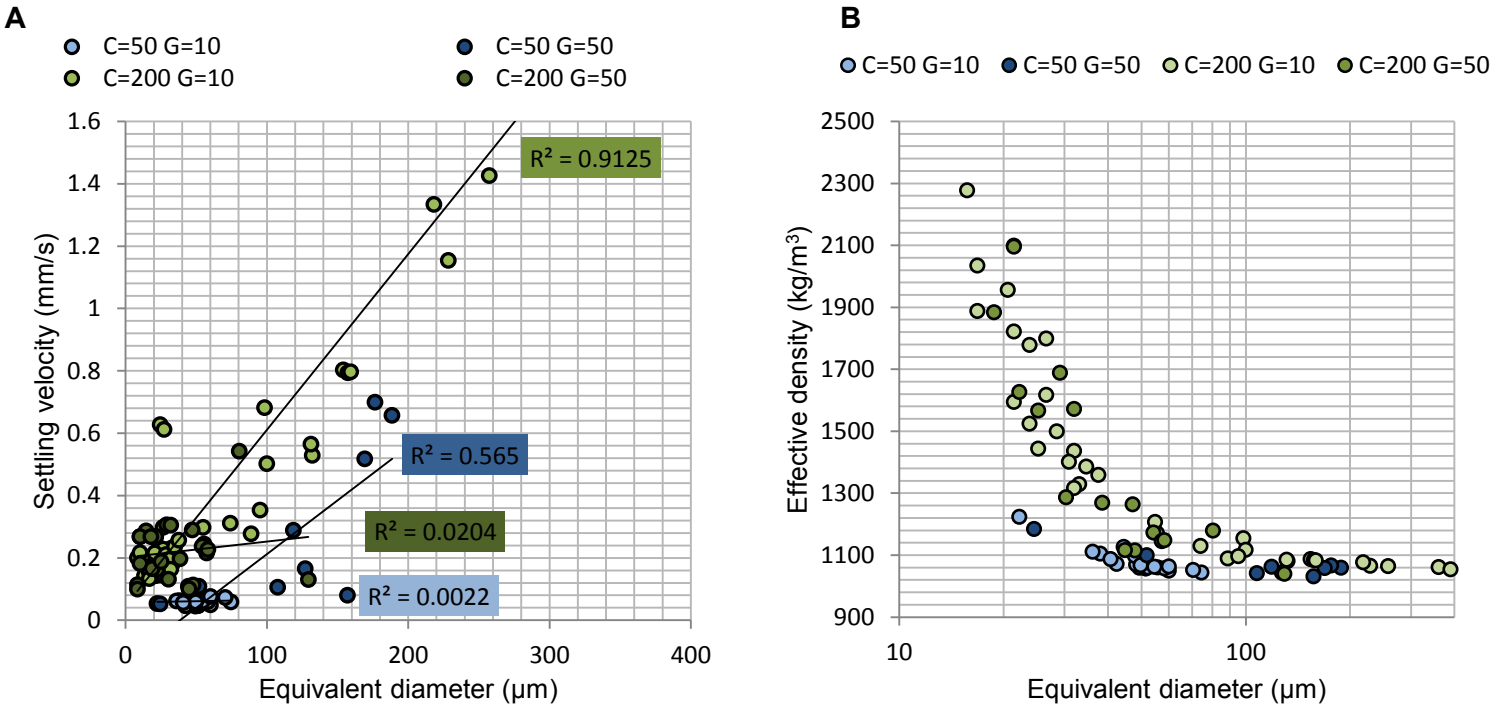

Figure 4-23: A: Settling velocity results for Mfolozi sediment at different shear rates. B: Effective density results for Mfolozi sediment at different shear rates. Key: C – concentration (mg/L), G – shear rate (s^{-1}).

Influence of shear rate on settling velocity

Settling tests were conducted on flocs from aggregation tests performed at a shear rate of $50s^{-1}$. The settling velocities were compared to those measured at $10s^{-1}$. The results are presented in figure 4-23. Flocs sampled from the $10s^{-1}$ 200mg/L aggregation test were larger than those sampled from the $50s^{-1}$ 200mg/L test. The effective densities of flocs from both tests were similar. There were too few flocs observed in the 50mg/L settling tests to make reasonable comparisons. The range of floc sizes produced under the conditions was small. Furthermore there was variability in the densities of the flocs which formed under these conditions. Figure 4-23 suggests that larger flocs were sampled from the $50s^{-1}$ aggregation test than the $10s^{-1}$ test. It is likely that only large flocs were tracked due to difficulties imaging smaller flocs. The results of the aggregation tests have shown that larger flocs form during the $10s^{-1}$ 50mg/L test than the $50s^{-1}$ test.

Despite the limited results of the 50mg/L tests, it is reasonable to say that the shear rate of the aggregation test merely affects the size of the flocs formed. The settling velocity is a function of the floc size. At high shear rates, smaller flocs will form, and the settling rate of the suspension will be lower.

The shear rate is expected to significantly affect in situ settling velocities. Boundary shear stresses at high shear rates exceed the critical shear stress for deposition and prevent settlement from occurring. It is not possible to observe this in a still settling column. An annular flume would be better suited to this purpose.

4.4.4. Settling velocity of quartz particles

The settling velocity of the equivalent sized quartz particle was calculated for each floc that was tracked. A comparison between floc settling velocities and those of equivalent quartz particles are provided in figure 4-24. The equivalent quartz settling velocities are significantly higher than the measured floc settling velocities. The difference increases with particle size. Figure 4-24 suggests that sediment flocs are significantly less dense than quartz particles. Measured effective densities in figures 4-20, 4-22 and 4-23 show that floc effective densities are low. Figure 4-24 distinctly shows the difference in behaviour of cohesive and non-cohesive sediments. Non-cohesive sediments settle quicker than cohesive sediments. The density of non-cohesive sediments does not vary with the size of the sediments. By contrast the density of cohesive sediment flocs has been shown to vary with floc size and other factors such as salinity.

The difference in settling velocity between quartz particles and flocs was small when flocs were small. The small difference in settling velocities is attributed to higher effective densities of smaller flocs. Smaller flocs are denser packed combinations of fewer particles. The difference is also smaller because of the quadratic nature of Stokes law. Settling velocity is increases with the square of the particle diameter. When the diameter is small, the settling velocity is small. It however increases quadratically. The high settling velocities of the larger equivalent quartz particles are not likely to be observed in the field.

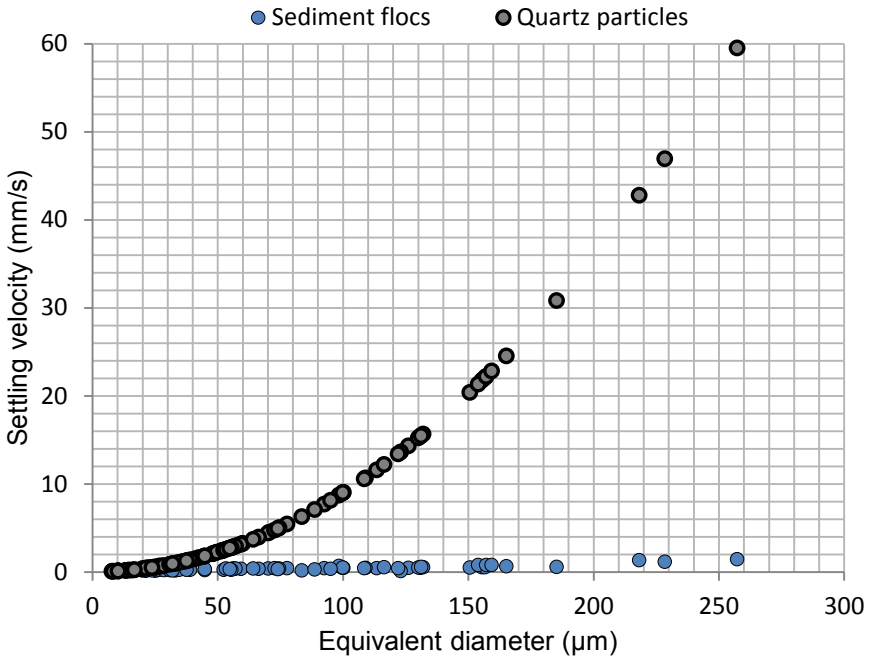

Figure 4-24: Comparison between the settling velocity of Mfolozi sediment flocs and their equivalent-sized quartz particles

4.4.5. Limitations of the settling tests

There were several problems encountered while developing the technique to measuring particle settling velocities. Note that these problems were rectified and the results presented above have not been affected. The most significant problem was the development of density currents within the settling column. The formation of currents was a continuous problem in preliminary tests. These currents accelerated the settlement of flocs at one side of the column, while lifting flocs at the other side of the column. The settling velocities obtained were inaccurate. The formation of currents during the initial experiments may be attributed to the following sources (of which the first is the most likely):

1. The incandescent sidelight initially used generated heat. This warmed one side of the column during the test. The thermally induced density gradient across the column caused a density current to form. The current circulated around the column. All particles within the column moved with the current. Settling velocities were amplified by the current.

2. If the fluid inside the settling column was less dense than that of the pipette, a jet formed. The sample fluid from the pipet would rapidly flow through the column to the bottom. This increased the settling velocities of the particles within the fluid.

   It is possible to correct for fluid flow within the column using particles image velocimetry. This is however computationally demanding and there was insufficient time and resources to develop a PIV system. The PIV approach assumes that the fine particles move at the same speed as the fluid. Their movement is used as the fluid movement and it is used to correct the settling velocity of larger particles. The approach is also unsuitable due to the low density of fine particles observed in the column.

   The formation of density currents was eliminated by using the beam of an overhead projector instead of the strong incandescent sidelight. The overhead projector beam did not heat the fluid within the column. A thinner settling column was used in place of the larger original column. Currents were did not develop as before. If a current was observed, the results of the test were rejected.

   Out of focus particles:

   The depth of field of the macro lens used to observe the settling flocs was limited. Many settling flocs appeared out of focus. These flocs may have been incorrectly processed. Particles closer to the camera may appear larger and with rounded edges. Particles further away may appear smaller. The settling velocity of the apparently smaller particles will be higher than anticipated. The effective density estimate will also be higher than expected. This estimate is amplified when the diameter of the floc is small due to the quadratic nature of the Stokes law estimation.

   Lighting conditions and camera resolution:

   The ability to detect and track small particles was limited by the lighting conditions and camera resolution. The resolution of the camera was at best 4.79μm. Fine flocs were difficult to detect under strong lighting. Fine flocs are also difficult to track because of ambiguity. There are generally many objects with areas of 1, 2 and 3 pixels. These objects are easily confused. If the pixel co-ordinates of another object are used, the settling velocity calculated will be incorrect.

   Camera timing:

The continuous interval-timer shooting mode of the D7000 was used. Images were captured at 2 second intervals. The D90 did not have this feature. The continuous shooting mode was used. The frame rate was measured repeatedly. The time interval between 10 frames did not vary and was thus used.

The frame rates of both cameras during both shooting modes can vary. It was therefore necessary to verify the frame rate for the settling column experiment. If the time interval between images of settling flocs is incorrect, the settling velocity will be incorrectly estimated.

Pipette sampling

Pipette sampling was performed in accordance with the recommendations of Gibbs & Konwar (1982). Pipetting was not observed to cause flocs to break up. Care was taken to ensure than the pipette was held upright. It is uncertain as to whether aggregation due to differential settlement occurred in the pipette. The fluid in the settling column was prepared at the same density as that of the solution tested in the jar test. This prevented currents from forming. If the density of the pipette fluid exceeded that of the settling column, a strong jet current would form.

4.4.6. Fractal dimension and particle shape:

The shape of the observed flocs was investigated during the settling column test. The intention was to establish whether a relationship existed between floc shape, floc size and possibly the flocculation drivers. Floc shape showed variation. The majority of flocs were ellipsoidal in shape. Very few flocs were circular. Floc shape was investigated using two parameters: the aspect ratio and fractal dimension. The fractal dimension is expressed by nf below.

$$logA = n_f \log(d) \qquad (4.1)$$

When a floc is circular, nf =2, where A= f(d^2). The aspect ratio is defined by the ratio of the major axis length to the minor axis length. The aspect ratio of a circular floc is 1. Elongated flocs will have a higher aspect ratio. The mean aspect ratio of all flocs observed was 1.513. The mean fractal dimension was 1.85. Fractal dimensions were investigated for trends. No trend was observed when comparing fractal dimension to equivalent diameter. Furthermore no trends were observed when investigating fractal dimensions over different salinities, shear rates and concentrations. The fractal dimensions of flocs observed in each test are presented in figure 4-25. The results show significant scatter. It appears that floc shape is random and not influenced by any of the drivers investigated.

The accuracy of the fractal dimension measurement may be reduced if the qualities of the images are poor. Flocs out of focus tend to appear more circular than they actually are. The finest particles are only 1-6 pixels in area. At this size, the resolution is too low to give an accurate estimate of particle shape. The results for finer particles showed more scatter.

In summary the majority of observed flocs were ellipsoidal in shape. There was no relationship between equivalent diameter and fractal dimension. Concentration, turbulence and salinity did not influence fractal dimension.

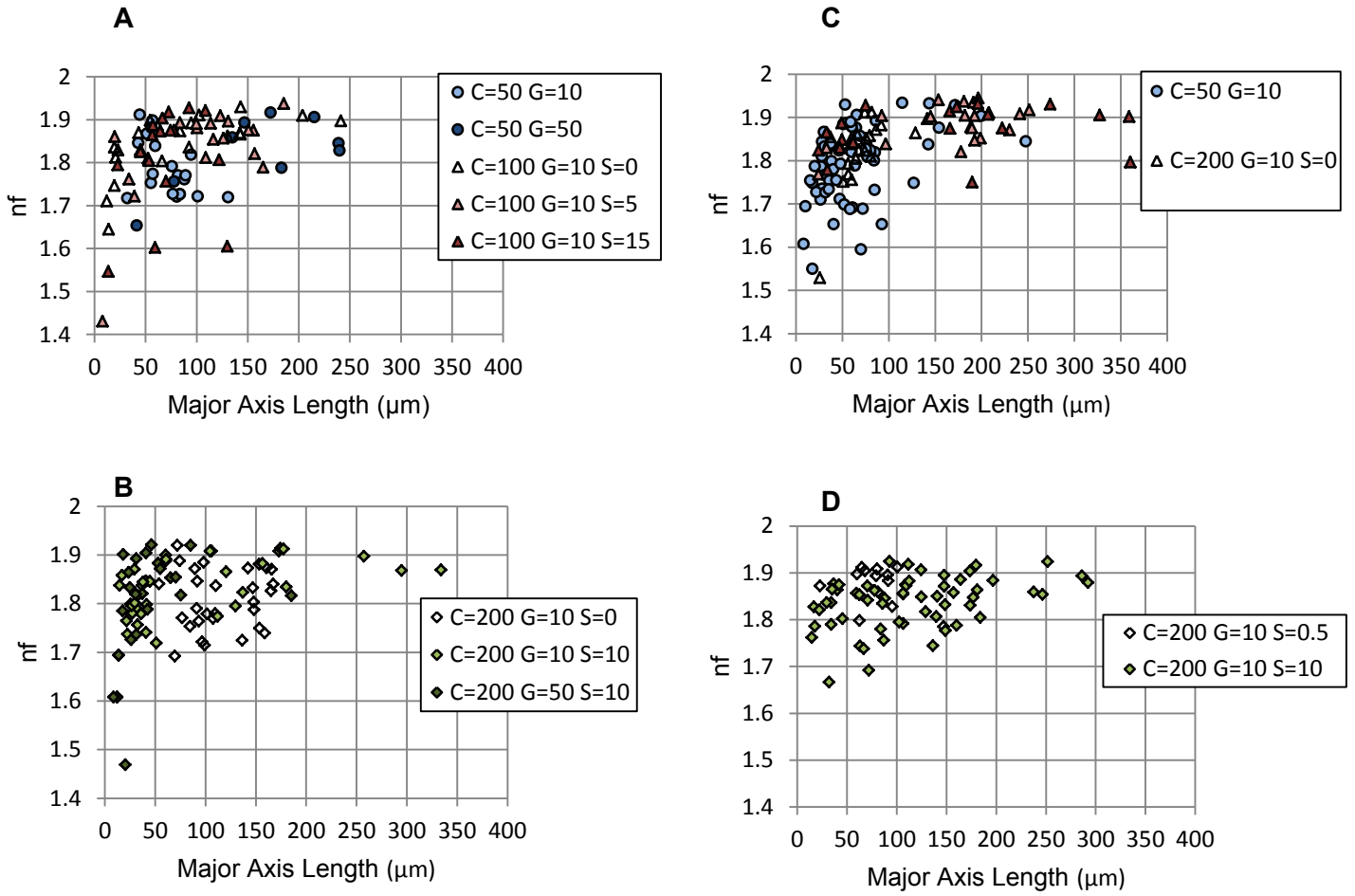

Figure 4-25: A-D showing fractal dimensions versus major axis length for different conditions. A&B: Mfolozi. C&D: Charters Creek sediment

4.4.7. Summary of effects:

The settling velocity of flocs was observed to be dependent on floc size and effective density. These are dependent on the drivers of flocculation, such as concentration, shear rate, and salinity. Settling velocity is therefore indirectly dependant on the drivers of flocculation. Floc settling velocity is directly proportional to floc size. The finest flocs were observed to settle less than 0.05mm/s while large microflocs and macroflocs settled at velocities in excess of 1 mm/s. Flocs settled significantly slower than their equivalent sized quartz particles. This was due to low effective density.

The effective density of large microflocs (>100µm) and macroflocs was generally between 1050 and 1100kg/m^3. The low effective densities indicated that they are loosely bonded porous structures. The effective density of smaller flocs was typically higher than 1100kg/m^3. Certain effective densities matched those of quartz particles. This suggested that fine flocs were more compact and closely packed. Effective density was observed to decrease when floc size increased. Results suggested that effective density increases in saline conditions and at higher suspended sediment concentrations.

There were limitations to the test which were discussed. The pipette sampling technique was found to be effective in transferring flocs without breakage. Flocs were generally ellipsoidal in shape. Floc shape was observed to be unrelated to floc size, effective density, or any of the drivers of flocculation.

4.4.8. Suggestions for application

The results of the aggregation tests in sections 4.2.1 and 4.2.5 show that sediment mass was generally concentrated in large microflocs and macroflocs. A characteristic settling velocity can be found for the floc size range over which the mass is concentrated. This settling velocity can be used to describe the mass settling flux of the sediment. Additional settling velocities can also be found for the floc sizes over which the remaining mass is distributed. The mass settling rate of suspended sediment can therefore be calculated empirically using information on the distribution of floc sizes and floc settling velocities. The influences of concentration, shear rate, and salinity are accounted for by the floc size distribution.

Results from the 200mg/L Mfolozi settling tests in figure 4-26 have been used to obtain a characteristic settling velocity for the size range over which the sediment mass is concentrated. Figure 4-27 below shows this range. 76% of the suspended mass in found in flocs 62.5 - 162.5µm in size. The suitable settling velocity for this size range is 0.5mm/s. Therefore 76% of the observable floc mass settled at 0.5mm/s. This settling velocity may be applied as a sink term in sediment transport models.

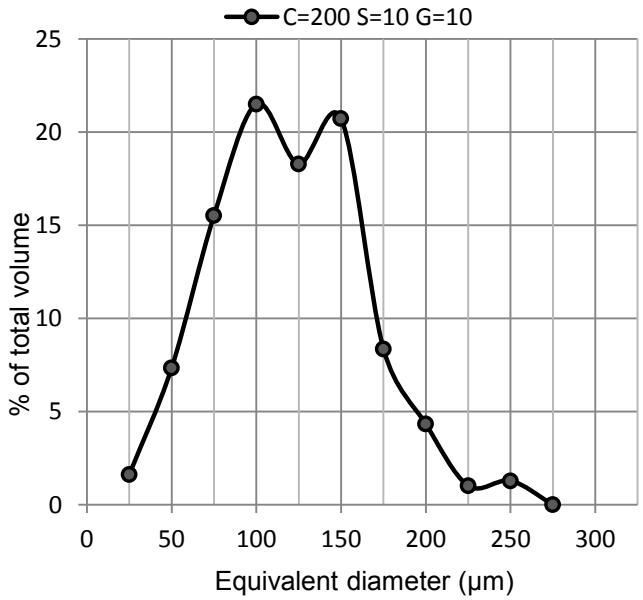

Figure 4-26: Volume distribution of 200mg/L Mfolozi sediment after 70minutes aggregation (S=10ppt, G=10s^{-1})

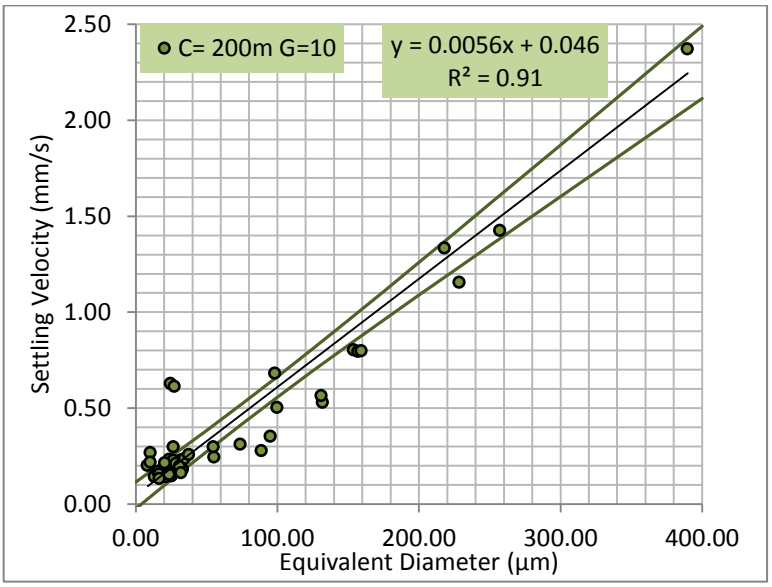

Figure 4-27: Settling velocity results for 200mg/L Mfolozi sediment (S=10ppt, G=10s^{-1}) showing 95% confidence intervals.

This above approach is dependent on the accuracy of the volume-based floc size distribution and settling velocities. It does not account for the numerous particles which could not be detected due to imaging difficulties. The application of the results was therefore checked using a simple jar test to measure the still settling velocity of the sediment.

Quiescent settling test:

This test was performed on selected solutions. Each solution was agitated for 70minutes in the beaker. The agitation was stopped and the agitator was removed. The turbidity at the centre of the water column was measured at regular time intervals from this point forward. The concentration was inferred by using turbidity as a proxy. A HACH P2100 turbidity-meter was used. This was used to determine the percentage of mass settled at regular time intervals. Plate 4-9 shows the quiescent settling test.

There were certain limitations to the test. Only one turbidity sample was taken for each measurement. Turbidity readings varied with the position of the sample point. It was difficult to sample at precisely the same position throughout the test.

Results:

The results of these tests are shown in figures 4-28 and 4-29. The observed settling rates differed to those measured in the settling column tests. Two distinct settling rates were observed, indicating bimodal behaviour. Settlement was initially fast, thereafter settlement

occurred slowly. The initial settling rates were lower than those observed in the settling column. The visible aggregates which formed during aggregation settled rapidly. The settling rate then decreased significantly. This settlement was not detected in the settling column test because the particles were too fine to detect. Fine microflocs were observed to settle at less than 0.01mm/s. There were variations in the initial settling velocity. Solutions prepared under similar conditions displayed differences in the initial settling behaviour. Some displayed rapid initial settlement while others displayed slower initial settlement. Thereafter certain solutions settled out completely while others did not.

The bimodal behaviour is attributed to the difference in settling rates of macroflocs and fine microflocs. It is evident that the entire population does not flocculate. Only a portion of the population will undergo flocculation to form larger particles. The remainder of the population remains composed of fine microflocs. These flocs form a slow-settling background concentration. Such flocs are shown in plate 4-10. The proportion of the mass which flocculates is dependent on the flocculation potential of the sediment. The material composition tests found that the sediment was silt-dominant. It is assumed that the fine slow-settling suspension was dominated by fine silt particles. These particles displayed a significantly lower potential to flocculate.

The results of the test in figure 4-28 A and B show that a considerable portion of the total mass may settle in the form of these particles. If a single constant settling velocity is used, it will not consider the bimodal behaviour. If a characteristic settling velocity is developed from the results of the settling tests, it will over-estimate the settling flux. This requires correction.

It is acknowledged that the settling velocities observed in the column provide reasonable estimates of individual floc settling velocity when compared to observations in literature. However they are unsuitable for direct application to the estuarine environment. The settling velocity estimates from the still settling column need to be reduced. In the still settling column, the large flocs were isolated and tracked while the background unflocculated materials remained undetected. These often constituted a significant portion of the mass flux. Furthermore an estimate of the background settling velocity is required.

In conclusion, settling columns are limited in their ability to predict field settling behaviour. Settling behaviour should be validated using simple tests in quiescent conditions. Furthermore it is desirable to obtain in-situ settling velocity estimates.

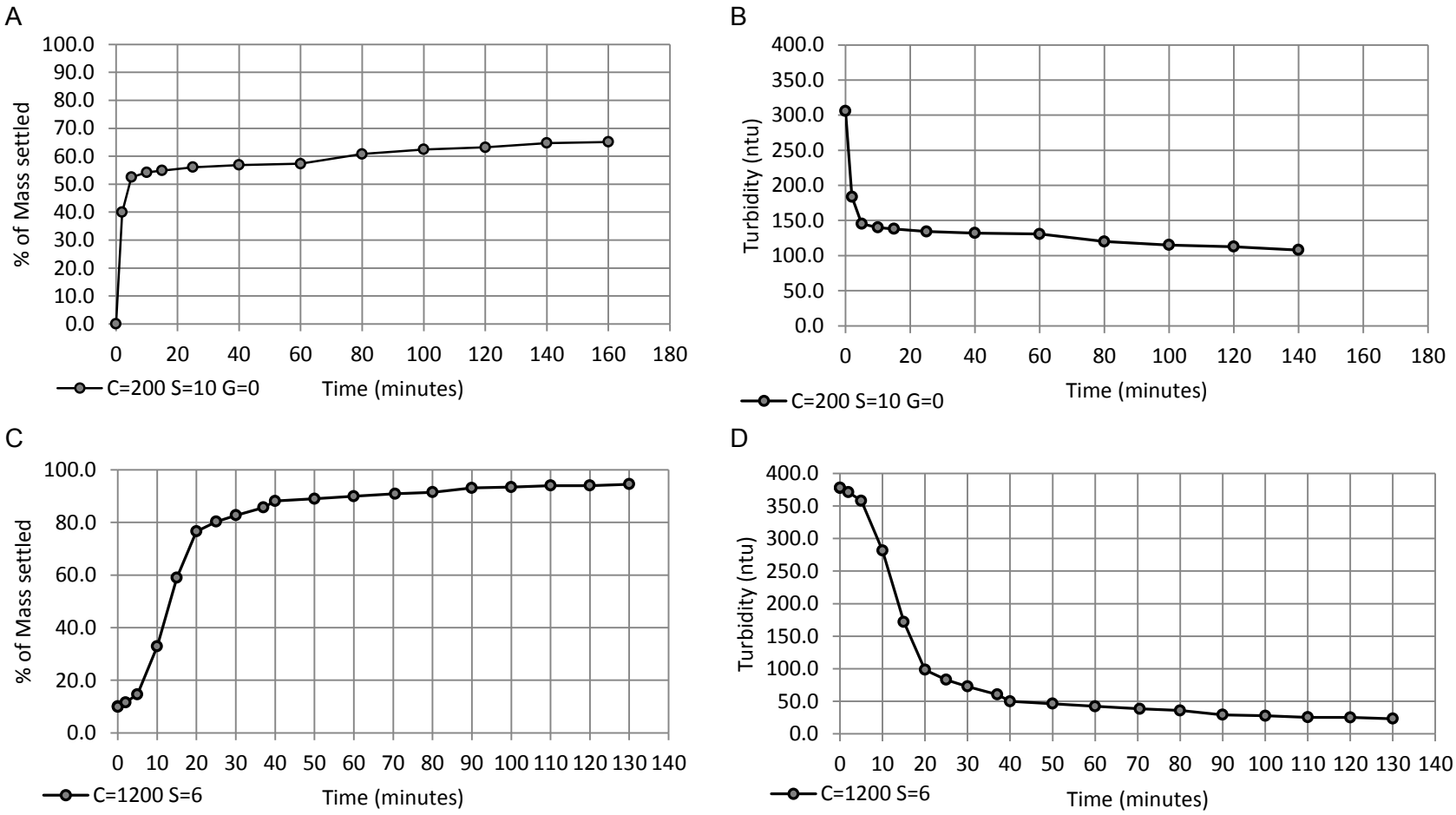

Figure 4-28: A: Mass settling rate of 200mg/L Mfolozi sediment in quiescent conditions. B: Turbidity readings for A. C; Mass settling rate of 450mg/L Mfolozi sediment in quiescent conditions. D: Turbidity readings for C.

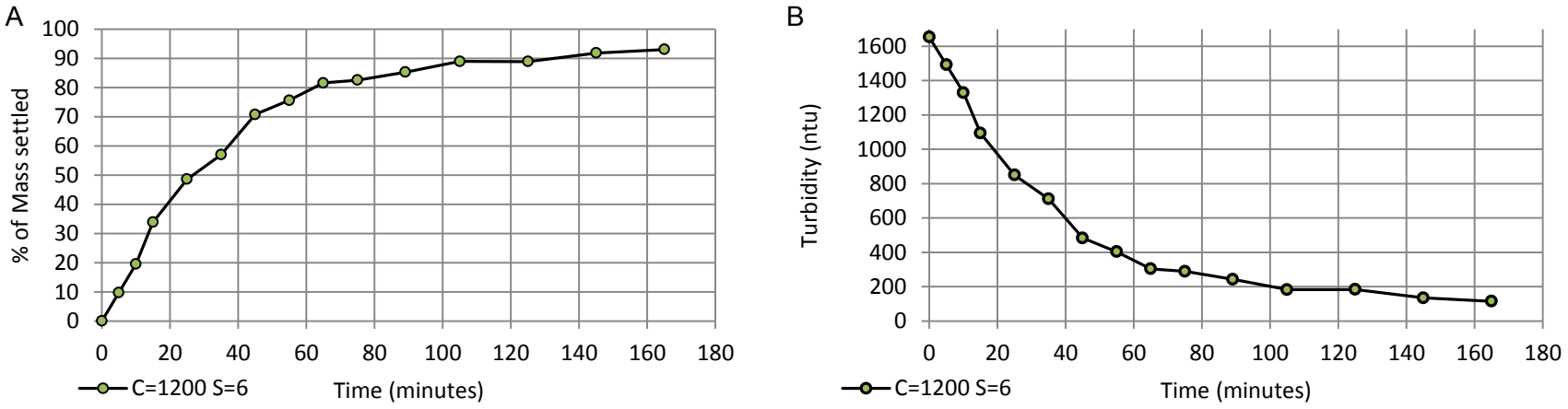

Figure 4-29: A: Mass settling rate of 1200mg/L Mfolozi sediment in quiescent conditions. B: Turbidity readings for A.

The settling velocities for 25, 50 and 75% of the suspended mass are shown in the tables below. Notice that the initial settling velocities are similar, yet lower than those measured in the settling column test. However the effective settling velocities for 75% of the mass were significantly lower than those measured in the settling column test. The diameter of the particles was estimated using by Stoke's Law. A constant density was assumed.

Table 4-9: Effective settling velocities of 200mg/L Mfolozi sediment in quiescent conditions. (See figure 4-28 A and B)

% Settled	H (mm)	t (min)	t (s)	Ws (mm/s)	Equivalent Diameter (µm)
25%	67	1	60	1.117	45
50%	67	5	300	0.223	20
60%	67	80	4800	0.014	5

Table 4-10: Effective settling velocities of 450mg/L Mfolozi sediment in quiescent conditions. (See figure 4-28 C and D)

% Settled	H (mm)	t (min)	t (s)	Ws (mm/s)	Equivalent Diameter (µm)
25%	82	8	480	0.171	18
50%	82	13	780	0.105	14
75%	82	20	1200	0.068	11

Table 4-11: Effective settling velocities of 1200mg/L Mfolozi sediment in quiescent conditions. (See figure 4-29 A & B)

% Settled	H (mm)	t (min)	t (s)	Ws (mm/s)	Equivalent Diameter (µm)
25%	82	12	720	0.114	15
50%	82	26	1560	0.053	10
75%	82	55	3300	0.025	7

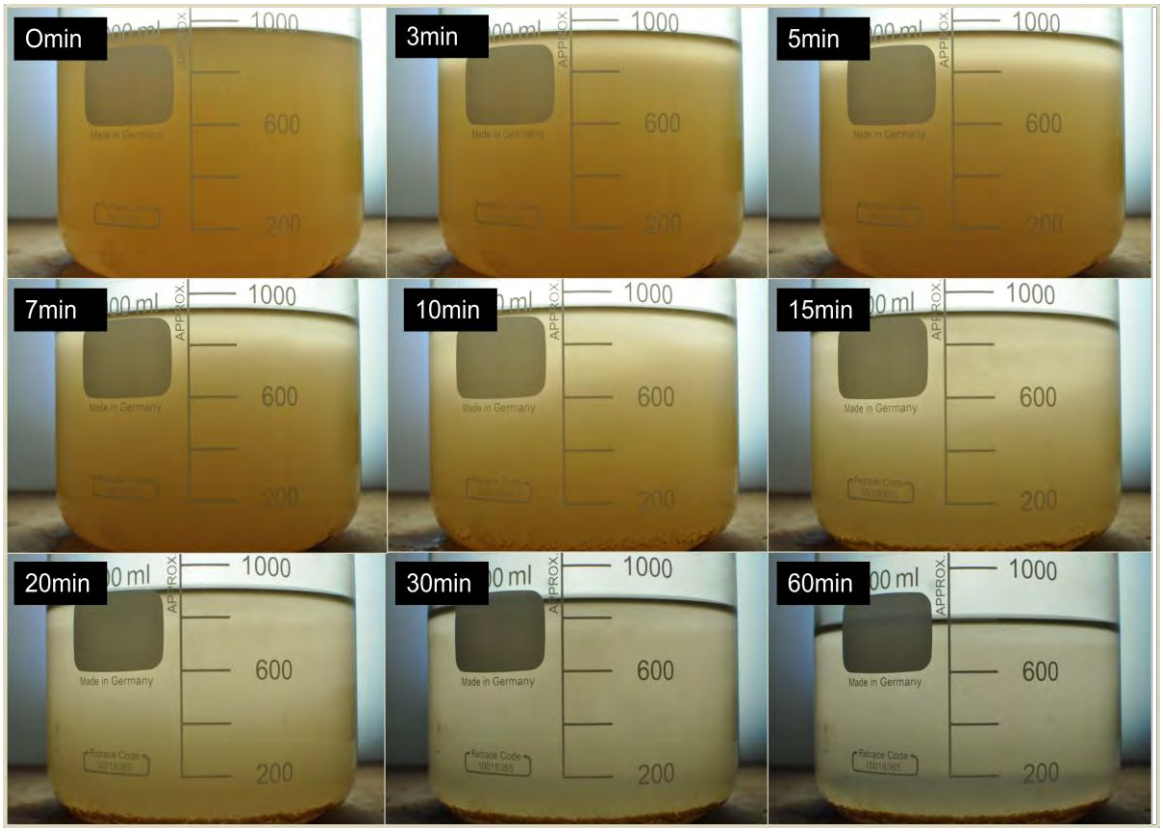

Plate 4-9: A schematic display of the settlement of fine sediments in quiescent conditions. (450mg/L quiescent settling test)

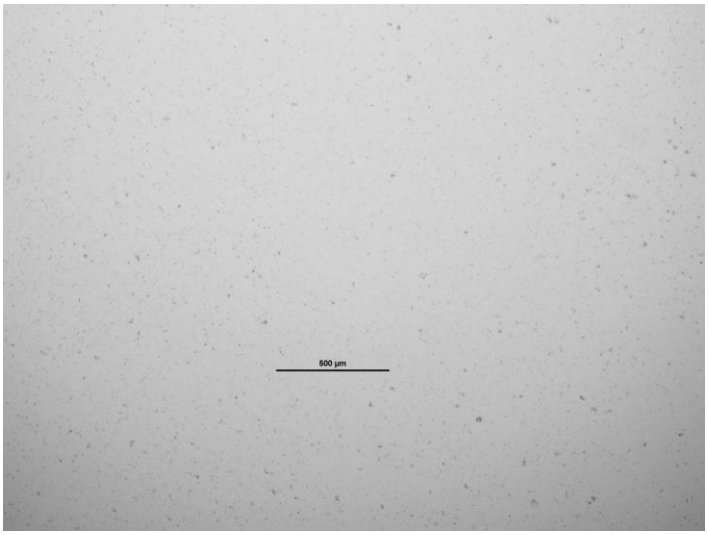

Plate 4-10: Microscope images of fine suspended material in the 200mg/L quiescent settling test at 60minutes. The solid bar represents 500µm.

Relevance of observations:

The background concentration of slow settling particles is likely to correspond to that of the Mfolozi estuary after settlement. Sediment is most likely to settle under quiescent conditions. Initial settlement will be rapid when such conditions occur. The remainder of the suspended mass will not settle unless conditions are sustained for long period of time (a few days). Such an event is unlikely in the Mfolozi estuary as it is influenced by both wind and tidal currents while Lake St Lucia is influenced by wind waves.

The background concentration is expected to scale with the suspended sediment concentration. More fine flocs will remain in suspension after high sediment loads. The sustained presence of these sediments in suspension increases turbidity. This may adversely impact the biology of the system as was briefly discussed in section 2-9. However if a flood occurs in a closed system, significant initial settlement will occur. If the systems were combined, the slow-settling fraction will likely enter the St Lucia estuary, significantly increasing the turbidity and settling over a longer period of time.

Implied limitations of aggregation and settlement column tests:

The application of settling column tests is limited to materials of high flocculation potential unless specialized equipment used. There is a finite limit to the size range of observable particles. The results are only applicable to observable particles. The background particle size distribution and settling rate needs to be estimated. This could be done with specialized equipment such as a Malvern Mastersizer or Coulter Counter, neither of which were available for regular use.

The limitations restrict the application of the results of the settling column test. The settling column results provide relevant, useful and reasonably accurate information, but do not provide all the information necessary for application.

The results of the quiescent settling tests above suggest that the volume-based distributions obtained are bimodal, with a peak, or at least large proportion of mass concentrated below 20um. This second peak could not be observed in the aggregation tests.

<u>Conclusions:</u>

The results of the settling column tests alone are insufficient for practical applications. The settling behaviour of the sediments tested was bimodal. The jar test and settling column tests were only able to show one aspect of the bimodal behaviour. The settling flux of the fine undetectable portion needs to be estimated.

SUMMARY AND CONCLUSIONS

The investigation set out to understand cohesive sediment flocculation and its influence on the settling characteristics of the Mfolozi and St Lucia estuaries. The objectives were to investigate the drivers of flocculation and their influence on the formation and destruction of aggregates. The objective was also to investigate the settling velocities of aggregates and their sensitivities to flocculation drivers. It was intended that the outcomes of these objectives would together provide a deeper understanding of the settling characteristics of cohesive sediments. A laboratory technique using digital imaging was developed for the purpose of this investigation. This chapter summarized the results and conclusions drawn from the investigation. The chapter is concluded with recommendations for future research.

5.1. Summation

A laboratory technique was developed to investigate flocculation of fine sediments from the Mfolozi and St Lucia estuaries. The tests were performed on suspended sediments sampled from the Mfolozi and St Lucia estuaries. The sediments were silt-dominant with a small clay fraction. Sediment behaviour corresponded to that of cohesive sediment. The technique involved the use of an agitated beaker, still settling column and digital imaging to monitor sediment behaviour. Flocculation was simulated in the agitated beaker. Flocculation drivers were varied and their influence on the formation or destruction of aggregates was measured by digital imaging. The settling velocities of aggregates were measured by analysing images of settling flocs in the still settling column. The laboratory technique was able to fulfil the objectives of the investigations. Different aspects of sediment behaviour were investigated: aggregation, deflocculation, settling velocity, effective density and particle shape. The results of these are summarized in the subsections which follow.

5.1.1. Aggregation behaviour

The development of aggregates in the agitated beaker over 70minutes was measured. The suspended sediment concentration, shear rate, and salinity of the sediment solution were varied in different tests. The flocculation timescale of both sediments tested was observed to be

70 minutes Aggregate growth was observed to occur at low shear ($10s^{-1}$) in the presence of salt. Aggregate growth was most visible in the 90^{th} percentile of the floc size distribution. Aggregate populations were dominated by microflocs (fine aggregates generally smaller than 100µm). By contrast macroflocs formed a small fraction of the population. The volume-based floc size distribution of aggregates did not follow the population size distribution. It instead showed that the sediment mass was concentrated over a particular size range. This size range depended on the drivers of flocculation. Fine microflocs could not be detected. It is uncertain as to the percentage of total mass these particles constituted. Crude investigations suggested that a bimodal volume-based floc size distribution was present.

Aggregate growth occurred in the presence of salinity. Salinity increased the flocculation potential of the cohesive sediments. Aggregates which formed in saline conditions were larger than those which formed in fresh conditions.

Aggregate growth increased when the suspended sediment concentration increased. The frequency of effective collisions between particles increased with the concentration. This was difficult to observe at high concentrations due to floc overlap in images. Aggregate growth was inhibited at high shear rates. Any flocs which formed were broken up by the high shear stress.

5.1.2. Influence of turbulence

The influence of turbulence on aggregate breakup was investigated in deflocculation tests. This was done by incrementally increasing the shear rate in the agitated beaker. Aggregate size decreased when the shear rate increased. The flocs were broken up due to shear stresses. The size of aggregates was limited by the Kolmogorov microscale. The largest aggregates observed were smaller than the size of the smallest eddies present.

Turbulence is necessary for aggregation to occur as it induces mixing. At low shear rates, turbulence stimulates aggregation while at higher shear rates it inhibits flocculation by breaking up aggregates. The interaction between turbulence and suspended sediment concentration drives flocculation. It is the combination of these drivers which generates collisions between particles. The probability of aggregate formation as a result of collisions is influenced by the chemical properties of the sediment and solution. This is largely controlled by salinity. The strength of aggregates formed is dependent on this chemical property. Turbulence interacts with the chemical properties to control the rate of aggregate break-up. The points made in this summary have been substantiated by observations in the aggregation and deflocculation tests.

5.1.3. Settling velocity

The settling velocities of flocs which formed during the aggregation tests were measured in a still settling column. Flocs were sampled using a pipette with an opening of sufficient width to prevent floc breakup. Floc size, effective density, and shape parameters were also measured. Floc settling velocity increased with floc size. Settling velocities ranged from 0.05mm/s to 2mm/s. Fine particles settled at the lower end of this range while macroflocs settled at the upper end. The range of settling velocities observed corresponded to those discussed in chapter 2. The settling velocity of fine microflocs could not be detected. This was however investigated in quiescent settling tests. The settling velocity of these particles was shown to be significantly lower than macroflocs and large microflocs. Bimodal settling behaviour was observed where larger particles settled rapidly during the initial part of the test, thereafter fine particles settled very slowly.

The effective density of flocs decreased as floc size increased. The densities of macroflocs ranged from 1050 to 1100kg/m^3 while those of finer particles were typically higher, often matching those of quartz particles. The observed densities suggest that macroflocs are loosely bonded-porous particles while microflocs are denser and more compact particles.

The settling velocities, densities and size range of flocs formed in fresh water were lower than those which formed in saline water. Flocs were typically ellipsoidal in shape. Floc shape did not vary with the drivers of flocculation. Floc shape also did not vary with floc size.

Floc settling velocity did not vary directly with the drivers of flocculation. It varied with floc size. The floc size distribution varied with the drivers of flocculation. It is therefore necessary to view settling velocities together with the results of aggregation tests in order to understand settling behaviour.

5.1.4. Effectiveness of laboratory technique

The techniques employed were able to demonstrate the behaviour of cohesive sediment as discussed in chapter 2. Aggregate formation, breakup, settlement, and other parameters were all measured. Digital imaging techniques in conjunction with simple laboratory tests may be effectively used to study flocculation. There were however some limitations to the test. The resolution was insufficient to allow the observation of particles finer than 20μm in size. This hindered the analysis of fine and unflocculated solutions. Images could not be analysed at high concentrations due to floc overlap and poor light transmission through the beaker. There are a limited range of conditions in which the technique may be effectively employed.

In situ sediment behaviour may differ to laboratory behaviour. The laboratory experiment involved isolating and precisely controlling various drivers and conditions (shear rate, salinity, concentration). This does not occur in the field where drivers vary temporally and spatially. Field conditions are more complex than the simple, controlled environment of an agitated beaker. Sediment will likely respond similarly to drivers in the field. However it is unlikely that the lab conditions will occur in the field for a period of time corresponding to the laboratory timescale. These comments reflect the shortcomings common to most laboratory investigations, which limit their ability to accurately simulate estuarine processes.

5.1.5. General conclusions

Cohesive sediments are present in solution as aggregates. Aggregates are predominantly microflocs, which are fine, robust, densely-compacted particles formed from a combination of primary particles (silt and clay particles). Large flocs known as macroflocs form under certain conditions favour aggregate formation. This typically occurs at low shear rates in the presence of salt. Macroflocs are porous, loosely-bound, low density aggregates which are easily broken up by turbulence. Macroflocs have higher settling velocities than microflocs. When formed, macroflocs dominate the vertical settling flux a suspension. The settling velocities of cohesive sediments are significantly lower than those quartz particles. Flocculation influences the size distribution and settling velocities of cohesive sediments. Flocculation enhances the rate at which settlement occurs. The results of this investigation have implications when considered in the context of the estuarine environment.

Given the observed flocculation timescale of 70minutes, aggregates grow in situ under various conditions. There is potential for aggregation in the saline regions of estuaries, particularly at the freshwater-saline water interface. This is likely to occur in regions of low turbulence. Flocculation may potentially enhance in situ settling rates. Furthermore large settled aggregates may be resuspended and broken up to form part of a flocculation cycle which occurs with the tidal cycle. These comments require investigation in the field. Laboratory results also require validation. From this it is recommended that a field investigation be undertaken to validate laboratory results and to provide insight into the field processes which occur in the St Lucia and Mfolozi estuaries.

5.16. Potential application of results

In the settling tests it was observed that floc settling velocity is primarily a function of floc size. Settling velocity can be expressed as a function of equivalent diameter as shown in section

4.4.8. Volume-based floc size distributions were obtained from the aggregation tests. These distributions indicated that the sediment mass is concentrated over a range of floc sizes. A characteristic settling velocity may be obtained from this size range. This settling velocity may be used as a constant settling velocity in a sediment transport model. This settling velocity is however unsuitable for application because the settling column tests were unable to measure the settling velocities of fine microflocs. Furthermore the results were not able to show the bimodal settling behaviour observed in settling tests in quiescent conditions. The settling velocities of fine microflocs require investigation.

Characteristic settling velocities obtained may be applied as a sink terms in sediment transport equations. They may also be applied in a simpler manner. A constant settling velocity for Charters Creek sediments may be used to describe still settling behaviour in Lake St Lucia after high energy events. This is already in the process of being used as a check in a wind re-suspension model for the south part of Lake St Lucia.

5.2. Suggestions for Further Research

5.2.1. Recommendations for the improvement of laboratory investigation

There were several limitations to the laboratory technique employed. These were discussed in chapters 3 and 4. Suggested improvements to the laboratory procedure and apparatus are suggested below:

1. Use a better quality source of lighting to illuminate flocs in the beaker and in the settling column. This will improve the contrast and hence improve the ability to detect finer particles.
2. Use a digital camera of superior resolution. Superior resolution will allow finer flocs to be detected. The resolution may also be increased by using superior quality optics. This may require a specialized lens.
3. Perform the full range of tests on a reference solution such as kaolinite.
4. Perform the tests on the full range of concentrations, shear rates and salinities in order to “fill in the gaps “
5. Decrease the thickness of the baffles used in the agitated beaker
6. Use different shaped jar to reduce settlement. A cone shape is recommended.
7. Improve the calibration of the turbulent agitator with a laser Doppler velocimeter.
8. Perform more detailed material composition tests. This includes a more frequent monitoring of the organic matter content. Chemical analysis tests such as X-ray diffraction or X-ray fluorescence may be used to identify clay minerals present.

5.2.2. Suggestions for further research:

There is potential for extensive further research into the behaviour of cohesive sediments in the Mfolozi and St Lucia systems. A short list of suggestions follows:

- A field investigation should be done to validate the findings of the laboratory investigation. The primary aim of this investigation should be to measure in situ settling velocities. It should investigate the how the drivers of flocculation vary with estuarine processes. A field investigation may be performed using a settling column (commercial Braystoke tube) and a CTB probe. Discharge and turbulent parameters may be estimated using acoustic techniques. Both estuaries are however shallow, hazardous (dangerous animals) and difficult to access. This should be kept in mind when planning a field investigation.
- Further investigation into the influence of organic matter content on aggregate growth is suggested. This could include the regular monitoring micro-organism populations followed by aggregation tests.
- This investigation forms a basis for understanding the influence of flocculation on cohesive sediment transport characteristics. The ultimate aim is to investigate the influence of Mfolozi river sediments on a restored combined Mfolozi-St Lucia estuary mouth. The development of a sediment transport model is suggested as further research. This will require investigation into settling velocity as a sink term in the model.

REFERENCES

Agrawal Y.C., and Pottsmith H.C., 2000. Instruments for particle size and settling velocity observations in sediment transport. *Marine Geology* 168, 89-114

Alldredge A.L., Gotschalk C., Passow U., and Riebesell U., 1994. Mass aggregation of diatomic blooms: insights from a mesocosm study. *Deep Sea Research II* 42(1), 9-27

Berry, W., Rubinstein, N., Melzian, B., and Hill, B., 2003.*The biological effects of suspended and bedded settlement (SABS) on aquatic systems*. Internal report U.S. EPA Office of Research and Development, National Health and Environmental Effects Laboratory, Atlantic Ecology Division and Midcontinent Ecology Division.

Bouyer D., Escudie R., and Line A., 2005. Experimental analysis of hydrodynamics in a jar-test. *Process safety and environmental protection* 83(B1), 22-30

Coufort C., Bouyer D., and Line A., 2005. Flocculation related to local hydrodynamics in a Taylor-Couette reactor and in a jar. *Chemical Engineering Science* 60, 2179-2192.

Bureau of Reclamation, 2006. Erosion and Sedimentation Manual, US Department of the Interior, Denver, pp. 4-1-4-46

Cyrus D.P. and Blaber S.J.M., 1988.The potential effects of dredging activities and increased silt load on the St Lucia system, with special reference to turbidity and the estuarine fauna. *Water SA* 14 (1), 43-47

Das B.M., 2007. Principles of Geotechnical Engineering, Thomson, Toronto

Dearnaley M.P., 1996. Direct measurements of settling velocities in the Owen tube: a comparison with gravimetric analysis. *Journal of Sea Research* 36, 41-47

Dyer K.R., 1989. Sediment processes in estuaries: future research requirements. *Journal of Geophysical Research* 94(c10)-14, 327-332.

Dyer K.R., Cornelisse J., Dearnaley M.P., Fennessey M.J., Jones S.E., Kappenberg J., McCave I.N., Pejrup M., Puls W., Van Leussen W., and Wolfstein K., 1996. A comparison of in situ techniques for estuarine floc settling velocity measurements. *Journal of Sea Research* 36, 15-29

Eisma D., Bale A.J., Dearnaley M.P., Fennessey M.J., Van Leussen W., Maldiney M.A., Pfieffer A., and Wells J.T., 1996. Intercomparison of in situ suspended matter floc size measurements. *Journal of Sea Research* 36, 3-14

Fennessey M.J. and Dyer K.R., 1996. Floc population characteristics measured with INSSEV during the Elbe estuary intercalibration experiment. *Journal of Sea Research* 36, 55-62

Fugate D.C. and Friedrichs C.T., 2002. Determining the concentration and fall velocity of estuarine particle populations using ADV, OBS and LISST. *Continental Shelf Research* 22, 1867-1886

Fugate D.C. and Freidrichs C.T., 2003. Controls on suspended particle size in partially mixed estuaries. *Estuarine, Coastal and Shelf Science* 58, 389-404

Gibbs, R.J. and Konwar, L.N., 1982. Effect of pipetting on mineral flocs. *Environmental Science and Technology* 16 (2), 119–121.

Graham G.W. and Manning A.J., 2007. Floc size and settling velocity with a Spartina anglica canopy. *Continental Shelf Research* 27, 1060-1079

Grenfell S.E. and Ellery W.N., 2009. Hydrology, sediment transportation dynamics and geomorphology of a variable flow river: The Mfolozi River, South Africa. *Water SA* (35), 271-282

Ha H.K., Hsu W.Y., Maa J.P.Y., Shao Y.Y. and Holland C.W., 2009. Using ADV backscatter strength for measuring suspended cohesive sediment concentration. *Continental Shelf Research* 29, 1310-1316

Kranenburg, C., 1994. The fractal structure of cohesive sediment aggregates. *Estuarine, Coastal and Shelf Science* 39 (5), 451–460.

Kranenburg, C. 1999. Effects of floc strength on viscosity and deposition of cohesive sediment suspensions. *Continental Shelf Research* 19: 1665–1680.

Krishnappen B.G., Haralimpides K., McCorquodale J.A., 2003. Deposition properties of fine sediment. *Journal of Hydraulic Engineering* 129(3), 230-234

Krone R.B., 1963.A study of rheological properties of estuarial sediments. Tech. Bul. 7, USAE Comm. on Tidal Hydr., Vicksburg, MS.

Kumar R.G., Strom K.B. and Keyvani A., 2010. Floc properties and settling velocity of San Jacinto estuary mud under variable shear and salinity conditions. *Continental Shelf Research* 30, 2067-2081

Kwon J.I. and Maa J.P.Y., 2007. Using ADV for suspended sediment settling velocity measurements. *Estuarine, Coastal and Shelf Science* 73, 351-354

Larsen T., 1999. Measuring the variations of apparent settling velocity for fine particles. *Water Research* 34 (4), 1417-1418

Larsen T. and Johansen C., 1998. Measuring the settling velocity of fine sediment using a recirculated settling column. *Journal of Coastal Research* 14 (1), 132-139

Lawrie R.A. and Stretch D.D., 2008. Evaluation of the short-term link between the Mfolozi estuary and St Lucia Lake. Report, Centre for Research in environmental, coastal and hydrological engineering, University of Kwa-Zulu Natal, Durban

Lawrie R.A. and Stretch D.D., 2011. Anthropogenic impacts on the water and salt budgets of St Lucia estuarine lake in South Africa. *Estuarine, Coastal and Shelf Science* 93, 58-67

Lindsay P., Mason T.R., Pillay S. and Wright C.I., 2006. Suspended particulate matter and dynamics of the Mfolozi estuary, Kwa-Zulu Natal: Implications for environmental management. *Environmental Geology* 28(1), 40-51

Maggi, F., 2006.Flocculation dynamics of cohesive sediment. PhD Thesis, University of Technology Delft, Delft, 136 pp.

Maine C.M., 2010.Flocculation and sedimentation in the Mfolozi and St Lucia estuaries. Honours Thesis

Manning A.J. and Dyer K.R. 1999.Observation of the size, settling velocity and effective density of flocs and their fractal dimension. *Journal of Sea Research* 41, 87-95

Manning A.J., Friend P.L., Prowse N.and Amos C.L., 2007. Estuarine mud flocculation properties determined using an annular mini-flume and the LabSFLOC system. *Continental Shelf Research* 27, 1080-1095

Mantovanelli A. and Ridd P.V., 2006. Devices to measure the settling velocities of cohesive sediment aggregates: A review of the in situ technology. *Journal of Sea Research* 56, 199-226

Mietta, F., Chassagne, C., Manning, A. and Winterwerp, J., 2009a. Influence of shear rate, organic matter content, pH and salinity on mud flocculation. *Ocean Dynamics* 59 (5), 751–763.

Mietta, F., Chassagne, C.and Winterwerp, J., 2009b. Shear-induced flocculation of a suspension of kaolinite as function of pH and salt concentration. *Journal of Colloid and Interface Science* 336 (1), 134–141.

Mikes D., Verney R., Lafite R. and Belorgey M. 2002. Controlling factors in estuarine flocculation processes. Experimental results with material from the Seine Estuary. *Journal of Coastal Research* SI 41, 82-89

Mikeš D., Verney R., Belorgey M., and Lafite R. 2004. Controlling factors in estuarine flocculation processes: Experimental results with material from the Seine Estuary, North-western France. *Journal of Coastal Research* 41, 82–89.

Mikes D. and Manning A.J., 2010. Assessment of flocculation kinetics of cohesive sediments from the Seine and Gironde estuaries, France, through laboratory and field studies. *Journal of Waterway, Port, Coastal, and Ocean Engineering* 136 (6), 306-318

Mikes D., 2011. A simple floc growth function for natural flocs in estuaries. Submitted manuscript

Mikes, 2011, personal communication

Milburn D. and Krishnappen B.G., 2003.Modelling erosion and deposition of cohesive sediments from Hay river, Northwest Territories, Canada. *Nordic Hydrology* 34(12), 125-138

Milligan, T. G., and Hill, P. S. 1998.A laboratory assessment of the relative importance of turbulence, particle composition, and concentration in limiting maximal floc size and settling behaviour. *Journal of Sea Research*, 39, 227–241.

Nagata S., 1975. Mixing: Principles and Applications, Halsted Press Wiley, Chichester

Nikora V.I. and Goring D.G., 2002. Despiking acoustic Doppler velocimeter data. *Journal of Hydraulic Engineering* 128(1), 117-126

Nortek, 2009. Vectrino Velocimeter user guide, Nortek AS, Norway

Ockendon M.C., 1993. A model for the settling velocity of non-uniform cohesive sediment in a laboratory flume and an estuarine field setting. *Journal of Coastal Research* 9(4), 1094-1105

Russelo P.J., ADV measurements in high shear and near boundaries. Cornell University, Ithaca

Serra, T. and Casamitjana, X., 1998. Structure of the aggregates during the process of aggregation and breakup under a shear flow. *Journal of Colloidal and Interface Science* 206 (2), 505–511.
Serra T., Colomer J. and, Logan B.E., 2008.Efficiency of different shear devices on flocculation. *Water Research* 42, 1113-1121

Spicer P.T. and Pratsinis S.E. 1996. Shear-induced flocculation: the evolution of floc structure and shape of the size distribution at steady state. *Water Research* 30, 1049-1056.

Spicer P.T., Keller W. and Prastsinis S.E., 1996. The effect of impellor type on floc size and structure during shear-induced flocculation. *Journal of colloidal and interface science* 184, 112-122

Stone M., Krishnappan B.G.and Emelko M.B., 2008. The effect of bed age and shear stress on the particle morphology of eroded cohesive river sediment in an annular flume. *Water Research* 42, 4179-4187

Tennekes H. and Lumley J.L. 1973.A first course in turbulence. MIT Press

Van Leussen W. and Cornelisse J.M., 1993. The determination of the sizes and settling velocities of estuarine flocs by an underwater video system. *Netherlands Journal of Sea Research 31*(3), 231-241

Van Leussen W. 1994. Estuarine Macrofocs and their role in fine grained sediment transport. Ph.D. Thesis, University of Utrecht.

Van Leussen W., 1996. The RWS field settling tube. *Journal of Sea Research* 36, 83-86.

Van Leussen W. and Cornelisse J.M., 1996. The underwater video system VIS. *Journal of Sea Research* 36, 77-81

Van Rijn, L., 1993. Principles of Sediment Transport in Rivers, Estuaries and Coastal Seas, Aqua Publications, The Netherlands

Verney, R., 2006. Processus de controle de la dynamique des sédiments cohésifs; mesures in situ, expérimentales et modélisation; application à l'estuaire de la Seine. PhD Thesis, Université de Rouen, Rouen, 323 pp.

Verney R., Lafite R. and Brun-Cottan J.C., 2009. Flocculation potential of estuarine particle: the importance of environmental factors and of the special and seasonal variability of suspended particulate matter. *Estuaries and Coasts* 32, 678-693

Verney R., Lafite R., Brun-Cottan J.C., and Le Hir P., 2010.Behaviour of a floc population during a tidal cycle: Laboratory experiments and numerical modelling. *Continental Shelf Research*

Verney R., 2011. Personal communication

Whitfield .A.K., Taylor R.H. 2009. A review of the importance of freshwater inflow to the future conservation of Lake St Lucia. *Aquatic Conservation: Marine and freshwater ecosystems*.19 (7), 838-848

Winterwerp J.C. 1999. On the dynamics of high-concentrated mud suspensions. Ph.D. Thesis, Delft University of Technology.

Wolanksi E., Gibbs R.J., Mazda Y., Mehta A. and King B., 1992. The role of turbulence in the settling velocity of mud flocs. *Journal of coastal research* 8(1), 35-46

Wolanski E., Li Y., and Xie Q., 1993.Coagulation and settling of suspended sediment in the Jiaojiang River Estuary, China. *Journal of Coastal Research* 9 (2), 390-402

Wolanski E. and Gibbs R.J., 1995. Flocculation of suspended sediment in the Fly River estuary, Papua New Guinea. *Journal of Coastal Research* 11 (3), 754-762

Wolanski E., Huu Nahn N., and Spagnol S., 1998.Sediment dynamics during low floc conditions in the Mekong river estuary. *Journal of Coastal Research* 14 (2), 472-482

APPENDICES

Contents of appendices:

Appendix A: Calibration of the turbulent agitator.

Appendix B: Material composition test results. Suspended sediment concentration measurements.

Appendix C: Selected results from flocculation tests

Appendix D: Selected results from settling tests and camera timing measurements

Appendix E: Other items of interest

Appendix A

Table A-0-1: Table showing calibration of turbulent agitator. The motor speed was controlled by a frequency drive. Speed was related to frequency. The calibration was done in steps of 0.1 Hz. This has been reduced in the table to 0.5 Hz in order save space. Related to section 3.2.5.

Frequenc y	n (rpm)	n(s^{-1})	Re	Npmax	Np	G(s^{-1})	η (µm)
0.1	2.7	0.28	1186	1.718	1.701	0.2	2187
0.5	13.4	1.40	5931	1.683	1.667	2.3	657
0.8	**21.4**	**2.25**	**9489**	**1.680**	**1.664**	**4.7**	**462**
1.0	26.8	2.81	11862	1.679	1.663	6.5	391
1.3	**34.8**	**3.65**	**15420**	**1.678**	**1.662**	**9.7**	**321**
1.5	40.2	4.21	17793	1.678	1.662	12.0	288
2.0	53.6	5.62	23724	1.677	1.661	18.5	232
2.1	**56.3**	**5.90**	**24910**	**1.677**	**1.661**	**19.9**	**224**
2.5	67.0	7.02	29655	1.677	1.661	25.8	196
2.8	**75.0**	**7.86**	**33214**	**1.677**	**1.661**	**30.6**	**180**
3.0	80.4	8.42	35586	1.677	1.660	33.9	171
3.5	93.8	9.83	41517	1.676	1.660	42.8	152
3.9	**104.5**	**10.95**	**46262**	**1.676**	**1.660**	**50.3**	**141**
4.0	107.2	11.23	47448	1.676	1.660	52.2	138
4.5	120.6	12.63	53379	1.676	1.660	62.3	126
5.0	134.0	14.04	59310	1.676	1.660	73.0	117
5.5	147.4	15.44	65242	1.676	1.656	84.2	108
6.0	160.8	16.85	71173	1.676	1.660	95.9	102
6.5	174.2	18.25	77104	1.676	1.660	108.2	96
7.0	187.6	19.65	83035	1.676	1.660	120.9	91
7.5	201.0	21.06	88966	1.676	1.660	134.1	86
8.0	214.4	22.46	94898	1.676	1.660	147.7	82
8.5	227.8	23.86	100829	1.676	1.660	161.8	79
9.0	241.2	25.27	106760	1.676	1.660	176.3	75
9.5	254.6	26.67	112691	1.676	1.660	191.1	72
10.0	268.0	28.08	118622	1.676	1.659	206.4	70
10.5	281.4	29.48	124553	1.676	1.659	222.1	67
11.0	294.8	30.88	130484	1.676	1.659	238.2	65
11.5	308.2	32.29	136415	1.676	1.659	254.6	63
12.0	321.6	33.69	142346	1.675	1.659	271.4	61
12.5	335.0	35.10	148277	1.675	1.659	288.5	59
13.0	348.4	36.50	154208	1.675	1.659	306.0	57
15.0	402.0	42.11	177933	1.675	1.659	379.2	51

Appendix B

Material composition test results and suspended sediment concentration measurements

Table B-1: Suspended sediment and organic matter content test results

Date	Sample	Filter (g)	Filter+Sediment (g)	Sediment (g)	SSC (mg/L)	Combusted (g)	OMC (g)	OMC (%)	mean OMC%		
06-Oct	Mfolozi virgin	0.1573	0.1794	0.0221	221	0.1764	0.0030	13.57	13.26	14.21	17.84
06-Oct	Mfolozi virgin	0.1573	0.1793	0.0220	220	0.1764	0.0029	13.18			
06-Oct	Mfolozi virgin	0.1604	0.1812	0.0208	208	0.1784	0.0028	13.46			
06-Oct	Mfolozi virgin	0.1617	0.1812	0.0195	195	0.1787	0.0025	12.82			
07-Nov	Mfolozi virgin	0.1596	0.1777	0.0181	181	0.1745	0.0032	17.68	16.11		
07-Nov	Mfolozi virgin	0.1485	0.1650	0.0166	166	0.1626	0.0024	14.55			
06-Oct	Mfolozi 50mg/L	0.1600	0.1642	0.0042	42	0.1633	0.0009	21.43	21.24	23.28	
06-Oct	Mfolozi 50mg/L	0.1573	0.1611	0.0038	38	0.1603	0.0008	21.05			
31-Oct	Mfolozi 50mg/L	0.1493	0.1534	0.0041	41	0.1523	0.0011	26.83	25.32		
31-Oct	Mfolozi 50mg/L	0.1587	0.1629	0.0042	42	0.1619	0.0010	23.81			
07-Nov	Charters virgin	0.1490	0.2130	0.0640	640	0.2035	0.0095	14.84	14.43	13.88	15.45
07-Nov	Charters virgin	0.1481	0.2116	0.0635	635	0.2027	0.0089	14.02			
31-Oct	Charters virgin	0.1596	0.2204	0.0608	608	0.2124	0.0080	13.16	13.33		
31-Oct	Charters virgin	0.1593	0.2215	0.0622	622	0.2131	0.0084	13.50			
01-Nov	Charters 200mg/L	0.1471	0.1623	0.0152	152	0.1598	0.0025	16.45			
01-Nov	Charters 50mg/L	0.1482	0.1535	0.0053	53	0.1524	0.0011	20.75			
05-Dec	Mfolozi 1200	0.1562	0.2780	0.1218	1218	0.2654	0.0126	10.34	10.34	11.05	11.05
05-Dec	Mfolozi 450 (V)	0.1600	0.2063	0.0463	463	0.2008	0.0055	11.88	11.75		

05-Dec	Mfolozi 450 (V)	0.1557	0.2013	0.0456	456	0.1960	0.0053	11.62			

- The term 'virgin' is used to describe suspended sediment samples obtained from the Mfolozi and St Lucia estuaries.
- Samples of certain concentrations were mixed from the virgin samples. Their concentrations are checked here.
- "V" refers to a virgin sample taken at a later stage of the investigation.

Table B-2: Organic content of dried sediments

Date	Sample	Crucible (g)	Crucible+sediment(g)	Sediment (g)	Combusted (g)	OMC (g)	OMC (%)	mean OMC
08-Nov	Mfolozi	42.9246	43.3955	0.4709	43.3148	0.0807	17.14	
08-Nov	Mfolozi	45.5152	46.0829	0.5677	45.9693	0.1136	20.01	18.57
08-Nov	Charters	48.5481	49.5723	1.0242	49.4408	0.1315	12.84	12.84

- The "dried sediments" were obtained by settling, decanting and drying out suspended sediment solutions.

Table B-3: Summary of suspended sediment concentrations and OMC

Sample	Date	OMC (%)	SSC (mg/L)
Mfolozi bulk water sample (mean)	06-Oct	13.26	211
Mfolozi bulk water sample (mean)	07-Nov	16.11	174
Charters bulk water sample (mean)	31-Oct	14.43	615
Charters bulk water sample (mean)	07-Nov	13.33	638
Mfolozi dried sediment	08-Nov	18.57	
Charters dried sediment	08-Nov	12.84	

Table B-4: Results of particle size analysis using Malvern Mastersizer 2000. Note that results are condensed (see note below).

Sample Name	Measurement date and time	Result Below 2.000 µm	Result Below 63.000 µm	Result 2.00µm-63.00µm	Result 63.00µm-2000.00µm	Result 2.00µm-4.00µm	Result 4.00µm-8.00µm	Result 8.00µm-16.00µm	Result 16.00µm-32.00µm	Result 32.00µm-63.00µm	Result 63.00µm-125.00µm	Result 125.00µm-250.00µm	Result 250.00µm-500.00µm	Result 500.00µm-1000.00µm	Result 1000.00µm-2000.00µm
C2	2011/11/09 12:13	5.072	97.282	92.21	2.718	12.802	28.824	30.3	14.986	5.298	2.01	0.708	0	0	0
C2	2011/11/09 12:14	5.287	97.453	92.166	2.547	13.251	29.158	30.019	14.569	5.168	1.973	0.574	0	0	0
C2	2011/11/09 12:14	7.469	96.42	88.951	3.58	14.047	26.872	27.205	14.69	6.135	3.024	0.557	0	0	0
C4	2011/11/09 12:19	3.321	68.15	64.829	31.85	3.222	6.018	9.574	16.52	29.495	24.388	7.057	0.405	0	0
C4	2011/11/09 12:20	3.341	68.323	64.982	31.677	3.244	6.058	9.624	16.612	29.444	24.219	7.025	0.433	0	0
C4	2011/11/09 12:20	3.343	68.371	65.028	31.629	3.245	6.059	9.634	16.609	29.482	24.225	7.019	0.385	0	0
C1	2011/11/09 12:27	8.021	96.681	88.66	3.319	14.557	27.103	26.781	14.236	5.984	2.48	0.839	0	0	0
C1	2011/11/09 12:27	8.183	96.743	88.56	3.257	14.784	27.225	26.607	14.069	5.877	2.392	0.864	0	0	0
C1	2011/11/09 12:28	8.337	96.871	88.533	3.129	15.005	27.342	26.422	13.875	5.89	2.365	0.765	0	0	0
C5	2011/11/09 12:32	7.934	96.436	88.503	3.564	14.49	27.81	27.313	13.128	5.763	2.762	0.802	0	0	0
C5	2011/11/09 12:33	8.091	96.425	88.334	3.575	14.73	27.973	27.118	12.843	5.67	2.744	0.831	0	0	0
C5	2011/11/09 12:34	8.22	96.408	88.188	3.592	14.95	28.128	26.931	12.611	5.569	2.756	0.836	0	0	0
C3	2011/11/09 12:39	5.669	97.811	92.142	2.189	10.642	15.422	22.131	28.163	15.784	2.05	0.139	0	0	0
C3	2011/11/09 12:40	5.68	97.806	92.126	2.194	10.655	15.448	22.163	28.159	15.701	2.025	0.168	0	0	0
C3	2011/11/09 12:41	5.695	97.762	92.067	2.238	10.668	15.454	22.224	28.09	15.632	2.068	0.17	0	0	0
M3	2011/11/09 02:24	11.924	96.455	84.531	3.545	15.623	15.994	16.157	20.811	15.946	3.545	0	0	0	0
M3	2011/11/09 02:25	12.17	97.375	85.205	2.625	15.945	16.314	16.241	20.824	15.881	2.625	0	0	0	0
M3	2011/11/09 02:26	11.63	97.458	85.829	2.542	16.292	16.45	16.661	20.837	15.589	2.542	0	0	0	0

M5	2011/11/09 02:30	14.632	96.542	81.91	3.458	17.642	18.884	15.848	16.447	13.088	3.458	0	0	0	0
M5	2011/11/09 02:31	15.151	96.898	81.748	3.102	18.202	19.243	15.838	16.092	12.372	3.102	0	0	0	0
M5	2011/11/09 02:31	15.473	97.197	81.724	2.803	18.589	19.463	15.816	15.937	11.919	2.803	0	0	0	0
M2	2011/11/09 02:35	23.116	95.962	72.845	4.038	23.76	24.55	15.859	5.33	3.346	2.182	0.887	0.732	0.237	0
M2	2011/11/09 02:36	24.072	97.505	73.433	2.495	24.281	24.875	15.735	5.227	3.315	1.981	0.514	0	0	0
M2	2011/11/09 02:37	24.345	96.816	72.471	3.184	24.412	24.616	15.287	5.01	3.148	1.998	0.823	0.362	0	0
M1	2011/11/09 02:41	24.887	97.493	72.606	2.507	25.588	24.708	14.851	4.635	2.824	1.676	0.831	0	0	0
M1	2011/11/09 02:42	25.562	97.82	72.258	2.18	25.761	24.633	14.561	4.511	2.791	1.626	0.554	0	0	0
M1	2011/11/09 02:42	25.742	97.803	72.061	2.197	25.992	24.652	14.409	4.377	2.631	1.782	0.415	0	0	0
M4	2011/11/09 02:46	3.278	86.395	83.117	13.605	3.629	6.237	10.842	27.268	35.141	13.34	0.265	0	0	0
M4	2011/11/09 02:47	3.305	86.529	83.224	13.471	3.654	6.261	10.876	27.324	35.109	13.216	0.255	0	0	0
M4	2011/11/09 02:48	3.341	86.591	83.25	13.409	3.67	6.267	10.88	27.38	35.053	13.163	0.246	0	0	0
C2_av	2011/11/09 12:13	5.18	97.367	92.188	2.633	13.026	28.991	30.16	14.778	5.233	1.991	0.641	0	0	0
C4_av	2011/11/09 12:19	3.335	68.281	64.946	31.719	3.237	6.045	9.611	16.58	29.474	24.277	7.034	0.407	0	0
C1_av	2011/11/09 12:27	8.18	96.765	88.585	3.235	14.782	27.223	26.603	14.06	5.917	2.412	0.823	0	0	0
C5_av	2011/11/09 12:32	8.082	96.423	88.342	3.577	14.723	27.97	27.121	12.861	5.667	2.754	0.823	0	0	0
C3_av	2011/11/09 12:39	5.681	97.793	92.112	2.207	10.655	15.441	22.173	28.137	15.706	2.049	0.158	0	0	0
M3_av	2011/11/09 02:24	12.047	96.915	84.868	3.085	15.784	16.154	16.199	20.818	15.914	3.085	0	0	0	0
M5_av	2011/11/09 02:31	15.312	97.048	81.736	2.952	18.396	19.353	15.827	16.014	12.146	2.952	0	0	0	0
M2_av	2011/11/09 02:36	24.209	97.16	72.952	2.84	24.346	24.745	15.511	5.118	3.231	1.99	0.669	0.181	0	0
M1_av	2011/11/09 02:41	25.397	97.705	72.308	2.295	25.78	24.664	14.607	4.508	2.749	1.695	0.6	0	0	0
M4_av	2011/11/09 02:46	3.308	86.505	83.197	13.495	3.651	6.255	10.866	27.324	35.101	13.24	0.255	0	0	0

Note: Selected results from the particle size analysis have been used in order to save space. More detailed output is available at the end of the appendix.

Five samples of Mfolozi and Charters Creek sediments were tested. The Malvern Mastersizer tests each sample 3 times and computes the average result.

Appendix C

Tabulated results of flocculation tests

The results of the aggregation and deflocculation tests formed large tables. Two tests were performed for each condition. The mean, d25, d50, d75, d90 and maximum sizes for particle Area, Equivalent diameter and Major Axis length were measured. The results of two tests are shown in tables C-2 and C-3. The remainder of the results have been omitted to reduce the volume of the appendices. The results followed the same format as those it tables C-2 and C-3. Table C-1 shows the Kolmogorov microscale values associated with the shear rates measured (with respect to section 4.2.2.)

Table C-1: The Kolmogorov microscale values and shear rates

G (s-1)	K (m)	K (um)
1	0.00100	1000
5	0.00045	447
10	0.00032	316
20	0.00022	224
30	0.00018	183
50	0.00014	141
100	0.00010	100
1000	0.00003	32
10000	0.00001	10

Table C-2: Aggregation and deflocculation test results of Mfolozi 200mg/L 10ppt test 1

200mg/L 10ppt Mfolozi	G (s^{-1})	10	10	10	10	10	10	20	30	50
	Time (min)	0	5	15	30	50	70	defloc20	defloc30	defloc50
Area (µm2)	mean		1927	2226	3315	3581	4140	2592	1439	1654
	d25		680	611	805	778	861	778	604	514
	d50		1042	1069	1805	1860.8	1944	1583	889	958
	d75		2486	2722	4721	4110.4	5721	3486	1583	1861
	d90		4985	4985	8909	8409.6	11145	5818	3055	3588
	max		11859	18025	21385	36744	24940	28328	10526	11470
Equivalent diameter (µm)	mean		41	44	54	55	60	49	37	40
	d25		25	26	28	29	31	278	26	25
	d50		33	35	42	46	48	42	32	35
	d75		47	56	72	70	79	64	44	47
	d90		78	78	102	101	118	84	61	65
	max		123	151	165	216	178	190	116	121
Major Axis Length (µm)	mean		37	41	50	55	53	51	40	32
	d25		23	24	24	25	24	25	25	23
	d50		27	30	33	37	34	37	34	25
	d75		41	46	60	69	64	67	49	34
	d90		70	76	107	110	121	103	65	46
	max		136	224	285	332	282	304	193	136

Table C-3: Aggregation and deflocculation test results of Mfolozi 200mg/L 10ppt test 2

200mg/L 10ppt Mfolozi	G (s^{-1})	10	10	10	10	10	10	20	30	50
	Time (min)	0	5	15	30	50	70	defloc20	defloc30	defloc50
Area (µm2)	mean		2512	3030	3886	5452	4673	3675	2379	1661
	d25		611	667	805	1048	1139	805	639	611
	d50		999	1472	1625	2888	2666	1916	1250	999
	d75		2368	3624	4333	6756	6124	4180	2972	1916
	d90		6866	7726	8757	13103	11798	9257	5305	3416
	max		24801	19969	61378	83097	50519	33689	24162	16247
Equivalent diameter (µm)	mean		43	51	55	68	64	55	44	38
	d25		25	27	28	34	34	28	25	24
	d50		32	39	41	58	54	45	32	31
	d75		51	64	70	89	86	71	50	46
	d90		85	99	104	126	120	104	84	61
	max		178	159	280	325	254	207	244	144
Major Axis Length (µm)	mean		43	53	59	69	66	56	44	39
	d25		25	27	25	26	28	25	24	24
	d50		32	38	38	44	50	38	32	30
	d75		47	68	73	90	91	73	50	46
	d90		77	109	123	144	131	114	84	65
	max		358	198	456	633	349	379	24	199

The results of the aggregation test at 400mg/L are shown below. The 50 and 70minute results are shown. The results were used to show that digital imaging was not possible at high concentrations due to floc overlap.

Table C-4: Aggregation test of Charters Creek sediment at 400mg/L. (G=10s^{-1}, S=5ppt)

Charters	50min results			70min results:		
400mg/L 5ppt	Area	Equivalent Diameter	Major Axis Length	Area	Equivalent Diameter	Major Axis Length
Mean	1696	34	29	1499	34	28
d25	472	22	22	472	22	22
d50	639	25	25	722	25	25
d75	1222	34	30	1291	35	30
d90	5777	62	39	3555	57	37
Max	17914	151	251	19136	156	208

The results of the aggregation test of Mfolozi sediment at 5s^{-1} are shown in table C-5 below. The results relate to section 4.2.3. Floc size decreased after 30minutes due to settlement. Large flocs were resuspended when the shear rate was increased to 10s^{-1} in the deflocculation test. Thereafter floc size decreased with increasing shear.

The aggregation time scale of 70minutes was established in section 4.2.4. This was supported by observations after 70minutes in an aggregation test. Observations showed that the floc size distribution stabilizes by 70minutes. The results are shown in table C-6 that follows.

Table C-5: Results of aggregation test performed on 200mg/L Mfolozi sediment at $5s^{-1}$.

200mg/L 10ppt Mfolozi	G (s^{-1})	5	5	5	5	5	5	10	20	30	50
	Time (min)	0	5	15	30	50	70	defloc10	defloc20	defloc30	defloc50
Area (µm2)	mean			2120.3	3101.8	1947.8	1273.1	9348.2	3365.7	1684.5	1752.5
	d25			569.3	638.8	611.0	583.2	1027.6	860.9	583.2	638.8
	d50			1097.0	1402.5	1083.1	916.5	2916.2	1888.6	999.8	1055.4
	d75			2207.9	3749.3	1999.6	1527.5	10200.0	4179.8	1749.7	1971.9
	d90			4990.8	8526.3	4221.5	2641.2	28800.0	8126.4	3518.8	4624.2
	max			25162.0	26914.0	16747.0	13109.0	136340.0	39882.0	26301.0	8998.4
Equivalent diameter (µm)	mean			41.4	47.3	40.7	35.6	79.5	55.1	38.7	39.1
	d25			24.5	24.5	25.2	25.2	29.1	30.3	24.5	23.8
	d50			33.1	35.2	33.6	31.5	52.0	46.6	32.6	34.2
	d75			49.2	57.8	47.7	42.0	105.0	69.6	44.1	44.5
	d90			74.6	96.2	69.0	55.5	180.0	100.1	64.2	72.8
	max			179.0	185.0	146.0	129.0	420.0	225.0	183.0	107.0
Major Axis Length (µm)	mean			35.7	40.2	38.5	44.3	53.7	57.5	39.9	37.2
	d25			22.7	23.2	23.6	25.6	23.6	25.9	23.9	24.2

	d50			26.2	27.3	28.2	35.0	27.9	42.1	30.2	29.4
	d75			36.4	42.0	42.8	53.8	51.0	74.1	46.2	41.3
	d90			57.3	80.2	68.3	79.3	129.0	112.7	68.8	63.6
	max			335.0	247.0	191.0	197.0	550.0	404.0	295.0	179.7

Table C-6: Results of aggregation test at $10s^{-1}$ of Mfolozi sediment. The results from 70 to 140 minutes are shown.

200mg/L 10ppt Mfolozi Sediment	G (s^{-1})	10	10	10	10	10
	Time (min)	70	90	105	120	140
Area (µm2)	mean	7270.1	7087.1	7843.3	8115.2	7440.9
	d25	1805.2	1583.1	1444.2	1242.8	1444.2
	d50	4554.8	4776.9	4832.5	4860.3	4735.3
	d75	9526.1	9276.1	11373	10498	9623.3
	d90	17516	16941	20005	19802	16955
	max	68766	66905	42048	118150	89706
Equivalent diameter (µm)	mean	80.7	78.3	81.5	79.9	79.2
	d25	43.3	37.1	352	30.9	36.2
	d50	73.8	72.8	72.1	70.6	73.3
	d75	108.1	104.5	117	111	108.2
	d90	147	140	154	154	145
	max	296	292	231	390	338
Major Axis Length (µm)	mean	74.1	68.5	81.9	73.1	82.6
	d25	25.4	25.1	27.1	25.4	28.5
	d50	44.1	36	52.2	39.8	56.6
	d75	106.9	97.8	117	103	118.6

	d90	162	153	179	164	171
	max	455	575	401	600	582

Images of the tests shown in tables C-5 and C-6 are shown below:

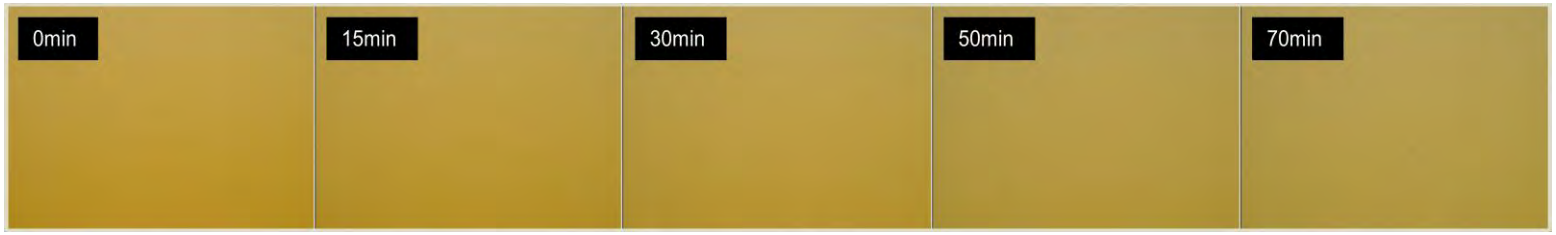

Plate C-1: Floc development for 200mg/L Mfolozi sediment $5s^{-1}$ (corresponding to table C-5)

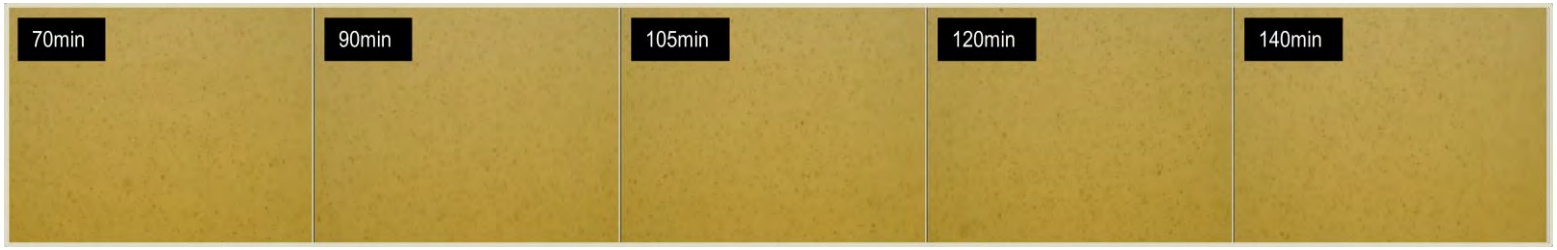

Plate C-2: Showing the results of the 200mg/L Mfolozi sediment from 70min to 140min (corresponding to table C-6)

Table C-7: Tabulated volume-based particle size distributions for Mfolozi sediment aggregation tests

			Mfolozi G=10 S=0	Mfolozi G=10, S=10	Mfolozi G=50, S=10	Mfolozi G=10, S=0	Mfolozi G=10, S=10	Charters G=10, S=0.5	Charters G=10, S=10	Charters G=50, S=10	Charters G=10, S=0.5	Charters G=10, S=10
Class Boundaries (µm)		Median	C=200	C=200	C=200	C=50	C=50	C=200	C=200	C=200	C=50	C=50
Lower	Upper	EQD (um)	Vol (%)	Vol (%)	Vol (%)	Vol (%)	Vol (%)	Vol (%)	Vol (%)	Vol (%)	Vol (%)	Vol (%)
20	37.5	25	7.1	1.6	24.2	30.2	33.8	8.9	16.5	20.8	5.4	3.1
37.5	62.5	50	21.5	7.3	34.6	15.8	39.7	22.3	29.9	37.7	16.6	16.8
62.5	87.5	75	21.9	15.5	23.7	10.7	18.1	22.3	19.8	33.0	15.3	25.5
87.5	112.5	100	23.0	21.5	6.4	20.0	5.2	17.7	11.7	7.0	18.2	24.1
112.5	137.5	125	10.9	18.3	4.3	14.0	1.9	12.6	7.8	1.5	17.6	11.0
137.5	162.5	150	12.9	20.7	0.0	3.8	1.2	3.8	3.9	0.0	9.5	6.5
162.5	187.5	175	2.8	8.4	6.7	5.4	0.0	6.9	4.3	0.0	10.5	4.7
187.5	212.5	200	0.0	4.3	0.0	0.0	0.0	0.8	2.6	0.0	3.3	7.0
212.5	237.5	225	0.0	1.0	0.0	0.0	0.0	2.8	2.9	0.0	0.0	1.3
237.5	262.5	250	0.0	1.3	0.0	0.0	0.0	2.1	0.8	0.0	0.0	0.0
262.5	287.5	275	0	0	0	0	0	0	0	0	3.4203	0
287.5	312.5	300	0	0	0	0	0	0	0	0	0	0
			100.0	100.0	100.0	100.0	100.0	100.0	100.0	100.0	100.0	100.0

Table C-0-2: Tabulated volume-based particle size distributions for Mfolozi sediment deflocculation test

			Mfolozi	Mfolozi	Mfolozi	Mfolozi
			G=10, S=10	G=20	G=30	G=50
Class Boundaries (µm)		Median	C=200	C=200	C=200	C=200
Lower	Upper	EQD (um)	Vol (%)	Vol (%)	Vol (%)	Vol (%)
20	37.5	25	1.6	7.2	18.0	21.3
37.5	62.5	50	7.3	19.7	27.9	38.0
62.5	87.5	75	15.5	25.1	26.6	19.5
87.5	112.5	100	21.5	17.8	14.7	13.2
112.5	137.5	125	18.3	16.7	6.0	5.0
137.5	162.5	150	20.7	4.0	2.8	3.1
162.5	187.5	175	8.4	3.0	4.0	0.0
187.5	212.5	200	4.3	6.5	0.0	0.0
212.5	237.5	225	1.0	0.0	0.0	0.0
237.5	262.5	250	1.3	0.0	0.0	0.0
262.5	287.5	275	0.0	0.0	0.0	0.0
287.5	312.5	300	0.0	0.0	0.0	0.0
			100.0	100.0	100.0	100.0

Appendix D

The results of the settling column tests are too numerous to include in this appendix. A sample of the results is shown in table D-1

Table D-0-3: Sample settling column test results

Image information	Image1 name (.jpg)	DSC_0157	DSC_0157	DSC_0157	DSC_0157
	Image 2 name (.jpg)	DSC_0167	DSC_0167	DSC_0167	DSC_0167
	Image 1 threshold	0.72	0.72	0.72	0.72
	Image 2 threshold	0.72	0.72	0.72	0.72
Test Conditions	Sediment type (M/C)	M	M	M	M
	S (ppt)	10	10	10	10
	C (mg/L)	200	200	200	200
	G (s^{-1})	10	10	10	10
	Δt (per interval)	0.364	0.364	0.364	0.364
	Intervals	10	10	10	10
	Δt (sec)	3.64	3.64	3.64	3.64
	Scale (1pxl: ?um)	5.27	5.27	5.27	5.27
floc in Image 1	area	155	29	671	274
	equiv. diameter (T)	14.0	6.1	29.2	18.7
	perimeter	14.0	6.1	29.2	18.7
	major axis length	21.2	7.8	32.8	22.8
	minor axis length	9.5	5.0	27.0	15.8
	centroid 1(y)	1066.8	255.8	763.3	395.0
Floc in Image 2	area	156	23	653	269
	equiv. diameter (T)	14.0	5.4	28.8	18.5
	perimeter	14.1	5.4	28.8	18.5
	major axis length	21.7	6.7	32.5	23.0
	minor axis length	9.6	4.3	26.3	15.6
	centroid 2(y)	1179.9	339.4	1055.7	643.2
Floc Properties	Area (µm sq.)	4304.8	805.4	18635.6	7609.8
	Equiv Diam (µm)	74.0	32.0	154.0	98.4
	Perimeter (µm)	112.0	41.3	173.0	120.4
	Major A. L. (µm)	112.0	41.3	173.0	120.4
	Minor A. L. (µm)	50.0	26.2	142.3	83.2
	ΔY (µm)	1131.0	836.0	2924.1	2482.2
	Vy(mm/s)	0.31	0.23	0.80	0.68
	eqd(um)	74.0	32.0	154.0	98.4
	effective density (kg/m^3)	1129.2	1436.5	1087.2	1154.3
	Quartz set vel (mm/s)	4.92	0.92	21.31	8.70
	Aspect ratio	2.24	1.58	1.22	1.45
	Fractal dimension - nf	1.77	1.80	1.91	1.87

Camera frame rate:

The frame rate of the D90 was measured to provide an accurate estimate of the time between images. This was discussed in sections 3.2.2 and 3.3.2. The results are shown in table D-2 below. The frame rate was measurement was repeated. A stopwatch was observed through the settling column. It was found that the time interval between 10 frames did not vary. It is acknowledged that the frame rate is not constant. This is compensated for by using images 10 frames apart.

Table D-0-4: Nikon D90 frame rate measurements

Image no.	Time (s)	ΔT (s)	Time (s)	ΔT (s)	Time (s)	ΔT (s)
1	7.66		30.96		48.87	
2	7.95	0.29	31.33	0.37	49.19	0.32
3	8.27	0.32	31.71	0.38	49.48	0.29
4	8.69	0.42	32.09	0.38	49.8	0.32
5	8.98	0.29	32.37	0.28	50.22	0.42
6	9.3	0.32	32.73	0.36	50.41	0.19
7	9.62	0.32	33.12	0.39	50.83	0.42
8	10.04	0.42	33.49	0.37	51.25	0.42
9	10.33	0.29	33.77	0.28	51.67	0.42
10	10.75	0.42	34.15	0.38	51.86	0.19
11	11.07	0.32	34.52	0.37	52.28	0.42
12	11.65	0.58	34.99	0.47	52.86	0.58
Mean ΔT (s)		0.36		0.37		0.36
St Deviation (s)		0.09		0.05		0.11
10*mean (s)		3.63		3.66		3.63
11*mean (s)		3.99		4.03		3.99
Total Δt (s)		3.99		4.03		3.99

Table D-3: Mean frame rate

Mean ΔT (s)	0.364
Mean St Dev. (s)	0.086
10 frame time interval (s)	3.64

The mean period for 10 intervals was calculated to be 3.64sec.

Appendix E

A copy of the image processing script and output has been included below. Prior to the script the binary images were created using the original images captured during testing. This appendix serves to illustrate the details of the image processing script. It begins by showing the details of the script; thereafter the output generated is displayed. This was originally produced in html form but has been subsequently copied into Microsoft word. The statistical data generated was used to prepare results for this dissertation. This script was used to process images captured at each stage of the flocculation and deflocculation tests.

MATLAB OUTPUT:

Contents

Microscope image analysis script

This script is designed to analyze 2 microscope/Camera images obtained from jar tests. Desired output: statistical properties of the size distribution of particles from the jar tests. Assumptions: It is assumed that the images have already been binarized. If the image is not binarized yet, then it should be binarized prior to running this script. Please make sure the scale is correctly entered

```
mtest='m1020010703';

IBW=imread('0017.tif');

JBW=imread('0018.tif');

KBW=imread('0019.tif');
```

```
scale=5.27;
```

Image I

```
[labeledI,numi]=bwlabel(IBW,8);
Idata=regionprops(labeledI,'all');
Iarea=[Idata.Area];
Iperim=[Idata.Perimeter];
Ieqd=[Idata.EquivDiameter];
Imal=[Idata.MajorAxisLength];
Imnl=[Idata.MinorAxisLength];
```

Image J

```
[labeledJ,numj]=bwlabel(JBW,8);
Jdata=regionprops(labeledJ,'all');
Jarea=[Jdata.Area];
Jperim=[Jdata.Perimeter];
Jeqd=[Jdata.EquivDiameter];
Jmal=[Jdata.MajorAxisLength];
Jmnl=[Jdata.MinorAxisLength];
```

Image K

```
[labeledK,numk]=bwlabel(KBW,8);
Kdata=regionprops(labeledK,'all');
Karea=[Kdata.Area];
Kperim=[Kdata.Perimeter];
Keqd=[Kdata.EquivDiameter];
Kmal=[Kdata.MajorAxisLength];
Kmnl=[Kdata.MinorAxisLength];
```

Combination of image data

```
IJKLarea=[Iarea Jarea Karea];
```

```
IJKLperim=[Iperim Jperim Kperim];

IJKLeqd=[Ieqd Jeqd Keqd];

IJKLmal=[Imal Jmal Kmal];

IJKLmnl=[Imnl Jmnl Kmnl];

numt=numi+numj+numk;
```

Scaling data

```
area=scale*scale*IJKLarea;

perim=scale*IJKLperim;

eqd=scale*IJKLeqd;

mal=scale*IJKLmal;

mnl=scale*IJKLmnl;
```

Output

```
disp(mtest);

disp('total sample population');

disp(numt);

areamean=mean(area);

areaptiles=prctile(area,[25 50 75 90 100]);

eqdmean=mean(eqd);

eqdptiles=prctile(eqd,[25 50 75 90 100]);

malmean=mean(mal);

malptiles=prctile(mal,[25 50 75 90 100]);

disp('Stats from left to right:');

disp('Area, EquivDiam, MajAxisLenght');

disp('mean');

disp([areamean eqdmean malmean]);

disp('d25');

disp([areaptiles(1) eqdptiles(1) malptiles(1)]);
```

```
        disp('d50');
        disp([areaptiles(2) eqdptiles(2) malptiles(2)]);
        disp('d75');
        disp([areaptiles(3) eqdptiles(3) malptiles(3)]);
        disp('d90');
        disp([areaptiles(4) eqdptiles(4) malptiles(4)]);
        disp('max');
        disp([areaptiles(5) eqdptiles(5) malptiles(5)]);
m1020010703
total sample population
       11082

Stats from left to right:
Area, EquivDiam, MajAxisLenght
mean
  353.6747   10.5126   13.2970

d25
   27.7729    5.9466    6.0853

d50
   27.7729    5.9466    6.0853

d75
   55.5458    8.4097   12.1705

d90
  111.0916   11.8931   18.2558
```

```
max
  1.0e+004 *

    4.4714    0.0239    0.0461
```

Filtering all flocs less than 20um in size:

```
areaf=area(area>400);

perimf=perim(perim>20);

eqdf=eqd(eqd>20);

malf=mal(mal>20);

mnlf=mnl(mnl>20);

figure, hist(areaf,15);title('Area
distribution');xlabel('Area (um sq)'); ylabel('number');

figure, hist(eqdf,15); title('Equivalent Diameter');
xlabel('Eq Diameter (um)'); ylabel('number');

figure, hist(malf,15);title('Major Axis Length');
xlabel('M.Axis Length (um)'); ylabel('number');

areafmean=mean(areaf);

areafptiles=prctile(areaf,[25 50 75 90 100]);

eqdfmean=mean(eqdf);

eqdfptiles=prctile(eqdf,[25 50 75 90 100]);

malfmean=mean(malf);

malfptiles=prctile(malf,[25 50 75 90 100]);

disp('Stats from left to right:');

disp('Area, EquivDiam, MajAxisLenght');

disp('mean');

disp([areafmean eqdfmean malfmean]);
```

```
        disp('d25');
        disp([areafptiles(1) eqdfptiles(1) malfptiles(1)]);
        disp('d50');
        disp([areafptiles(2) eqdfptiles(2) malfptiles(2)]);
        disp('d75');
        disp([areafptiles(3) eqdfptiles(3) malfptiles(3)]);
        disp('d90');
        disp([areafptiles(4) eqdfptiles(4) malfptiles(4)]);
        disp('max');
        disp([areafptiles(5) eqdfptiles(5) malfptiles(5)]);
Stats from left to right:
Area, EquivDiam, MajAxisLenght
mean
  1.0e+003 *

    6.4507    0.0780    0.0742

d25
  1.0e+003 *

    1.7358    0.0431    0.0257

d50
  1.0e+003 *

    4.3742    0.0723    0.0534

d75
```

```
  1.0e+003 *

    8.9151    0.1045    0.1069

d90
  1.0e+004 *

    1.5789    0.0140    0.0156

max
  1.0e+004 *

    4.4714    0.0239    0.0461
```

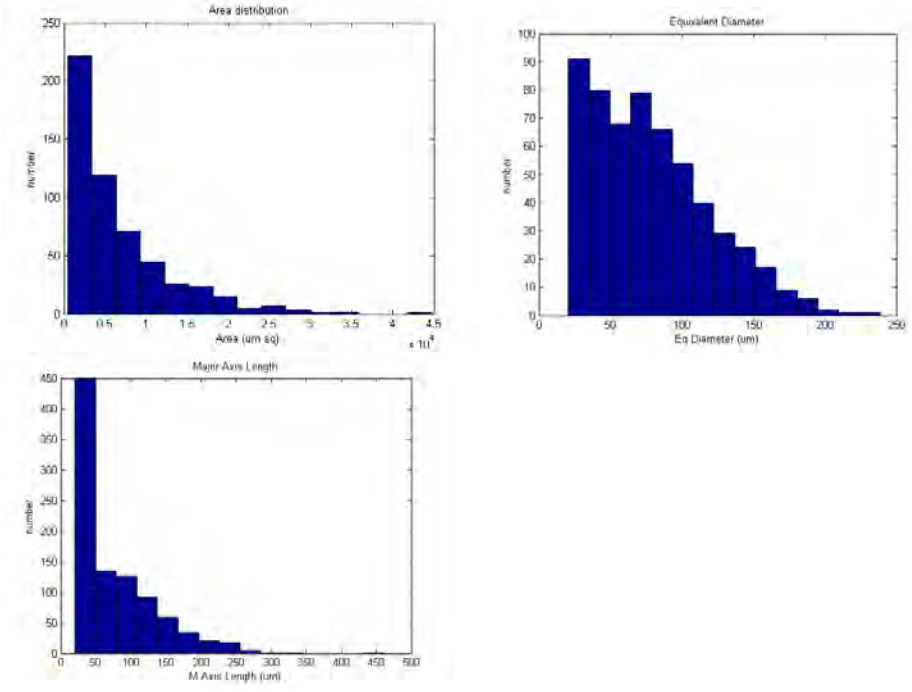

Published with MATLAB® 7.8